ABSTRACT

Title of Dissertation:	THERMODYNAMICS AND RELAXATION DURING ACTIN POLYMERIZATION
	Jermey N.A. Matthews, Ph.D., 2005
Dissertation Directed By:	Professor Sandra C. Greer, Department of Chemical Engineering

Actin is the most abundant cytoskeletal protein, accounting for 20% of the total protein content in all eukaryotic cells, especially muscle cells. Actin polymerizes from the globular state known as G-actin monomer to the filamentous semi-flexible polymer, F-actin. This polymerization is involved in cell motility, cell signaling, and even in regulation of ion transport.

Actin polymerization is known to be regulated *in vivo* by more than 150 actin-binding proteins, but was shown early on to be capable of thermodynamic regulation and this was proven under conditions of varying salt, ATP, initial monomer concentration and temperature. It was shown that actin polymerization is entropically driven, has a "floor" temperature for propagation, and is analogous to a second-order phase transition.

The purpose of this work was to measure the effect of pressure on the extent of actin polymerization as a function of temperature. The relaxations of the extent of polymerization after temperature jumps were also measured and analyzed in terms of the initial polymerization rates, r_p, as a function of temperature. The effects of

"thermal cycling" along the polymerization line were examined. The role of hydrogen bonding was studied by exchanging H_2O solvent for D_2O, which is known to have stronger "hydrogen" bonding.

The results show that actin polymerization under pressure follows the same trend as at atmospheric pressure, exhibiting a floor temperature, T_p, and showing the maximum in the extent of polymerization as reported earlier by Niranjan et al. New results show that increasing pressure increases T_p and that the volume change of polymerization is positive, a result expected for self-assembly of biological polymers, and varies between 300-500 cm^3/mol around 30 ^{0}C. The results also revealed the existence of a "ceiling" temperature, T_{p2}, above which the system re-enters the monomer region of the phase diagram. The relaxation studies revealed that r_p correlates with the equilibrium extent of polymerization and shows a peak near the transition temperatures. We also discovered that actin exhibits strong hysteresis upon temperature reversals, especially near the transition temperatures.

THERMODYNAMICS AND RELAXATION DURING ACTIN POLYMERIZATION

By

Jermey N.A. Matthews

Dissertation submitted to the Faculty of the Graduate School of the
University of Maryland, College Park, in partial fulfillment
of the requirements for the degree of
Doctor of Philosophy
2005

Advisory Committee:
Professor Sandra C. Greer, Chair/Advisor
Professor Mikhail Anisimov
Professor Timothy Barbari
Professor John Fisher
Professor Steven Rokita

Dedication

To my parents, Dr. Lionel and Walterine Matthews, who through consistent and persistent words and deeds of affirmation, made me believe that I could accomplish anything.

To my wife, Camesia, the most beautiful, intelligent, sophisticated woman that I know…who loves and supports me. *"You raise me up to more than I can be."*

Acknowledgements

I first want to thank the people whose names do not appear on this page, but know that they deserve an acknowledgement for their positive efforts in my academic and personal life.

Sincerest appreciation then goes to my advisor, Dr. Sandra Greer for guiding this dissertation and teaching me so much about professionalism and ethics, and being an example of discipline and organization. I would also like to thank Dr. Michael Harris of Purdue University, my master's thesis advisor, for encouraging me into the University of Maryland and for believing in me. I would like to thank all my group members and other peers at the University of Maryland, and especially Brittney Manvilla, and also Andrew Pomerance in Dr. Wolfgang Losert's group for their help in the lab and their support. I would like to thank Dr. Jeffrey Forbes at NIH, and Dr. Michael Alessi and Dr. Peter Yim, former group members for their advice and support. I also extend appreciation to all of my undergraduate and graduate school professors who instilled knowledge and had faith in me.

All of this would not be possible without the support of my family, friends and church family. They have always provided a safety net for me when falls were inevitable. I especially thank my sisters Jermella and Jonelle for their unconditional love and support.

Finally, I thank God for placing all these people in my life.

Table of Contents

List of Tables

List of Figures

Chapter 1: Introduction and Motivation

1.1 Introduction

In recent years, much research has been dedicated to unraveling the theory of macromolecular assembly. Macromolecules are extremely large molecules, especially when compared to common simple compounds such as table salt or methane. A variety of macromolecules abound in biological organisms. Plant cells, for example, contain cellulose and animals utilize DNA, RNA, and proteins for their composition and functions. Polymers are macromolecules which are large molecules made up of many repeating units. Synthetic polymers such as polyethylene, from which milk bottles are made, and virtually all plastics are seeing increased production and consumption. Moreover, since polymers have many unique and tunable properties, they are fast replacing wood, glass and metals as the choice material in many applications.

Although synthetic polymers have received considerable interest, success in polymer research has also lead to a renewed zeal to understand their biological counterparts - biopolymers. In fact, the longest known polymer is the biopolymer, DNA, which can have as many as ten billion monomer units.[1] The aid of modern tools and techniques has rendered the challenge to elucidate the structures of proteins and nucleic acids less daunting. The dynamics of polymerization remains a challenge and are critical towards understanding the functionality of a polymer.

Some polymers undergo reversible polymerization or equilibrium polymerization, a term that suggests that the polymerization reaction can shift in

either the forward or reverse direction. One biopolymer that exhibits this characteristic behavior is the protein, actin.

Equilibrium polymerization has been suggested and shown to conform to the theory of phase transition and critical phenomena.[2,3] In this study, the actin equilibrium polymerization is treated as a model phase transition system and some of the thermodynamic and kinetic properties of the polymerization are measured.

1.2 The Chemistry and Biochemistry of Actin

Actin is an important protein because it plays a central role, among other things, in muscle contraction, cell motility, and cell morphology. These functions are chiefly regulated by the ability of this biopolymer to reversibly self-assemble or (polymerize into filaments). Actin is commonly associated with muscle, accounting for about 25% of its protein content. It is the most abundant protein in the cytoskeleton and is found to comprise 15-20% of the protein content of a eukaryotic cell and can even be found in some protozoan and fungal sources. Although ubiquitous, variations in the amino acid sequence among its six isoforms, even within quite differing species, are minimal. There is only 5% variation between the isoforms of amoebas and humans.[4] This high degree of conservation suggests to biologists that all segments of the protein are essential for cellular functions. The actin isoform most commonly used and the one employed in this study is the α-actin from rabbit muscle. This actin "monomer" is a protein composed of approximately 375 amino acid residues with a molecular weight of 43 000 Dalton (g/mol), and exists as a globule at salt concentrations below typical intracellular concentrations of 150 mM K^+, 0.5 mM

Mg^{2+} and 0.0001 mM Ca^{2+}.[5] There is a slight excess of acidic residues, resulting in an isoelectric point of pH 5.5.

1.3 Actin Structure and Properties

Although protein molecules themselves are polymers, being made up of repeating amino acid segments, the native form of actin is commonly referred to as G-actin and is considered the monomer of an actin filament, or F-actin. Although F-actin is well known for its role in muscle contraction, G-actin can exist in the cell at concentrations as high as 100 μM even though it can polymerize to leave only 0.1 μM.[6] G-actin is resistant to crystallization because it is thermodynamically inclined towards polymerization. However, X-ray diffraction crystals of the complex of G-actin and the enzyme, deoxyribonuclease I, or Dnase I, which inhibits actin polymerization, have been obtained and the structure is shown in Figure 1.1.[7] The G-actin molecule is composed of two major domains of approximately equal size, the overall dimensions of the molecule being approximately 5.5 x 5.5 x 3.5 nm – not exactly spherical. The domains are further divided into subdomains 1 through 4, each with unique binding properties in the polymerization process. The cleft between the two domains can accommodate one molecule of ATP or ADP and one molecule of a divalent cation, typically Mg^{2+} or Ca^{2+} (Figure 1.1).

Figure 1.1 Schematic representation of the structure of G-actin. *Adapted from W. Kabsch.*[7]

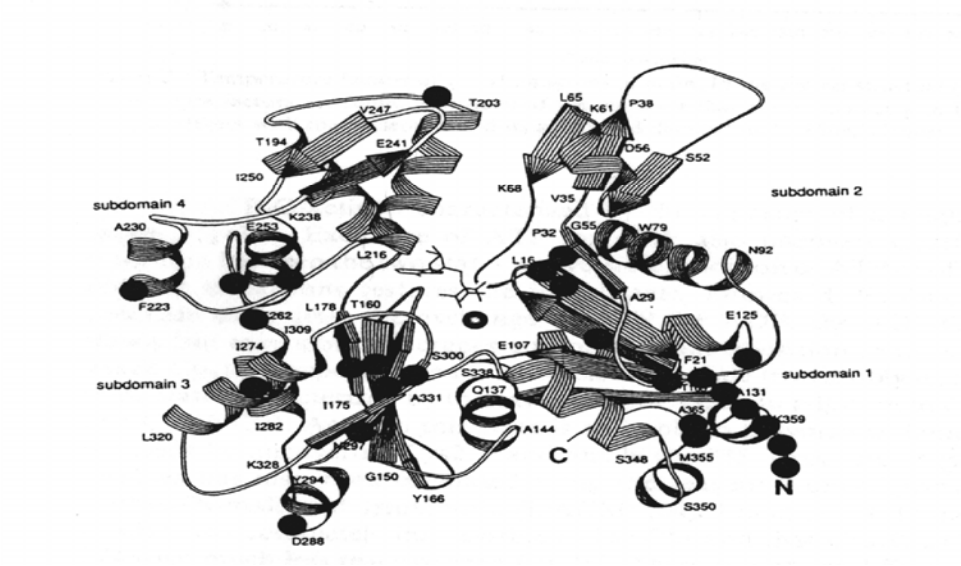

F-actin can be formed by increasing the salt concentration in G-actin. Crystallization of F-actin is also difficult because it forms amorphous filamentous aggregates. The structure of F-actin has been elucidated from models that apply the details of the monomer crystal structure to electron microscopy images and from an X-ray fiber diagram of F-actin complexed with the toxin, phalloidin. The overall shape resembles an arrow, with a barbed (or plus) end and a pointed (or minus) end (see Figure 1.2).[8] It is a helical structure that consists of two linear strands of actin monomers wrapped around each other, and the diameter of the double helix is around 8-10 nm.

Figure 1.2 (a) Lattice structure and (b) atomic model of F-actin. *Adapted from J. Howard.*[8]

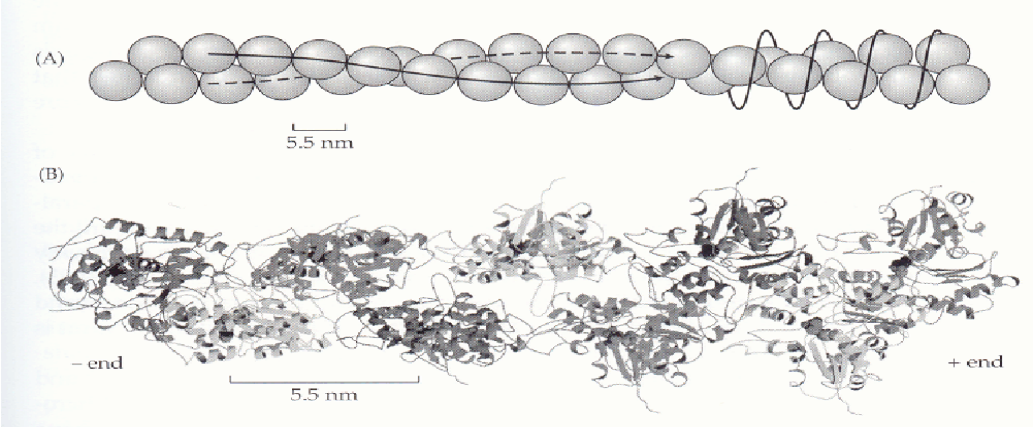

1.4. The Mechanism of Actin Polymerization

F-actin is formed from the self-association of G-actin due to hydrophobic/hydrophilic interactions between the amino acid residues and the aqueous solvent. The polymerization process is reversible at certain values of pH, G-actin monomer concentration, salt concentration, and temperature.[9] Actin self-assembly can therefore be viewed as a type of equilibrium polymerization reaction, where the concentrations of G-actin (monomer) and F-actin (polymer) are fixed at equilibrium. This is analogous to synthetic polymer systems that undergo equilibrium polymerization.

Polymerization of actin proceeds with activation of a G-actin monomer, followed by nucleation of two activated monomers to form a dimer or an activated dimer to form a trimer, then an elongation/propagation step of a trimer going on to form an actin filament.[10] All three steps are reversible. Nucleation is considered the rate-limiting step, and the rate of propagation is diffusion controlled.[11]

Activation: $A_1 \leftrightarrow A_1^*$

Nucleation: $A_1^* + A_1^* \leftrightarrow A_2$ and $A_1^* + A_2 \leftrightarrow A_3$

Propagation: $A_n^* + A_1 \leftrightarrow A_{n+1}^*$; $n \geq 3$

The two ends of the propagating filament polymerize at different rates because of the difference in polarity of the two domains of the monomer. The critical concentration, or the threshold concentration above which spontaneous polymerization can occur, of an actin solution containing ATP is lower at the barbed end and higher at the pointed end. Because of this, G-actin monomer travels to the barbed or rapidly polymerizing end from the pointed end, which actually depolymerizes after the solution falls below its critical concentration. This phenomenon is known as "treadmilling" and it is driven by the hydrolysis of ATP. Two actin filaments can be joined together in a process known as "annealing," and can be broken up under mechanical stress in a process known as "fragmentation." All these processes result in an exponential distribution of filament lengths and molecular weights.[12]

The Gibbs free energy dictates the requirement for the reaction to occur ($\Delta G < 0$) and the condition for chemical equilibrium ($\Delta G = 0$):

$$\Delta G_P = \Delta H_P - T \Delta S_P \qquad (1.1)$$

The subscript refers to the propagation of the reaction. The temperature T = T_p at which ΔG becomes negative can then be regarded as the polymerization or transition temperature. Calculations from the van't Hoff equation show that ΔH_p and ΔS_p for actin polymerization are positive,[2,13] though direct measurements of enthalpy have been unsuccessfully attempted.[15] Since ΔH and ΔS are both positive, the temperature must be greater than T_p for polymerization to proceed. This "floor" temperature, defined as the inflection point in Figure 1.3 below.[16] The maximum in figure 1.3 was unobserved until recently and may suggest a second transition temperature leading to depolymerization. Polymerization of actin may also be viewed as a "rounded" second-order phase transition with the extent of polymerization used as a sort of "order parameter."[17]

Figure 1.3 The extent of polymerization of actin as a function of temperature at different concentrations of KCl: Solvent = H_2O, $[G_0]$ = 2.93 mg/ml[18]

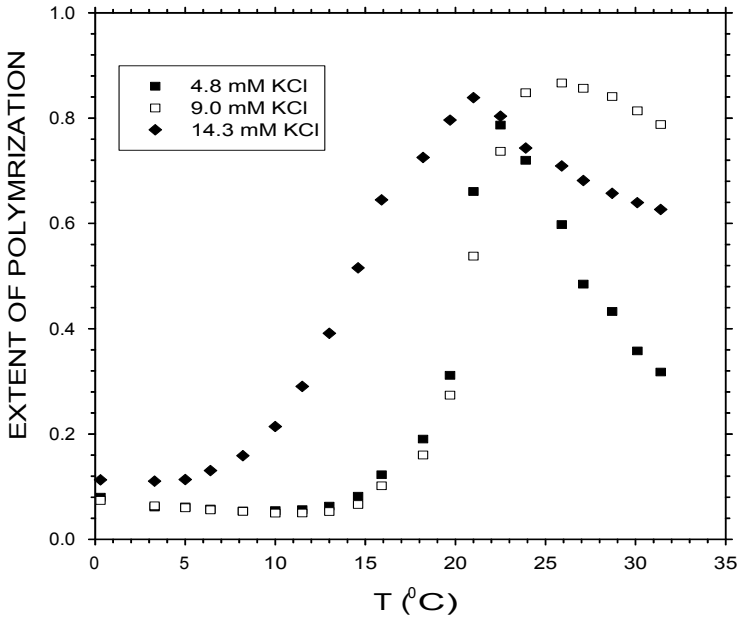

1.5 Significance

The actin polymerization equilibrium has recently received attention in neuroscience. Researchers at MIT's Picower Center for Learning and Memory deduced that, near the brain region linked to memory, F-actin under a particular electrical stimulus is formed to enlarge the synaptic spine and increase the ability of the brain cells to transmit information and under a different stimulus, G-actin forms and unravels the F-actin "information highway".[19] This ability of brain cells to shift their shape is directly related to memory retention or memory loss and is chiefly regulated by actin polymerization.

The role of actin in cell motility is an important one, as recently discussed in a review article in **Science**, entitled "*How Cells Step Out.*"[20] The article describes how a family of proteins/enzymes responds to motility signals and act in concert to polymerize and depolymerize actin and to form branched filaments. This filament growth pushes outward on the cell membrane and acts as the driving force for motion. The current research is intended to give the minimum thermodynamic and relaxation parameters for polymerization in the absence of the intracellular regulators. Actin polymerization is diffusion limited in the propagation step, so knowledge of the overall kinetics, especially near the transition point where concentration fluctuations should increase, will be revealing of solution transport properties.

One interesting and controversial new theory is that most cell functions, including cell motility, are primarily driven by the phase transition of the cell membrane "gel" due to mechanical stress, temperature, solvents, salts, etc.[21] This theory also underscores the importance of water and the fact that its

adsorption/desorption onto actin plays a role in trans-membrane solute transport. A measure of the volume change upon polymerization as well as altering the nature of the buffer (H_2O to D_2O) will give useful information on the role of the solvent. The phase transition approach has been, and continues to be a prominent one[14,16,18] in studying the effect of temperature, salt, solvent, and pressure on the extent of actin polymerization.

1.6 Project Summary

In this project, several issues will be addressed:

- **The effect of pressure on the extent of polymerization (Chapter 6)**. The extent of polymerization as a function of temperature will be measured at different pressures. The extent of polymerization is proportional to the intensity of fluorescence, which is monitored in a high pressure cell of a fluorescence spectrophotometer. This experiment allows for an analysis of the effect of pressure on the transition of G- to F-actin. This method can also be used to determine the volume change (ΔV) of the polymerization of actin, since the change in the extent of polymerization with pressure is related to ΔV.
- **The effect of "thermal cycling" on the dynamics of equilibrium polymerizations (Chapter 4 and 5)**.[22] Reversible polymers are reported to be ultrasensitive (that is, the length distribution is highly responsive) to external changes such as temperature or pressure, even exhibiting non-linear responses to linear perturbations. The goal is to understand how sensitive actin polymerization is to positive and negative temperature jumps in relation to both its thermodynamics and its kinetics.

- **The kinetics of actin polymerization (Chapter 4 -6).** The relaxation of the extent of polymerization after the positive (and/or negative) temperature jumps will also be measured. From these relaxation data, we will determine the initial rate of polymerization, taken as initial slope of monomer concentration versus time will be determined and studied with respect to temperature.
- A study of the **role of the solvent (Chapter 5)** on the properties of actin polymerization will also be performed by measuring the extent of polymerization of actin in D_2O versus H_2O buffer, since D_2O is considered to have stronger hydrogen bonds.[23]

Chapter 2: Experimental Framework

2.1 Measurement of the Extent of Polymerization under Pressure

The application of high pressure as a variable in the polymerization process of proteins is important because, in addition to providing information about the volume change, knowledge of pressure effects is important as much of our biosphere is not at atmospheric pressure (i.e. deep sea, high altitudes).[24,25] Pressure is also known to promote dissociation of proteins[26,27] and can, in general, give information on structural changes in protein solutions.[24]

Many techniques exist for quantifying actin polymerization. Viscometry techniques are frequently employed because of the significant viscosity increase from G-actin to F-actin. However, shearing the actin sample leads to fragmentation of the filaments. Electron microscopy, another technique useful in quantification of filament morphology, cannot track the polymerization process in real time in solution. Ikkai and Ooi[28] used flow birefringence to measure polymerization, but this technique shears the sample and distorts the molecular weight distribution. Fluorescence spectroscopy is a preferred technique because the signal to noise ratio is high, it is non-invasive, and it requires very little sample volume. Garcia et al.[27] observed the fluorescent spectral changes of actin dissociation under pressure. They performed the experiment at an unreported temperature and only observed depolymerization under pressure.

The current project will study the extent of polymerization as a function of temperature by observing the increase in fluorescence due to association in a sample

containing pyrene-labeled G-actin. The initial monomer concentration, initial salt concentration, solvent type, and ATP concentration are held constant as in a previous study,[18] with pressure as an additional parameter.

2.2 Theory of Volume Change from Pressure Effects

At equilibrium, where the change in Gibbs energy goes to zero, and for a system at constant temperature and composition (x), we derive the derivative of ln K_x , where K_x is the "equilibrium constant" in terms of concentrations with respect to pressure, to get the expression for the volume change ΔV:

$$K_x = [A_{n+1}]/[A_n]\,[A_n^*] \tag{2.1}$$

$$\left(\frac{\partial \ln K_x}{\partial P}\right)_{T,x} = \frac{-\Delta V}{RT} \tag{2.2}$$

In this equation, R represents the universal gas constant and T is the absolute temperature. The volume change is proportional to the derivative of the equilibrium constant with respect to pressure. The concern is that the concentrations (x) of the components in solution, i.e. pH and [ATP], may depend on pressure. A lower pH increases the rate of polymerization because proton binding induces a conformational change and stabilizes the dimers.[29] A study of the effect of pressure on Tris-HCl buffer[30] discovered that the volume change of ionization (or acid disassociation) due to pressure is slightly positive and that the pK_a, which is proportional to the pH decreases by less than 0.2 units. This is attributed to the fact that acid dissociation of Tris does not change the number of formal charges, which tends to typically cause a volume decrease due to solvation effects. Hence, the conclusion was that Tris buffer at pH = 8 is fairly insensitive to pressure changes over a pressure range of about 600

MPa. For ATP, the equation for hydrolysis during actin polymerization[31] (see Equation 2.3) indicates that the number of moles does not change, so it is not expected that the equilibrium will shift due to volume changes caused by pressure according to Le Châtelier's Principle. While ATP hydrolysis is not essential for actin polymerization,[32,33] ATP stabilizes F-actin against pressure denaturation over pressure ranges as high as 250 MPa and greater.[24]

$$\text{Actin.ATP} \rightarrow \text{Actin.ADP.P}_i \rightarrow \text{Actin.ADP} + \text{P}_i \qquad (2.3)$$

The extent of polymerization (ϕ) is formally defined as the ratio of the mole fraction of monomer in the polymer (X_p) to the initial monomer mole fraction (X_0):

$$\phi = X_p/X_0 = (M_0\text{-}M_f)/M_0, \qquad (2.4)$$

M_0 is the initial concentration (mol/L) of monomer present and M_f is the concentration of free or un-bound monomers in solution.

When the system is allowed to equilibrate at a specific temperature, ϕ remains constant and thus can be considered a thermodynamic parameter. The extent of polymerization, ϕ, is related to the "equilibrium constant" for the propagation, K_x:

$$K_x = 1/M_0\ (1- \phi) \qquad (2.5)$$

Chapter 3: Sample Preparation and Experimental Methodology

3.1 Introduction

In this chapter, a thorough description of the methods of sample preparation, the apparatus used, and the experimental procedures is provided. The actin used was derived from fresh rabbit muscle tissue obtained from NIH and was isolated in accordance with the protocol of Pardee and Spudich. Changes or variations to the protocol are noted. The tissue first underwent treatment in various solutions, followed by filtering of the solution and retention of the tissue. The tissue, which was primarily actin, was then converted to a dry powder form by precipitation in acetone. G-actin was then isolated and purified from the muscle acetone powder in buffer A (see Table 3.1), the solvent/buffer used in all of the experiments.

The final stage of purification involved fractionation through a gel filtration column which separates molecules according to size. When D_2O solvent was required, H_2O in buffer A was exchanged for 99.9 % pure D_2O by dialysis. We calculated the concentration of G-actin by measuring the absorbance with a UV/VIS spectrophotometer using the Beer-Lambert Law to make the correlation. Care was taken to maintain sterility and to meet the strict temperature requirements for sample integrity, which included sterilization of the containers and transfer equipment used, and maintenance of the sample at 4 ^{0}C in the cold room or at 0 ^{0}C on ice, as required by the protocol. All details are supplied in section 3.2.

The technique of fluorescence spectroscopy was used to measure the fraction of actin that had been polymerized. The actin sample was mixed with 3% by mass of

actin that was labeled with a fluorescent probe. The basic principle of actin labeling involves attachment of a fluorescent molecule to a reactive site on the protein. In these experiments, N-(1-pyrenyl) iodoacetamide, or "pyrene" dye, is attached to the reactive Cys-373 amino acid residue on actin. When the actin nuclei associate near that reactive group, they cause a local structural change and the intensity of the fluorescence of the molecule increases. The fluorescence of the pyrene dye provides up to a 25-fold enhancement over the intrinsic fluorescence of actin.[34]

3.2 Sample Preparation

3.2.1 Preparation of Muscle Acetone Powder

Rabbit muscle tissue was obtained and stored at -70 ^{0}C until it was ready to be used. The muscle was then minced and extracted with gentle stirring in various solvents in the cold room (4 ^{0}C), followed by filtration by hand through cheesecloth or over a Buchner funnel under vacuum. The residue was saved in each step. The solvents in order were:

a. 0.1 M KCl/0.15 M potassium phosphate

b. 0.05 M $NaHCO_3$

c. 1 mM EDTA

d. H_2O

At the final stage, the residue was stirred in acetone and filtered to precipitate the remaining proteins and to form muscle acetone powder, then air-dried overnight. A flow chart of the process with additional details is shown in Figure 3.1.

Figure 3.1 Flowchart of the preparation of muscle acetone powder from rabbit tissue. "Volume" represents the volume of extraction solution to be used per gram of tissue. The number in brackets refers to the number of times the extraction is performed.

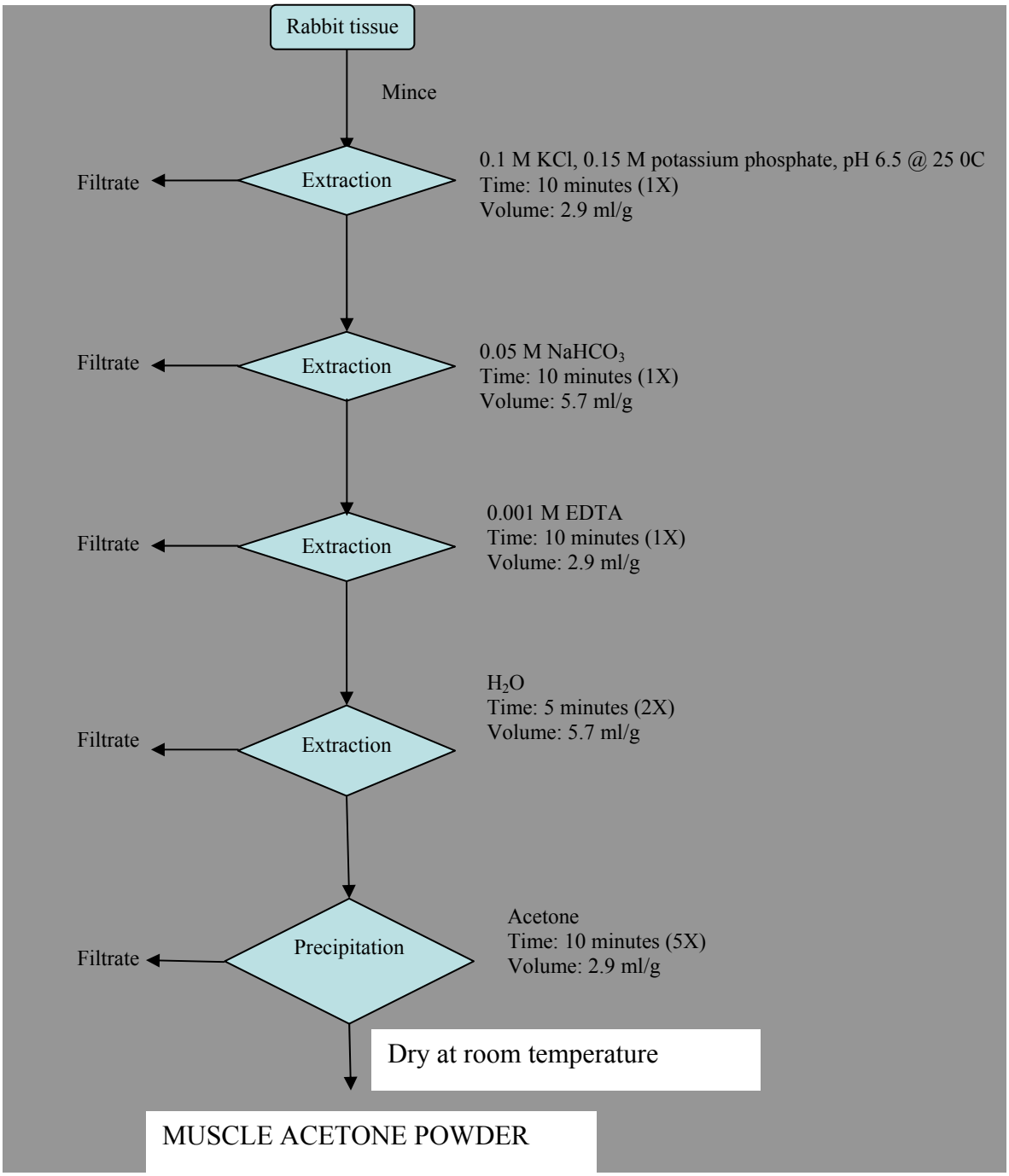

3.2.2 Actin isolation and purification

The actin was isolated from the muscle acetone powder by extraction with stirring into buffer A (see Table 3.1), followed by filtering through a cheesecloth. The residue was extracted again to increase the yield. The filtrate, which was retained, was centrifuged at 10k rpm for 1 hour in a Sorvall refrigerated super speed centrifuge that had been pre-chilled to 4 ^{0}C and the supernatant (primarily G-actin) was collected. The G-actin was polymerized to F-actin by bringing the concentration of KCl to 50 mM, $MgCl_2$ to 2mM, and Na_2ATP to 1mM. After a few hours of allowing the actin to polymerize at 4 ^{0}C, the F-actin solution was brought to a concentration of 0.6 M KCl by adding solid KCl and stirring for 30 minutes at 4 ^{0}C. This step was designed to remove tropomyosin.

Table 3.1 Buffer A components and their role.

Component	**Concentration**	**Role**
Tris(hydroxymethyl)aminomethane	4 mM	buffer pH = 8
$CaCl_2$	0.2 mM	actin stability
Na_2ATP	0.2 mM	actin stability
20 % NaN_3 in H_2O	0.005% (v/v)	inhibits bacterial growth
HCl	concentrated	lower to pH 8 @ 25 ^{0}C
Dithiothreitol (DTT)	0.5 mM	reducing agent/actin stability

Following the salt wash, the F-actin was pelleted at 52k rpm for 1.5 hours in a Beckman XL-90 preparative ultracentrifuge. The F-actin pellet was collected and homogenized in buffer A, and the sedimentation/homogenization process was repeated. After the second homogenization, the solution was first sonicated for a few minutes to break up the actin oligomers (which helps to speed the depolymerization) and then placed in regenerated cellulose dialysis tubing of molecular weight cutoff (MWCO) 12-14,000 Daltons and dialyzed/depolymerized by rapid stirring in a cylinder of buffer A over a period of 4 days at 4 ^{0}C, with daily buffer changes. This process simply takes advantage of the salt concentration difference between a large volume of buffer A (with no KCl or $MgCl_2$) and the salt-containing F-actin solution. The salts permeate the dialysis tubing and the removal of salts allows the actin filaments to depolymerize. The G-actin can then be recycled by polymerizing with 50 mM KCl, 2 mM $MgCl_2$, and 1 mM ATP, hereafter referred to as the "polymerization cocktail," followed by depolymerization via dialysis. This recycling process is helpful in removing unwanted oligomers and other impurities smaller than 14 000 g/mol that have remained in the sample.

The G-actin sample after dialysis was clarified by centrifugation at 45k rpm for 1.5 hours in the Beckman XL-90 ultracentrifuge and the supernatant was retained. This action removes very large or heavy constituents and impurities. At this stage, the sample can be polymerized and stored as F-actin at 0 ^{0}C, or used to make pyrene-labeled actin, hereafter referred to as "pyrene-actin." The labeling process is described later in section 3.2.3.

The final step involved eluting the sample (pure G-actin or pyrene-actin) through a gel filtration column (Sephacryl S-200 distributed by Amersham Pharmacia) with resolution in the molecular weight range of 5,000-250,000 Daltons. Gel filtration or size exclusion columns are designed for preparative purification of proteins and peptides according to hydrodynamic size. The largest particles pass through the void volume and are eluted fastest. The actin molecules fit into the pores and take longer to elute. The smaller particles are therefore eluted last. The column used here was packed with the cross-linked allyl dextran and N,N-methylenebisacrylamide gel particle co-polymer. This co-polymer is very rigid, able to withstand up to 1 ml/min of flow, inert to most chemicals, and stable within a pH range of 2-13.

A piece of filter paper was spotted with 3.5 μL of the fractions that were eluted from the gel filtration column. Protein existence was indicated by staining the filter paper with Coomassie Blue Staining Solution (0.5 % Coomassie BB R-250, 40% glacial acetic acid and 50% distilled water). The fractions that stayed blue upon treatment with the de-staining solution (20% methyl alcohol, 5% glacial acetic acid and 75% distilled water) were pooled and the concentration was measured with a UV/VIS spectrophotometer. The concentration can then be adjusted to the desired value, diluted with filtered buffer A, or concentrated by filtering the buffer through a low protein-binding centrifugal filter device with a 10-12 000 MWCO range. The buffer passes through the membrane but the actin is retained, thus lowering the volume of solution while keeping the mass of actin constant. At this point, the sample was utilized for experiments or polymerized to F-actin for storage at 0 ^{0}C. A

flowchart of the entire process of actin isolation and purification is shown in figure 3.2.

Figure 3.2 Flowchart of actin purification from muscle acetone powder.

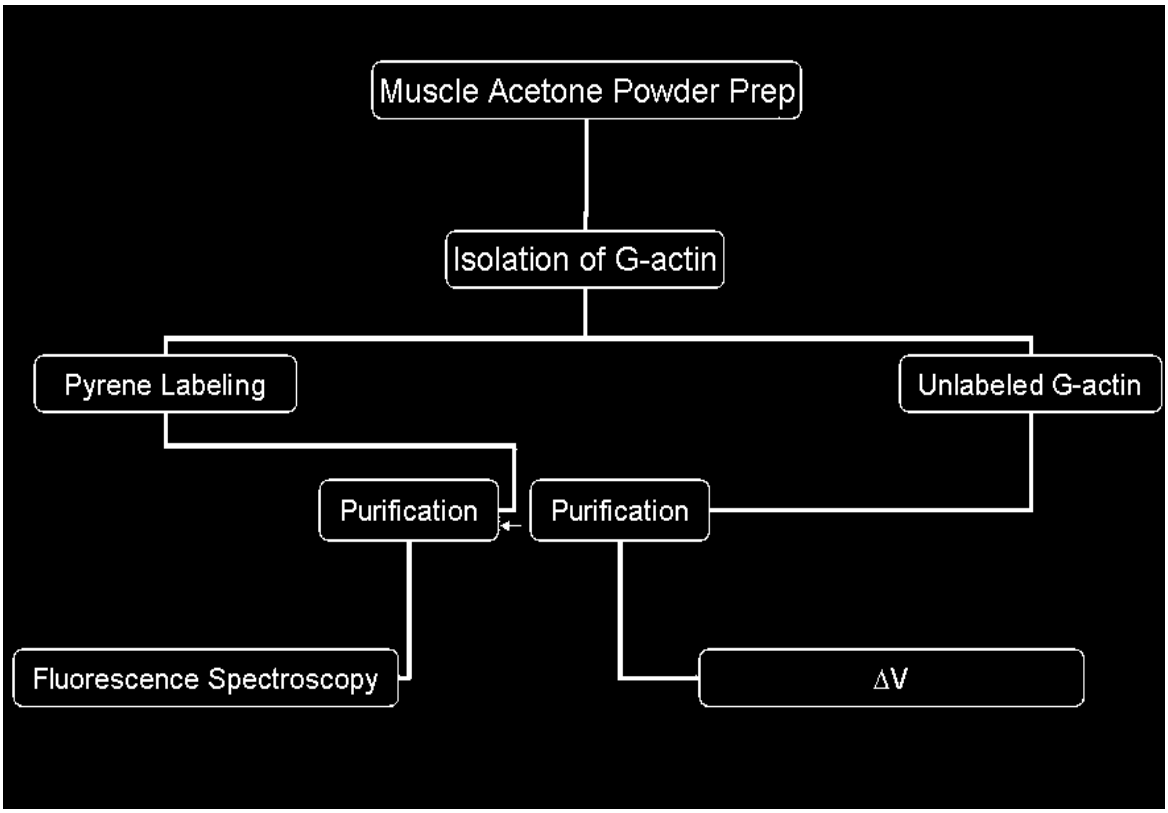

3.2.3 Labeling of actin with N-(1-pyrenyl) iodoacetamide

Following the four day dialysis step discussed above in section 3.2.2, the actin was brought to a concentration of approximately 1 mg/ml, polymerized with the polymerization cocktail and dialyzed against F Buffer (Buffer A minus DTT plus 100 mM KCl) for 12 hours. DTT was removed because, although it stabilizes the protein by protecting thiol groups from forming disulfide bonds, pyrene reacts covalently with the Cys-374 residue, a thiol containing group.[34] The pyrene dye was prepared

by dissolving in N,N-dimethyl formamide to a concentration of 4 mM. After dialysis, the dye was added slowly to a 4:1 molar ratio of dye to actin while stirring the solution. Stirring is essential because the organic solvent is incompatible with the aqueous solution and if added too quickly or if allowed to localize, can denature the protein. After 12 hours of allowing the reaction to proceed, DTT was added to stop the reaction and to protect against oxidation.

The now labeled actin was sedimented in a high speed centrifuge and the pellet was homogenized in Buffer A and dialyzed for 12 hours. The labeled actin was further purified by fractionation through the gel filtration column. The concentration of both pyrene and actin was measured by UV/VIS spectroscopy, with a ratio of the pyrene concentration to the actin concentration resulting in the fraction of actin that is labeled. Labeled G-actin or pyrene-actin was mixed with the unlabeled actin at a ratio of 3% by mass.

3.2.4. Solvent exchange of H_2O for D_2O

The thermodynamic and kinetic properties under consideration were also analyzed as a function of solvent type – namely the effect of D_2O based buffer A as compared to aqueous buffer A. It is therefore necessary to exchange the H_2O solvent in a sample of actin with D_2O. This was accomplished by solvent exchange via macrodialysis.

Macrodialysis is a technique which allows exchange of molecules smaller than the pore size of a dialysis membrane, the driving force being a concentration gradient. Macrodialysis offers a broader range of moderate volume requirements for sample and dialysate, where the small microdialysis tubing is not sufficient, or where

a large volume requirement for the dialysate or sample would be expensive. The design is also suitable for flow dialysis, where the dialysate is being replenished continuously. The chamber consists of two cell chambers with a membrane disc in between and two luer fittings in each half-cell. The two half cells are clamped together and the dialysate is inserted via a syringe into the lower chamber and the sample is inserted in like fashion into the upper chamber. A stir bar can be placed in the lower chamber to provide rapid exchange.

A Spectra/Por MacroDialyzer with a half cell volume of 10.0 mL and a 47 mm diameter membrane disc with a MWCO of 12-14 000 was used. Approximately 10 mL of the dialysate was placed into the lower chamber and exchanged or replenished at every stage (where 60 minutes equals one stage) under gentle stirring with a magnetic stir bar. The upper chamber contained 10 ml of gel-filtered G-actin in buffer A. For the dialysate, we used buffer A with a solvent base of 99.9% D_2O buffer, called buffer D. Since H_2O and D_2O are the only permeable molecules that have a concentration difference, they are exchanged for each other. The dialysate was replenished with buffer D for eight stages. Greater than 99% exchange for D_2O was accomplished after 6-8 stages of replenishing.[15]

3.2.5. Measuring concentration with UV/VIS spectroscopy

In this section, a description is given of how the concentrations of actin and pyrene-actin are measured by UV/VIS spectroscopy. It is known that a transition of pi bonds and nonbonding electrons between electronic energy levels occurs upon absorption of ultraviolet-visible light or radiation. UV/VIS spectrophotometers are

designed to measure the amount of light transmitted (T) which is inversely proportional to the amount of light absorbed. The concentration of a particular species in solution is directly proportional to the absorbance (A). This proportionality is represented by the Beer-Lambert Law:

$$A = \log (1/T) = \log (I_0/I) = \varepsilon c l \qquad (3.1)$$

I_0 is the intensity of incident light, I is the intensity of transmitted light, l is the path length or the length of the cuvette or sample holder, c is the concentration, and ε is a proportionality constant commonly known as the extinction coefficient. Absorbance is unitless whereas ε has units of mol^{-2} m^2 if concentration is given in units of mol m^{-3}. A standard curve of absorbance versus concentration is usually plotted to find the extinction coefficient.

Actin has an extinction coefficient of ε = 0.63 ml/mg at 290 nm.[35] The concentration is measured at 290 nm, the wavelength of maximum absorbance. Data are corrected for scattering due to large particles or oligomers by subtracting the absorbance value at 330 nm. Equation 3.2 shows the modified Beer-Lambert Law for determining the actin concentration:

$$[G_0](mg/ml) = \frac{A_{290} - A_{330}}{0.63(ml/mg)} \qquad (3.2)$$

Pyrene-actin is simply a solution of pyrene covalently attached to G-actin. It is therefore plausible that a measurement of the concentration of pyrene will give information as to how much pyrene-actin there is, since every pyrene molecule will be found bound to an actin molecule. Pyrene has an absorbance maximum at 344 nm and an extinction coefficient of 2.2 x 10^4 cm^{-1} M^{-1}.[34] Since attachment or labeling of 100% of the actin is rarely achieved, however, the concentration of actin (minus the

scattering correction) at 290 nm is also measured. The degree of labeling (DL) is given by the following relation:

$$DL = \frac{A_{344}}{\varepsilon_{pyrene}} \times \frac{MW_{actin}}{c}, \tag{3.3}$$

or more simply,

$$DL = 1.93\left(\frac{A_{344}}{c}\right) \tag{3.4}$$

Typical DL values of 70% to 80% are usually achieved.

3.3. Fluorescence Spectroscopy: Pressure Effects and Kinetics

3.3.1 Introduction

The extent of polymerization as a function of temperature and pressure is measured by the technique of fluorescence spectroscopy. This technique is ideal for the measurements proposed in this project because the pressure can be altered and controlled, thus giving information on the pressure effects on the extent of polymerization, forward and reverse kinetics, and the volume change. The apparatus requires very little sample, is sensitive, non-invasive, and provides rapid response time, resulting in reliable kinetic data. In this section, a description of the apparatus is provided as well as the procedure for measuring the extent of polymerization and the kinetics.

3.3.2 Description of the Spectrofluorimeter and Related Apparatus

Measurements of ϕ (t) under pressure were taken with an ISS PC1 Photon counting Spectrofluorimeter (see Figure 3.3), KOALA model, attached to a HiP

Pressure Generator The lamp is a Perkin-Elmer Compact Xenon Arc Lamp and the slit width is 0.5 mm. There is a 365 (+/-10) nm bandpass filter in front of the excitation monochromator and in place of an emission monochromator, there is a 405 (+/-10) nm bandpass filter. The KOALA sample compartment can handle temperatures from -40 ^{0}C to 60 ^{0}C and a pressure range from 1 to 3000 bar +/- 5 bar. The temperature is controlled by a circulating water/glycol bath with a range of -40 to 60 ^{0}C, and the temperature is measured by a calibrated thermistor in close proximity to the sample cell with an accuracy of 0.01 ^{0}C and a precision of 0.003 ^{0}C. In addition, the instrument is covered by insulating material to further reduce any thermal gradients and variations. Measurements at atmospheric pressure (0.1 MPa) were taken in the ISS 3-position sample compartment, and 600 μL quartz cuvettes were used to hold the samples.

A round quartz cuvette with a plastic cap and a 9 mm outer diameter is used as the sample cell for the pressures above 1 bar. Its height is 32 mm with the plastic cap. The cuvette holds 0.80 mL, but the cap, which holds 0.4 mL, must also be filled to allow for transfer of pressure from the hydrostatic fluid to the sample though the cap.[36] The total sample volume is therefore approximately 1.2 mL. The sample cell is placed into the sample compartment of the pressure cell, which is filled with low fluorescence background, spectroscopic-grade ethanol – the hydrostatic fluid. A manual pump (see Figure 3.4) compresses the fluid and the pressure is manually reset to a constant pressure over the period of the run if it changes due to thermal expansion of the ethanol (250 ppm) as temperature is varied.

Figure 3.3 Schematic of the spectrofluorimeter (courtesy of ISS).

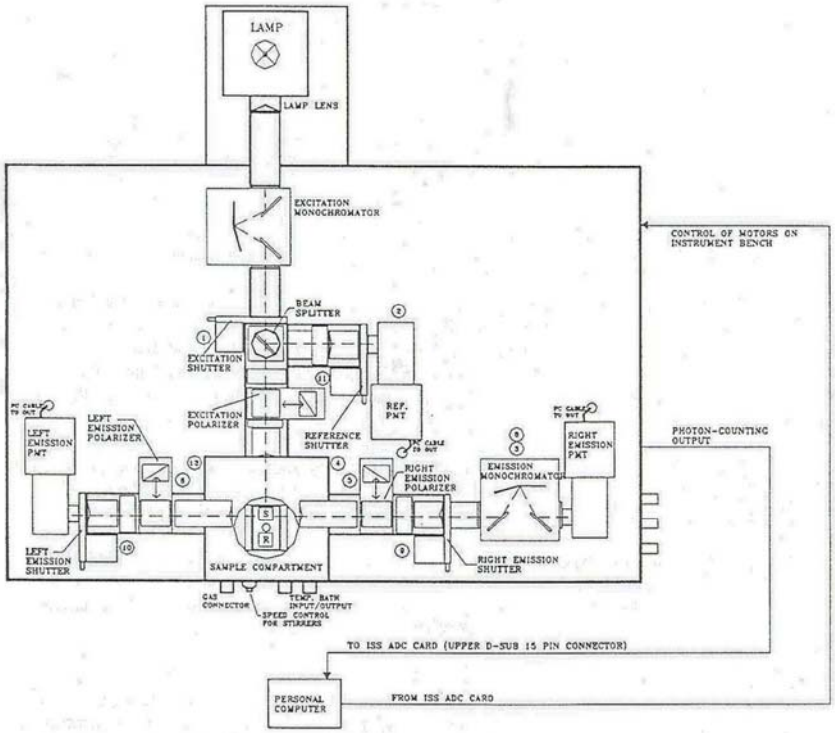

Figure 3.4 Schematic of the manual pressure pump (courtesy of ISS).

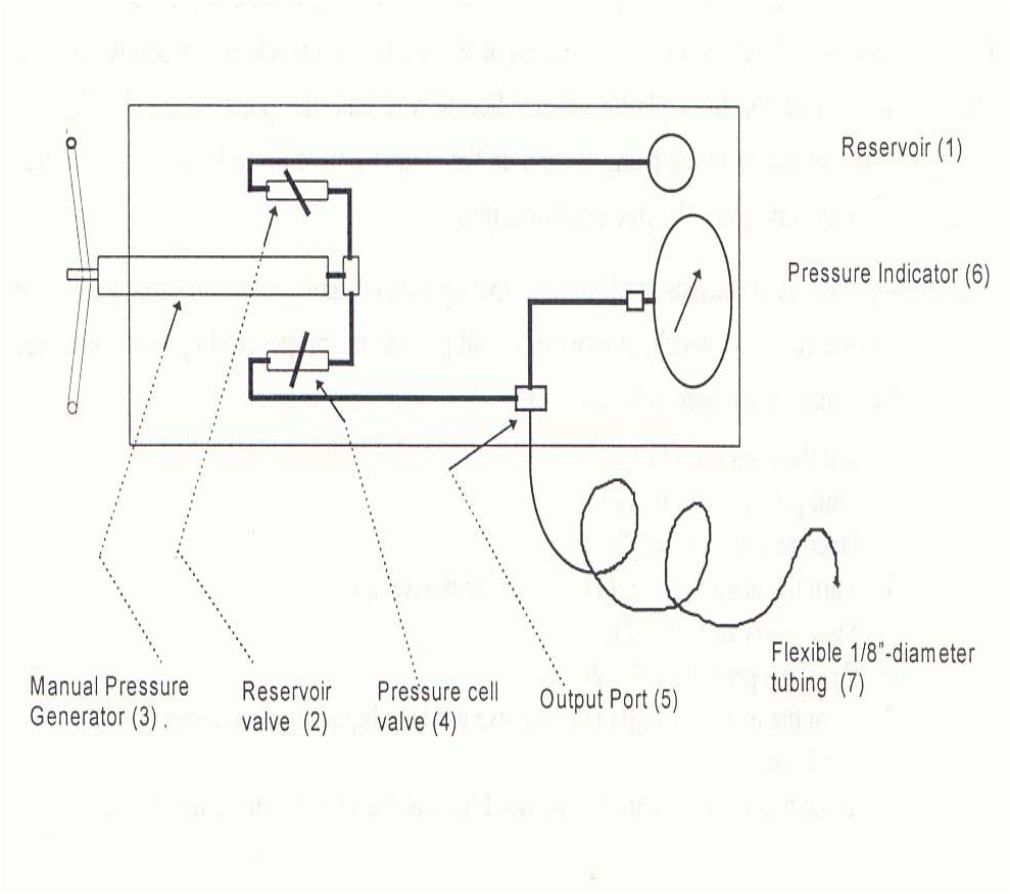

3.3.3 Procedure for Measuring ϕ (T) and Kinetics

After column purification and centrifugation to the desired concentration of G-actin, the actin sample was filtered through the Amicon Ultra centrifugal filter device, a low protein binding membrane with 10,000 MWCO. The pyrene-actin (3% by mass) and KCl to 15 mM were then added. The sample was degassed for a few minutes under vacuum and placed in the sample cuvette, which was then transferred from ice to the pre-chilled pressure cell, for 10 and 20 MPa, or the three-position chamber for atmospheric pressure experiments. The entire system was allowed to equilibrate at 0 ^{0}C for at least three hours. The pump was manually set to the desired pressure. The computer program was set to advance the temperature 3 ^{0}C every hour. The intensity was recorded every 10 seconds within that hour. Since we did not have an emission monochromator, the intensity was measured by placing a 405 +/- 5 nm bandpass filter between the sample and the PMT. After the final temperature, 2 mM of $MgCl_2$ was added to the sample to completely polymerize it. It was then allowed to equilibrate and the signal of maximum polymerization (I_{max}) was measured. The equation that relates the extent, ϕ, to the fluorescence intensity or signal is:

$$\phi = I_{total}/I_{max} \qquad (3.5)$$

where I_{total} is the intensity of all G-actin present in solution, including unbound G-actin which contributes less than 10% of the intensity.[15] For reverse kinetics studies, which were done for the atmospheric pressure experiments, the temperature was manually reversed 3 degrees, and the extent measured as before. A chart detailing the experimental conditions is given as Table 3.2.

Table 3.2 Design of pressure spectrofluorimeter experiments

Sample: G-Actin

$[G_0]$ = 3.0 mg/ml

[KCl] = 15 mM

$[MgCl_2]$ = 15 mM (added at the final temperature)

Solvents: H_2O Buffer A and D_2O Buffer D

Pressure	0.1 Mpa (~1 bar/atm)	10 MPa(~100 bar/atm)	20 MPa (~200 bar/atm)
Temperature range	0 -12 ^{0}C 9 -24 ^{0}C 21 -33 ^{0}C 30 -36 ^{0}C	0- 39 ^{0}C	0-42 ^{0}C
Chamber	three-position	pressure cell	pressure cell
Temperature increment	3^0 every hour	3^0 every hour	3^0 every hour
Total Time (hours)	~20	~14	~15

Chapter 4: Results/Discussion of Actin Polymerization at 0.1 MPa in H_2O Buffer

4.1 Run #1: Solvent = H_2O, P = 0.1 MPa, [Actin] = 3.1 mg/mL

The extent of polymerization was first studied under conditions of atmospheric pressure (~0.1 MPa) in buffer A. This experiment was performed in the three-position chamber as described in the Experimental Methods chapter. The initial concentration of actin monomer was $[G_0]$ = 3.1 mg/mL (Run #1). KCl, used as an initiating salt, was added to the sample at a concentration of [KCl] = 15 mM. The results of the 3.1 mg/mL sample are reported in this section.

4.1.1. Extent of Polymerization Results

The fluorescence intensity was measured at a series of bath temperatures starting at 0 °C, as a function of time for approximately one hour at each temperature. The results from the entire experiment of the equilibrium extent of polymerization as a function of temperature, $\phi(T)$, are presented in Table 4.1 and shown in Figure 4.1, where the various temperature ranges are represented by unique symbols. For the first bath temperature range, from 0 to 12 °C (see Figures 4.2, a and b), measurements were made as the temperature increased in three degree increments. The actual temperatures, which differed slightly from the controlled temperature of the water bath, were measured with a thermocouple, attached near the sample cell and monitored by an electronic datalogger, and were used in all results and analyses. After measurements at 12° were made, the bath temperature was lowered or reversed to 9°, in order to study the behavior due to temperature lowering or reversal (these

results will be presented and discussed in section 4.1.5). Data were taken in the second bath temperature range (see Figure 4.3, a and b) from 9 to 24 °C by increments of three degrees. The third bath temperature range (see Figure 4.4, a and b) was from 21 to 33 °C, and the fourth and final bath temperature range (see Figure 4.5, a and b) was from 30 to 36 °C. The maximum intensity (complete polymerization) was measured at the final bath temperature of 36 °C upon addition of $MgCl_2$ to 15 mM. The intensity values over time divided by the equilibrium value of the maximum intensity yields the extent of polymerization, both ϕ (T) which is the equilibrium value and ϕ (t) at each temperature.

The equilibrium extent of polymerization can also be expressed in terms of the molar fraction of monomers free in solution, X_f, and the free monomer concentration, M_f, both given by the following equation:

$$M_f = M_0 - M_p = M_0 - M_0\phi = M_0 (1-\phi) = M_0X_f, \quad (4.1)$$

where M_p is the concentration of monomers that have been converted to polymers. M_0 is the initial molar actin concentration given by:

$$M_0 \text{ (mole/L)} = [G_0] \text{ (mg/ml) x } 1/43\,000 \text{ g/mol (molar mass of actin)} \quad (4.2)$$

Figure 4.6 shows the equilibrium plot for the entire experiment in terms of ϕ (T), with arrows clearly illustrating the order in which the data were taken. Figure 4.7 shows ϕ ("bound" monomer molar fraction) and X_f (free monomer molar fraction) with temperature. Figure 4.8 is a comparison of the results of ϕ (T) with previous results from a similar experiment.[15] The tables of ϕ (t) can be found in Appendix A. Discussions of these results will be presented in sections 4.1.3.

Table 4.1. Extent of polymerization (ϕ (T)) values as a function of temperature. The "true" temperature was measured by a thermocouple at the sample cell: Solvent = H_2O, $[G]_0$ = 3.1 mg/mL, [KCl] = 15 mM, P = 0.1 MPa.

Bath Temperature (^{0}C)	**"True" Temperature (+/- 0.1 ^{0}C)**	**"True" Temperature (+/- 0.1 K)**	**Extent of Polymerization ϕ (T)**	**Reverse Extent of Polymerization ϕ (T)**
0	3.0	276.2	0.1538 (+/- 0.0001)	
3	5.5	278.7	0.1666 (+/- 0.0004)	
6	8.0	281.2	0.2126 (+/- 0.0014)	
9	10.8	284.0	0.2909 (+/- 0.0016)	0.5524 (+/- 0.0001)
12	13.0	286.2	0.4293 (+/- 0.0062)	0.5835 (+/- 0.0020)
15	15.5	288.7	0.7071 (+/- 0.0049)	
18	18.0	291.2	0.7623 (+/- 0.0028)	
21	20.7	293.9	0.7541 (+/- 0.0068)	0.6829 (+/- 0.0009)
24	23.7	296.9	0.6884 (+/- 0.0012)	0.6200 (+/- 0.0007)
27	26.5	299.7	0.5537 (+/- 0.0010)	
30	29.5	302.7	0.4818 (+/- 0.0009)	0.4069 (+/- 0.0001)
33	31.9	305.1	0.4268 (+/- 0.0009)	0.3604 (+/- 0.0001)
36	34.6	307.4	0.3217 (+/- 0.0006)	

Figure 4.1. Extent of polymerization as a function of "true" temperature: $[G]_0$ = 3.1 mg/mL, [KCl] = 15 mM, P = 0.1 MPa. Symbols represent the various temperature ranges, as discussed in the text.

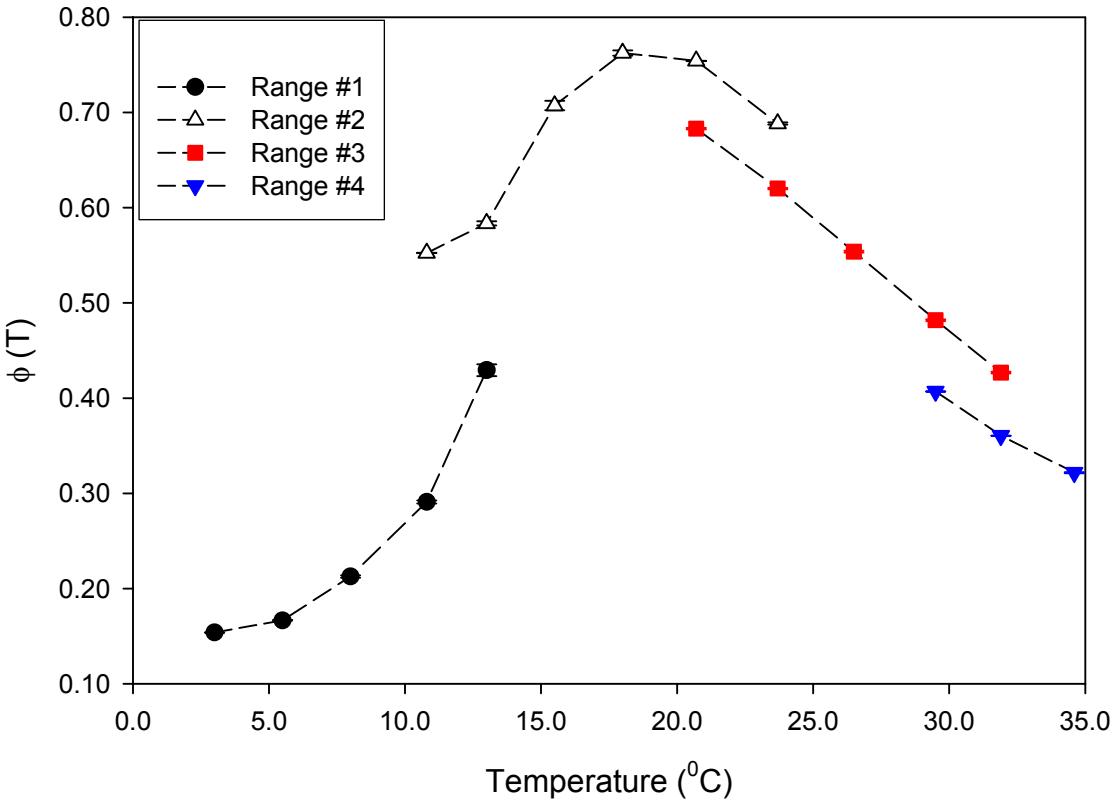

Figure 4.2a. Extent of polymerization as a function of time for temperature range #1: Solvent = H_2O, $[G]_0$ = 3.1 mg/mL, [KCl] = 15 mM, P = 0.1 MPa.

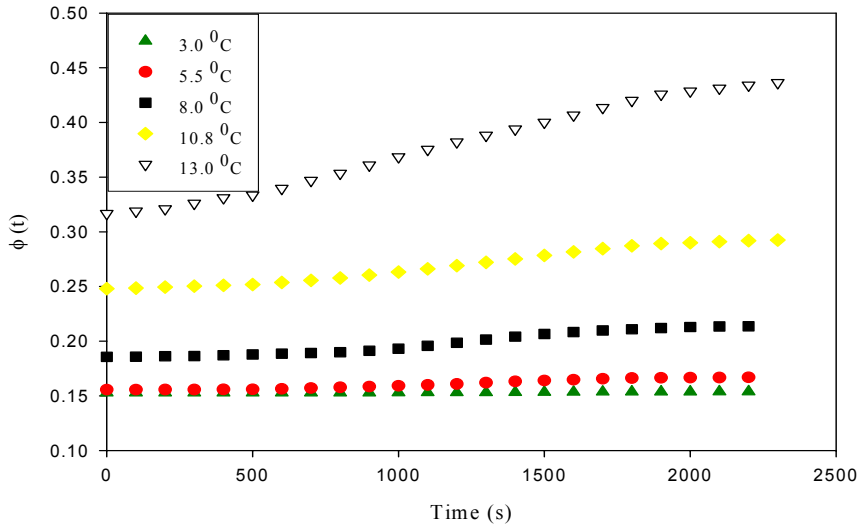

Figure 4.2b. Equilibrium extent of polymerization for temperature range #1: Solvent = H_2O, $[G]_0$ = 3.1 mg/mL, [KCl] = 15 mM, P = 0.1 MPa.

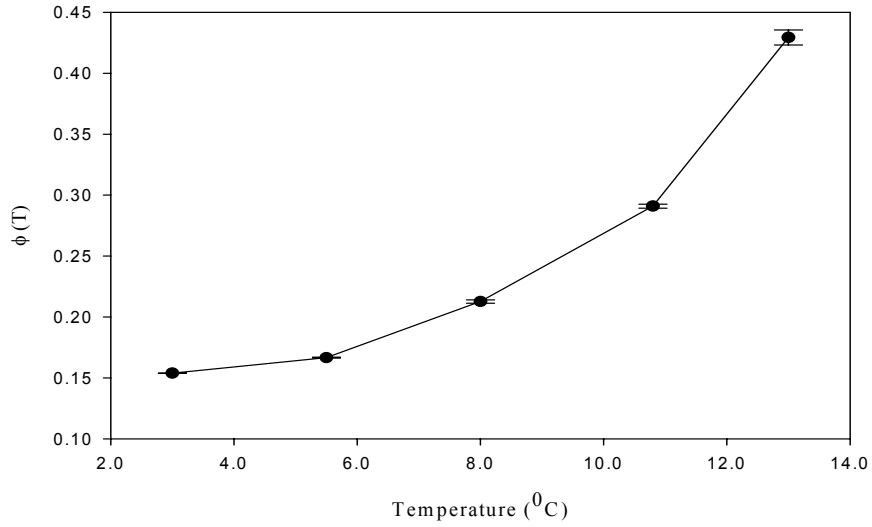

Figure 4.3a. Extent of polymerization as a function of time for temperature range #2: Solvent = H_2O, $[G]_0$ = 3.1 mg/mL, [KCl] = 15 mM, P = 0.1 MPa.

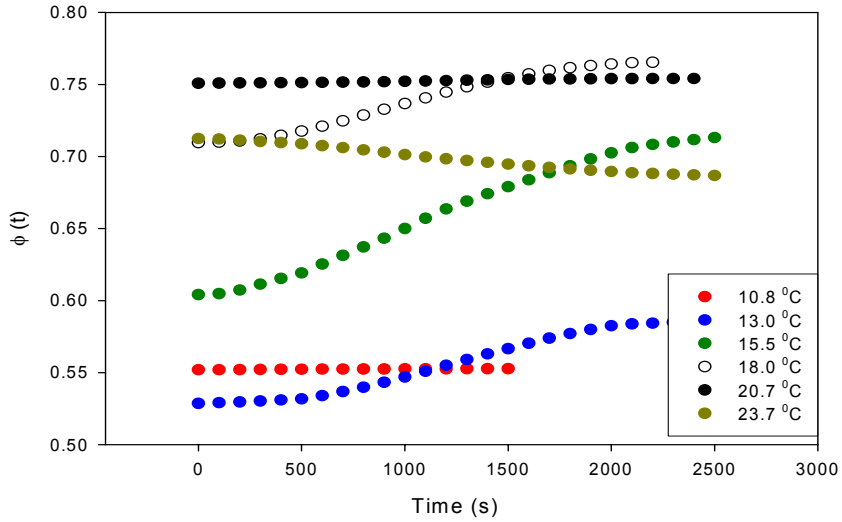

Figure 4.3b. Equilibrium extent of polymerization for temperature range #2: Solvent = H_2O, $[G]_0$ = 3.1 mg/mL, [KCl] = 15 mM, P = 0.1 MPa.

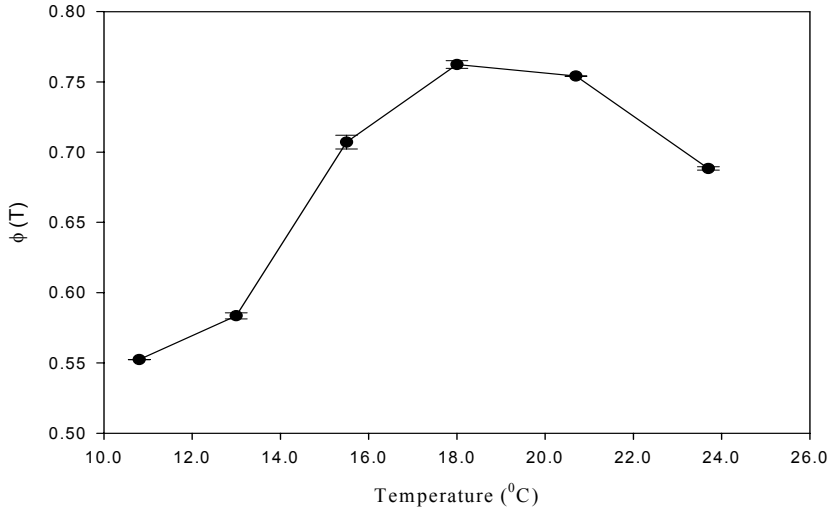

Figure 4.4a. Extent of polymerization as a function of time for temperature range #3: Solvent = H_2O, $[G]_0$ = 3.1 mg/mL, [KCl] = 15 mM, P = 0.1 MPa.

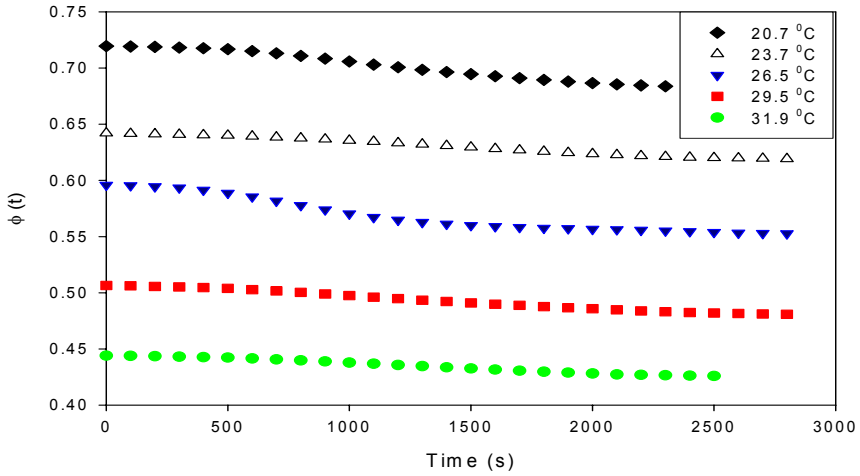

Figure 4.4b. Equilibrium extent of polymerization for temperature range #3: Solvent = H_2O, $[G]_0$ = 3.1 mg/mL, [KCl] = 15 mM, P = 0.1 MPa.

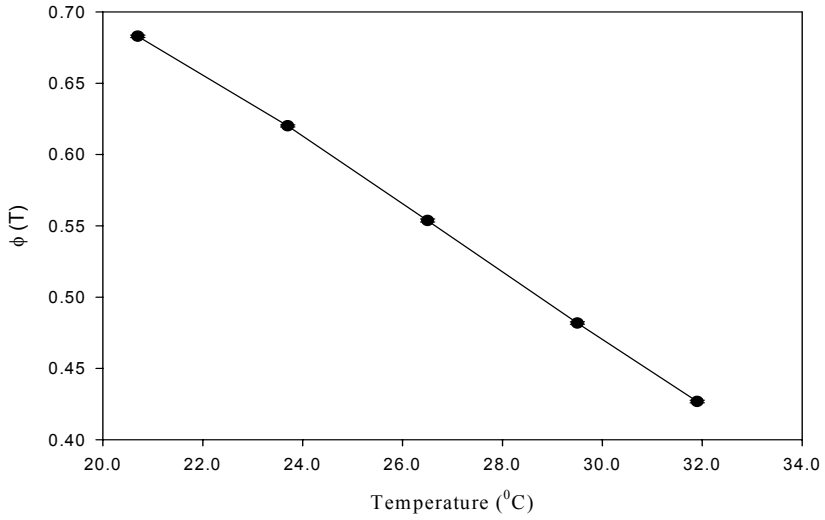

Figure 4.5a. Extent of polymerization as a function of time for temperature range #4: Solvent = H_2O, $[G]_0$ = 3.1 mg/mL, [KCl] = 15 mM, P = 0.1 MPa.

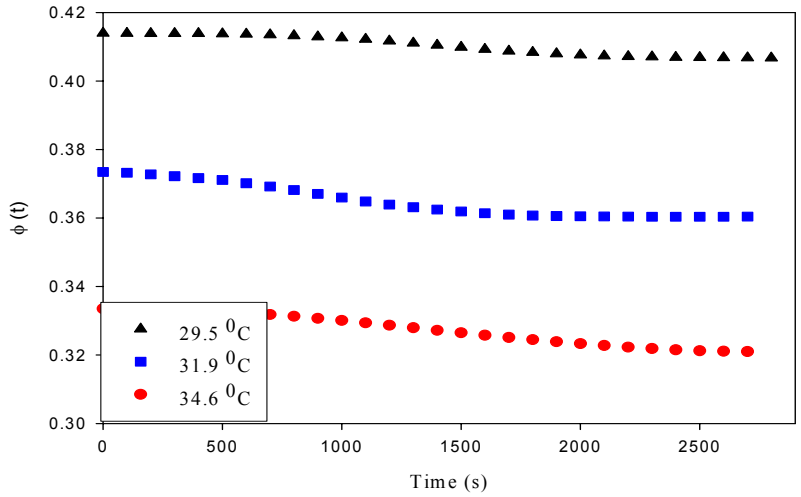

Figure 4.5b. Equilibrium extent of polymerization for temperature range #4: Solvent = H_2O, $[G]_0$ = 3.1 mg/mL, [KCl] = 15 mM, P = 0.1 MPa.

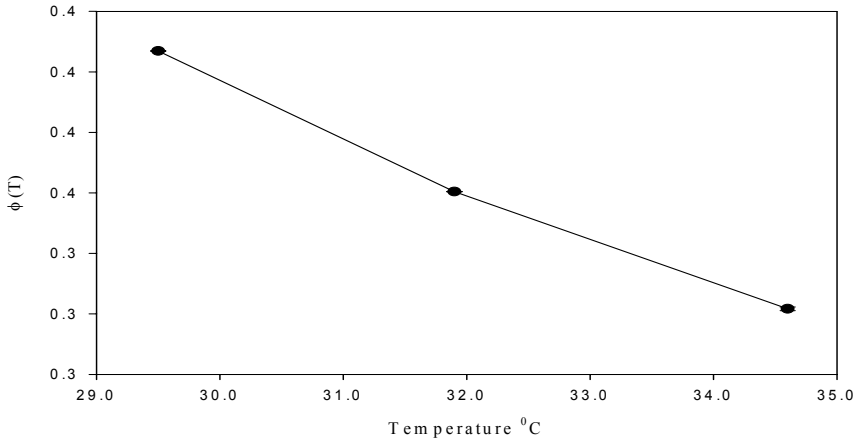

Figure 4.6. Equilibrium extent of polymerization showing points where temperature was reversed. Arrows indicate the order of measurements: Solvent = H_2O, $[G]_0$ = 3.1 mg/mL, [KCl] = 15 mM, P = 0.1 MPa.

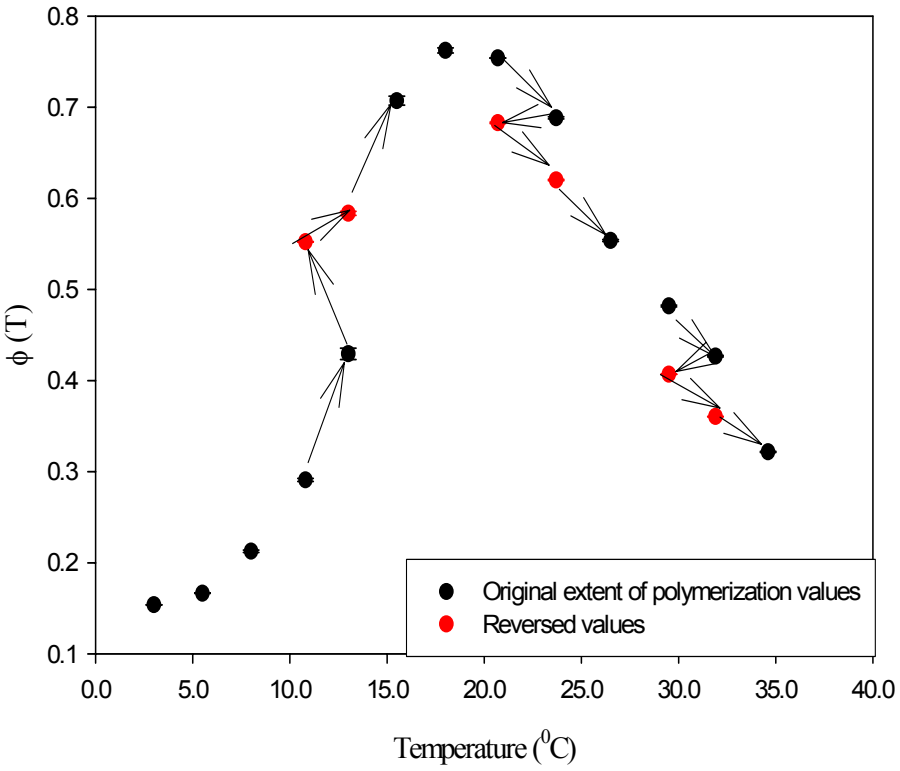

Figure 4.7. Plots of ϕ (T) and X_f (T) – fractions of bound versus free monomers. The intersecting point is T_p, the transition temperature: Solvent = H_2O, $[G]_0$ = 3.1 mg/mL, [KCl] = 15 mM, P = 0.1 MPa.

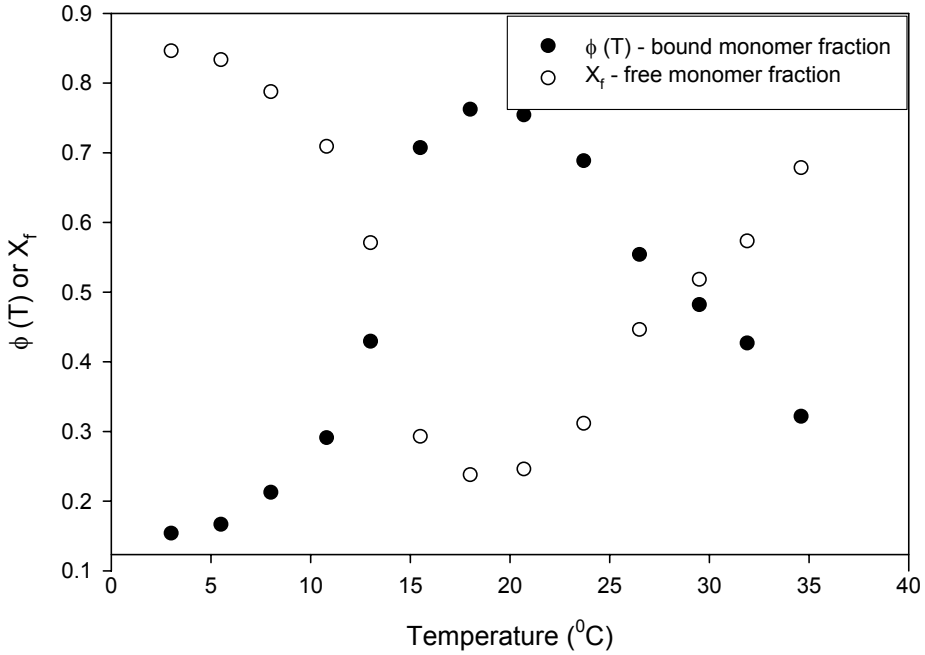

Figure 4.8. Extent of polymerization as a function of temperature: Solvent = H_2O, $[G]_0$ = 3.1 mg/mL, [KCl] = 15 mM, P = 0.1 MPa. Black symbols represent data from the current work. The reverse values have been omitted for clarity. The open (white) symbols are data taken from earlier work: Solvent = H_2O, $[G]_0$ = 2.93 mg/mL, [KCl] = 14.93 mM, P = 0.1 MPa.[18]

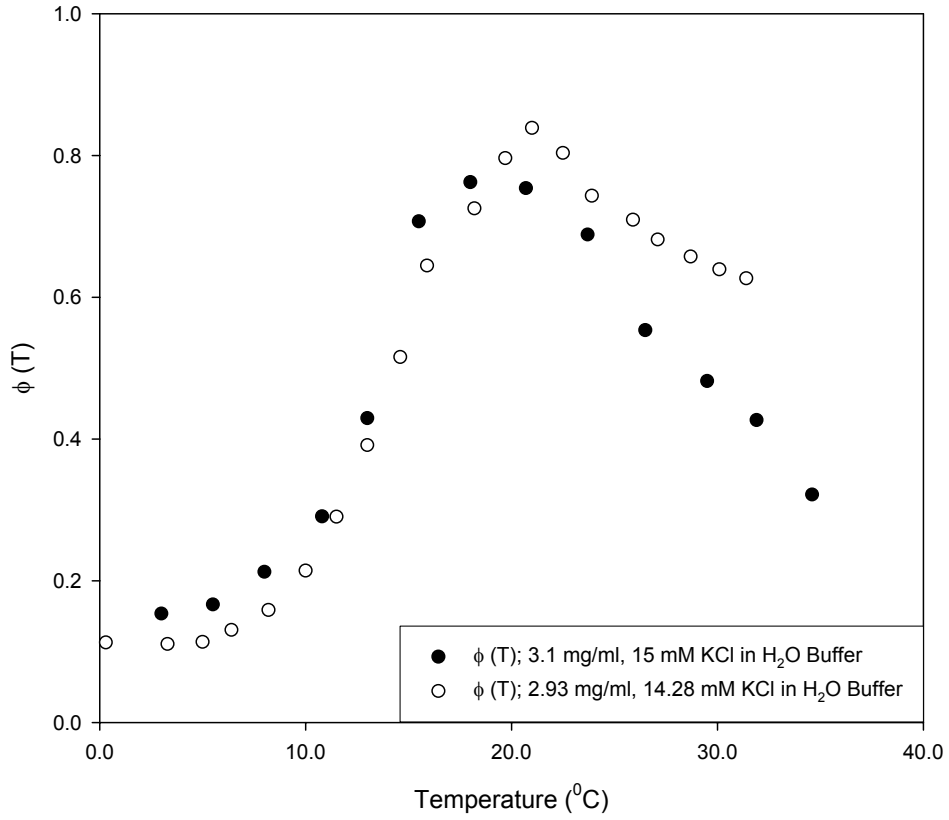

4.1.2 Initial Rates of Polymerization

Despite efforts to insulate the apparatus and to have a small enough yet experimentally discrete temperature change, it was not possible to perform an instantaneous temperature jump. Rather, the temperature bath took approximately one minute to change by three degrees, and the actual temperature near the cell as recorded by the datalogger required approximately 10 minutes to reach a steady value. A plot of temperature with time for the same apparatus, but for a different experiment (3.0 mg/ml actin in D_2O buffer), is shown in Figure 4.9. The vertical line marks the time at which the temperature equilibrated. The transient regions can actually be observed in the kinetics plots (see Figure 4.2 (a) for example) between 0 and 600 seconds. After the transient region in the kinetic plot, the slope in the "reaction" region increases dramatically and stays constant for about fifteen minutes before chemical equilibrium is achieved.

In analyzing the kinetics of polymerization, the data of $M_f(t)$ between 0 and 600 seconds (the transient temperature region) is first truncated and the time is set to t = 0 at the temperature equilibration time. A plot of the equilibrium values of $M_f(T)$ is shown in Figure 4.10. A sample plot of $M_f(t)$ at 8.0 ^{0}C is depicted in Figure 4.11 (see Appendix A for the remaining $M_f(t)$ plots). The slope of the first ten minutes of $M_f(T)$ data is taken as the initial polymerization rate, $r_p = -dM_f/dt$ (see Figure 4.12).

$$r_p = -dM_f/dt \qquad (4.1)$$

The results of r_p at all temperatures are shown in Table 4.2. Figure 4.13 depicts the initial rate as a function of temperature, $r_p(T)$, for the entire experiment. Discussions of these results are presented in sections 4.1.4.

Figure 4.9. Temperature near the cell in the three-position chamber as a function for time for T = 18 ^{0}C: P = 0.1 MPa, 3.0 mg/mL in D_2O Buffer. The vertical line indicates the point beyond which the temperature is fairly constant.

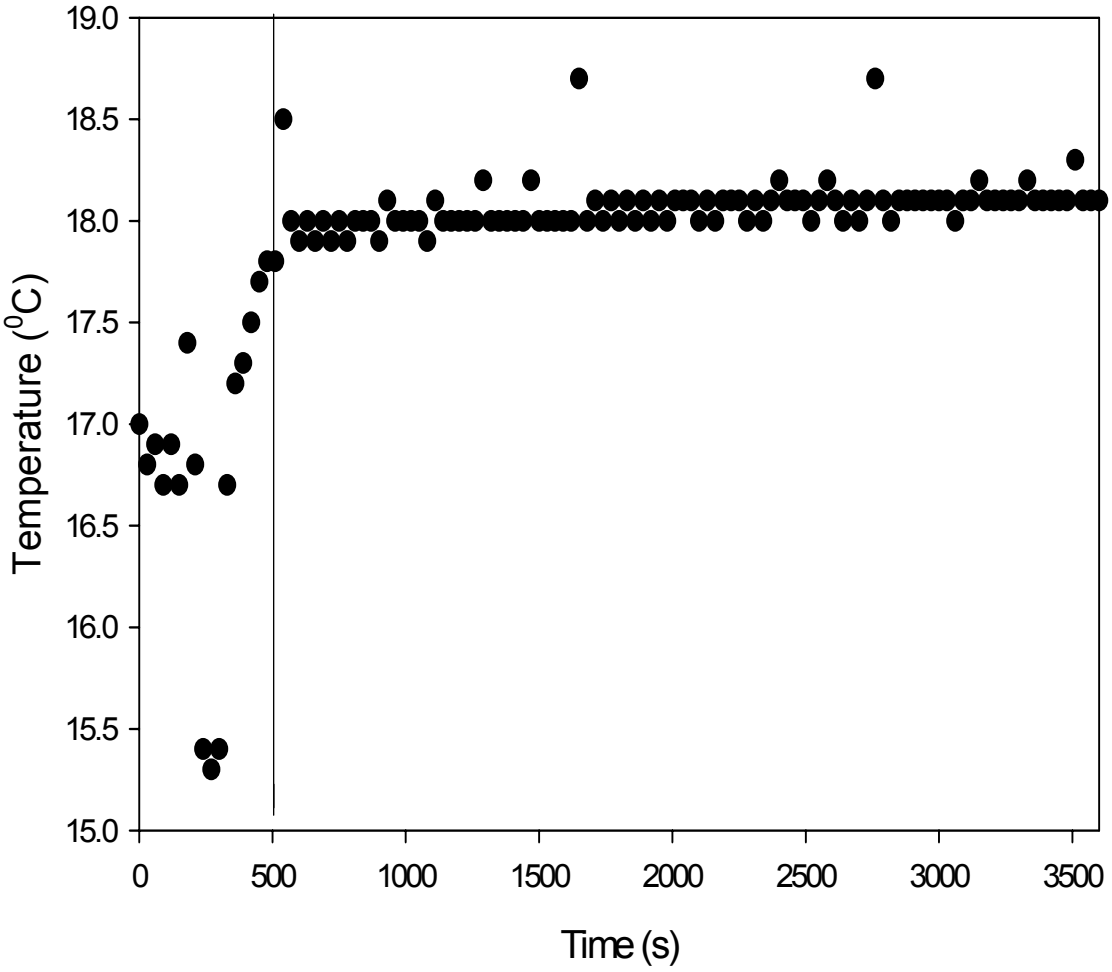

Figure 4.10. Equilibrium free monomer concentration, M_f, as a function of temperature: Solvent = H_2O, $[G]_0$ = 3.1 mg/mL, [KCl] = 15 mM, P = 0.1 MPa. Symbols represent the various temperature ranges.

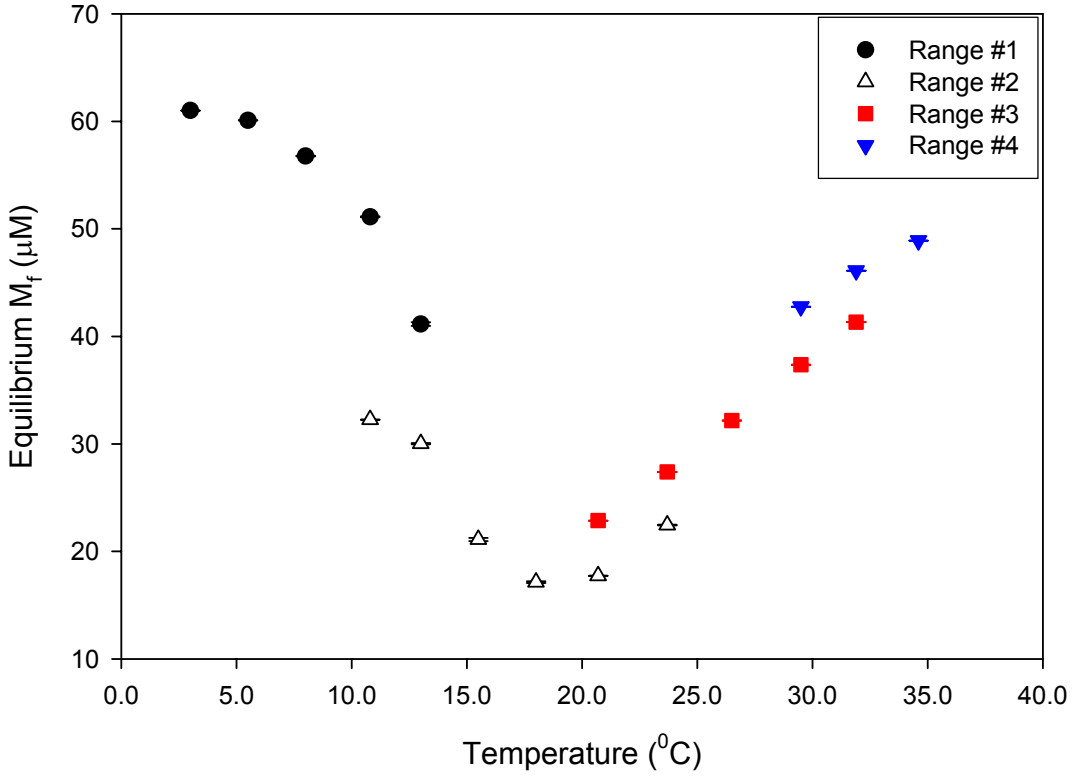

Figure 4.11. Free monomer concentration as a function of time for T = 8.0 ^{0}C: Solvent = H_2O, $[G]_0$ = 3.1 mg/mL, [KCl] = 15 mM, P = 0.1 MPa.

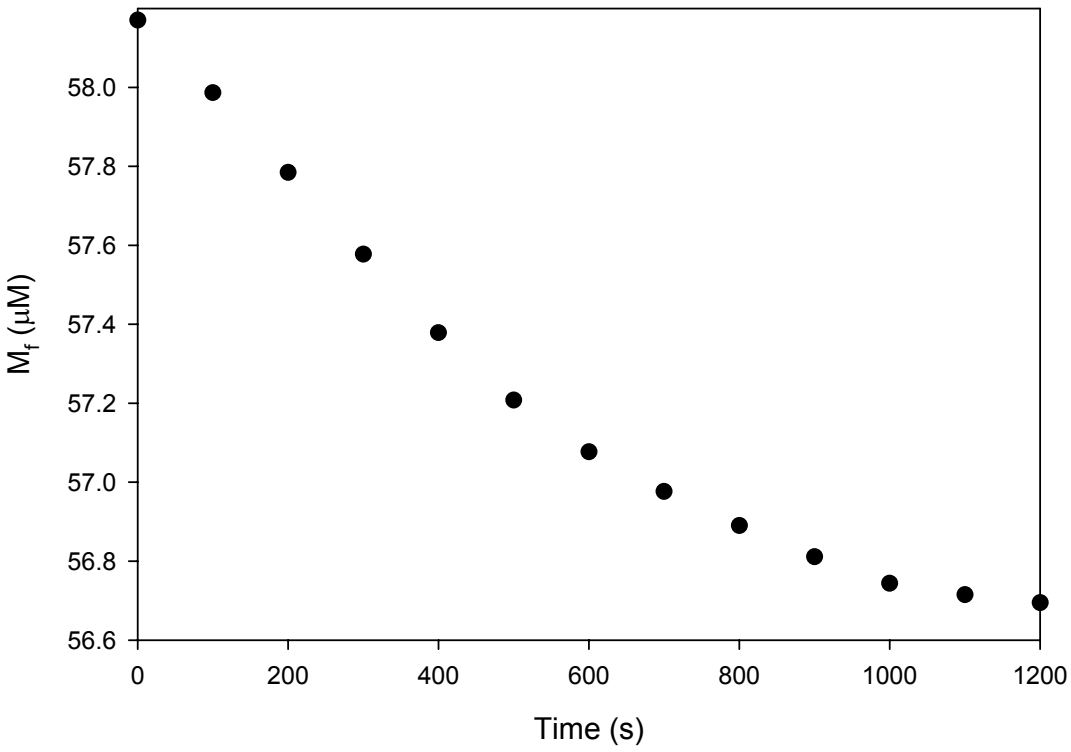

Figure 4.12. Free monomer concentration as a function of time for 10.8 ^{0}C. A linear fit is applied to the data within the ten minute period following the transient temperature region: Solvent = H_2O, $[G]_0$ = 3.1 mg/mL, [KCl] = 15 mM, P = 0.1 MPa.

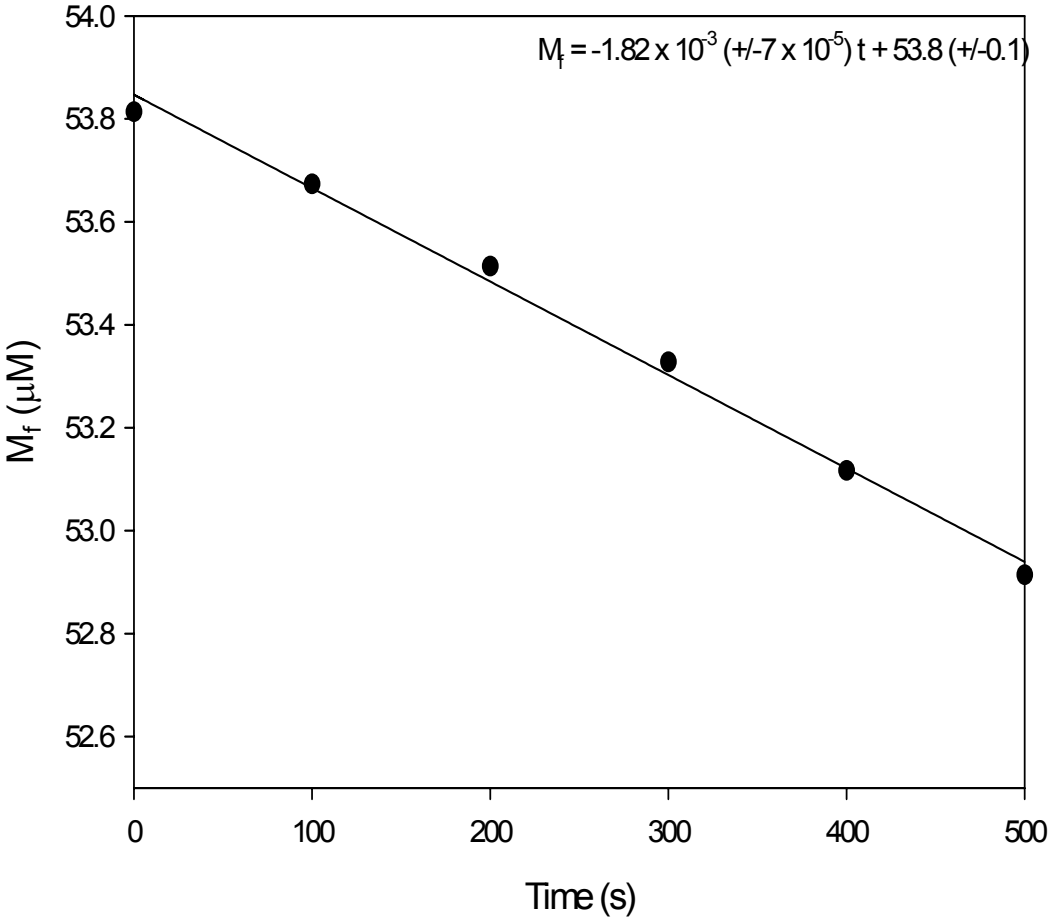

Table 4.2. Initial rate ($\mu M\ s^{-1}$) of polymerization as a function of temperature. The "true" temperature was measured by a thermocouple at the sample cell: Solvent = H_2O, $[G]_0$ = 3.1 mg/mL, [KCl] = 15 mM, P = 0.1 MPa.

Bath Temperature (^0C)	**"True" Temperature (+/- 0.1 ^0C)**	**Initial Rate, r_p ($\mu M\ s^{-1}$)**	**Reverse Initial Rate, r_p ($\mu M\ s^{-1}$)**
0	3.0	7.35×10^{-5} (+/-1.2×10^{-6})	
3	5.5	5.06×10^{-4} (+/-7×10^{-6})	
6	8.0	1.87×10^{-3} (+/-5×10^{-5})	
9	10.8	1.82×10^{-3} (+/-7×10^{-5})	5.70×10^{-5} (+/-3.1×10^{-6})
12	13.0	5.16×10^{-3} (+/-5×10^{-5})	2.64×10^{-3} (+/-8×10^{-5})
15	15.5	4.54×10^{-3} (+/-9×10^{-5})	
18	18.0	2.77×10^{-3} (+/-4×10^{-5})	
21	20.7	1.29×10^{-4} (+/-8×10^{-6})	-1.81×10^{-3} (+/-3×10^{-5})
24	23.7	-1.13×10^{-3} (+/-1×10^{-5})	-6.89×10^{-4} (+/-1.7×10^{-5})
27	26.5	-2.70×10^{-3} (+/-3×10^{-5})	
30	29.5	-9.74×10^{-4} (+/-1.8×10^{-5})	-2.22×10^{-4} (+/-1.3×10^{-5})
33	31.9	-6.84×10^{-4} (+/-1.5×10^{-5})	-7.69×10^{-4} (+/-1.0×10^{-5})
36	34.6	-4.17×10^{-4} (+/-1.5×10^{-5})	

Figure 4.13. Initial polymerization rate, r_p, as a function of temperature for each temperature range: Solvent = H_2O, $[G]_0$ = 3.1 mg/mL, [KCl] = 15 mM, P = 0.1 MPa.

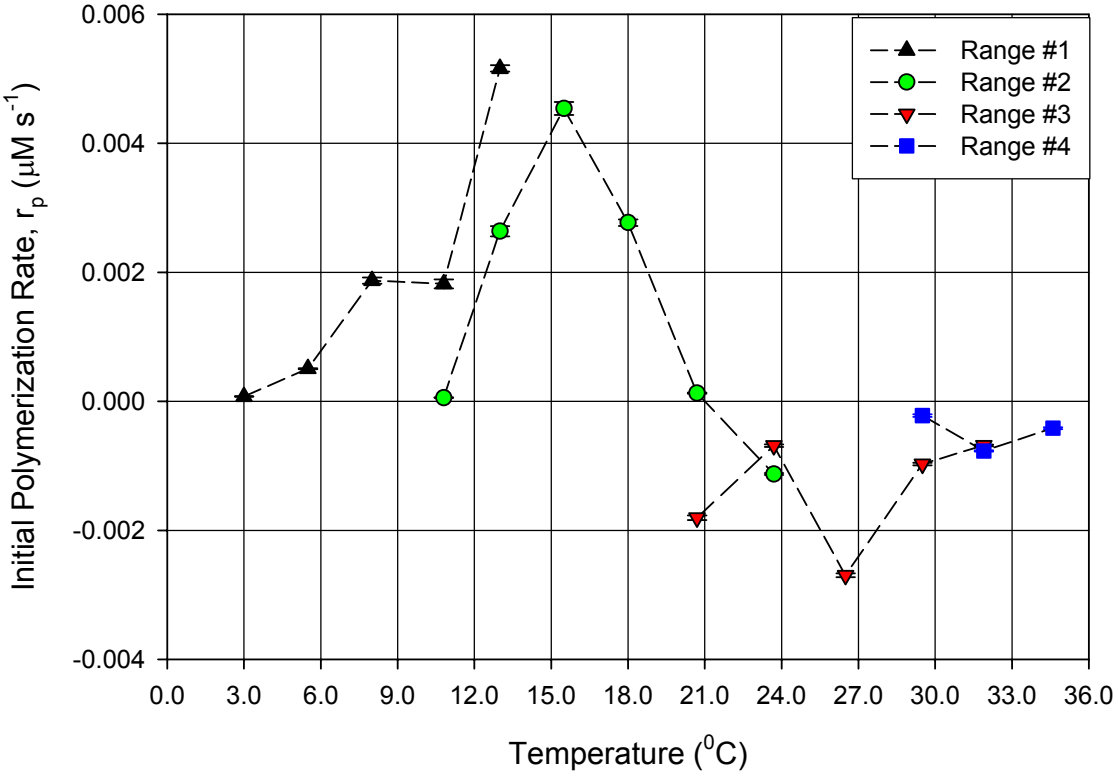

4.1.3 Discussion - Thermodynamics

The thermodynamic (extent of polymerization) data submitted in this chapter were collected at conditions that mimic the conditions of a previous experiment performed at 2.93 mg/mL, atmospheric pressure (0.1 MPa) and 14.93 mM KCl.[15] (see Figure 4.8) The experiment was repeated here because 1) the instrumental conditions are different, 2) the larger volume and accuracy of the data produced in the current study are more amenable to kinetic analysis, and 3) it is useful to confirm the validity of the previous results with a different source of rabbit muscle.

The mechanism of fluorescence enhancement due to monomer-monomer binding is suitable for tracking the polymerization process because a fluorescence intensity increase can only be attributed to dimerization and/or propagation due to a conformational change upon binding. The plots clearly indicate a sharp increase in fluorescence intensity, which is directly proportional to the extent of polymerization in the region around 13 ^{0}C (see Figure 4.8). The extent of polymerization, ϕ, is an ideal parameter to measure this critical "floor" temperature because it is a property, like the equilibrium constant, that depends only on thermodynamic variables such as temperature, as in this case, or pressure. The transition "floor" temperature, T_p, is defined as the inflection point in this sharp region.[17] At this point, the second derivative of ϕ (T) becomes zero. The thermodynamic theories that predict and explain much of the observations of the extent of polymerization of actin are effectively summarized in the work of Niranjan et al.[16]

The results of this study are in excellent agreement with the results of Niranjan et al. as shown in Figure 4.8, even with the appearance of a maximum in the

extent of polymerization at a temperature defined as T_{max}. A summary comparing the experimental conditions and the critical parameters are shown in Table 4.3. The effect of the temperature reversals on the thermodynamics and kinetics will be discussed in section 4.1.5.

Table 4.3. Comparison of results from current and prior work on actin polymerization in buffer A: 3 mg/mL, 15 mM KCl, and 0.1 MPa. Errors on T and ϕ are rough estimates based on visual extrapolation of the data in Figure 4.8.

Conditions/Parameters	**Current Work**		**Prior Work**[15]	
$[G]_0$	3.01 (+/-0.01) mg/mL		2.93 (+/-0.01) mg/mL	
[KCl]	15.0 (+/- 0.1) mM		14.28 (+/- 0.01) mM	
T_p, ϕ_p	13 (+/-1) ^{0}C	0.41 (+/-0.02)	13 (+/-1) ^{0}C	0.42 (+/-0.02)
T_{max}, ϕ_{max}	21 (+/-1) ^{0}C	0.76 (+/-0.02)	22 (+/-1) ^{0}C	0.83 (+/-0.02)

Other studies have also noted the existence of this critical "floor" temperature.[37] The results obtained in the current work lend credence to the theory predicted by Oosawa and Kasai[9] as well as the theory that suggests that biological self-assemblies are entropy-driven reactions.[38]

There seems to be evidence of a transition around 5 ^{0}C, where there is an abrupt change in the slope of the curve. This point is referred to in the theory[17] as T_x, the onset of polymerization. This defines the rough region about which propagation becomes favorable, whereas T_p, the inflection point, defines the thermodynamically

unique point that is analogous to a second order phase transition. Below T_x, the nonzero extent of polymerization is thought to be due to dimerization/nucleation,[18] since dimerization is universally spontaneous in this system $\Delta G < 0$ for every T).[37]

The nature of T_{max} is of considerable interest since it had not been observed for actin polymerization prior to Niranjan et al. and is now confirmed by the current work. While it may be a concern that protein denatures at higher temperatures, it is known that F-actin is more robust than G-actin and stable against thermal degradation up to about 60 ^{0}C since the T_m of G-actin (the melting or denaturation temperature) is 60.5 ^{0}C.[39,40] A visual inspection of the sample after the experiment revealed a viscous homogeneous gel, whereas denaturation should be indicated by a dilute solution of precipitates. Beyond T_{max}, near 27 ^{0}C (see Figure 4.8), there is also indication of a second inflection point, hereafter referred to as T_{p2}. This point would be analogous to a "ceiling" temperature for the propagation reaction. Arguments for the meaning of T_{max} and T_{p2} are presented below.

Dudowicz et al.[17] have proposed that the peak in $\phi(T)$ depolymerization for actin is due to a competition between activation of monomers and propagation, this due to activation also being entropically driven and having a floor temperature in the vicinity of the floor temperature for propagation. The depolymerization of F-actin would then serve to make the monomers available for activation. Another theory that describes the nature of double critical points[41] suggests that the dependence of H-bonding and hydrophobic bonding on temperature is an essential factor in the formation of a closed loop phase diagram. At lower temperatures, water molecules both occupy the cleft of the actin monomer and rearrange around the partially

hydrophobic actin to solubilize the monomer. Above the floor temperature, however, thermal disruption of the hydrogen bonds exposes the hydrophobic surfaces of the protein causing them to aggregate. Beyond an even higher temperature, the ceiling temperature, entropy favors a homogenous mixture of water and actin, and the water-monomer complex is re-formed.

In this section, experimental results have confirmed that actin polymerizes above a "floor" temperature T_p and that it reaches a maximum at a temperature T_{max}, beyond which depolymerization is evidenced. The apparent existence of a "ceiling" temperature, T_{p2}, suggests a temperature above which actin will not polymerize (see Figure 4.14). The existence and location of this second transition temperature, T_{p2}, is queried in the experiments in chapter 5 as a function of D_2O based buffer and in chapter 6 as a function of pressure.

Figure 4.14. Schematic phase diagram of the results of the actin polymerization experiment reported in this chapter: $[G]_0$ = 3.1 mg/mL, [KCl] = 15 mM, P = 0.1 MPa.

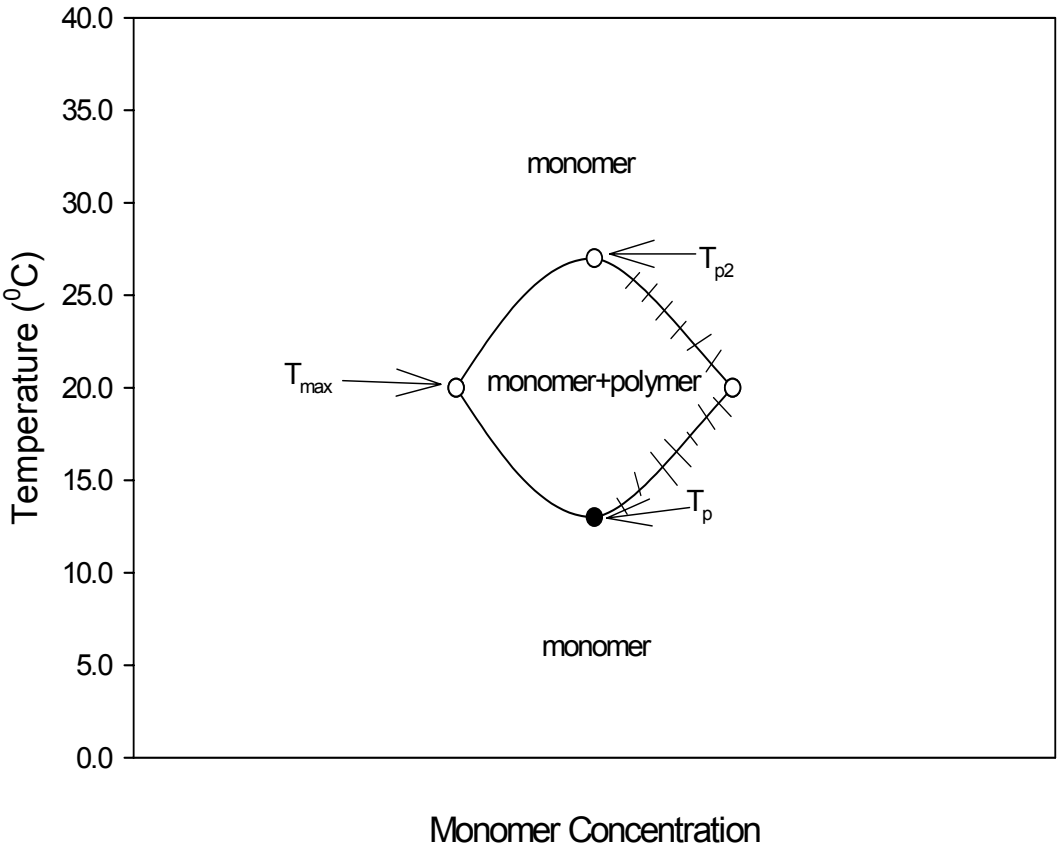

4.1.4 Discussion - Kinetics

The general form of the propagation step in actin polymerization and the corresponding equilibrium constant previously presented in chapter two are reproduced below.

$$A_n^* + A_1 \Leftrightarrow A_{n+1}^* \quad 4.4$$

$$K_{prop} = [A_{n+1}^*]/ [A_n^*] [A_1] = k_f/k_r \quad 4.5$$

$$\text{Rate of propagation} = -k_f[A_n^*] [A_1] \quad 4.6$$

As previously discussed in chapter two, A_n^* and A_{n+1}^* are polydisperse and the concentrations are unknown, so it is difficult and beyond the scope of these experiments to calculate an exact value for k_f or k_r independently. Consideration must also be made for the observed annealing and fragmentation of F-actin filaments.[42]

The approximation made in section 4.1.2 for r_p, the initial polymerization rate, taken at the steepest slope of $M_f(T)$, describes the fastest overall rate difference of the forward reaction and the reverse reaction of all species in solution – i.e. activated monomers, dimers, trimers, and the oligomers population having an exponential size distribution.[12] A plot of Figure 4.13 without the reversal points is reproduced as Figure 4.17. Figures 4.18 – 4.20 show the three regions separated by the two critical points, T_p and T_{p2}.

Figure 4.15. Initial polymerization rate, r_p, and ϕ as a function of temperature excluding the reverse points: $[G]_0$ = 3.1 mg/mL, [KCl] = 15 mM, P = 0.1 MPa.

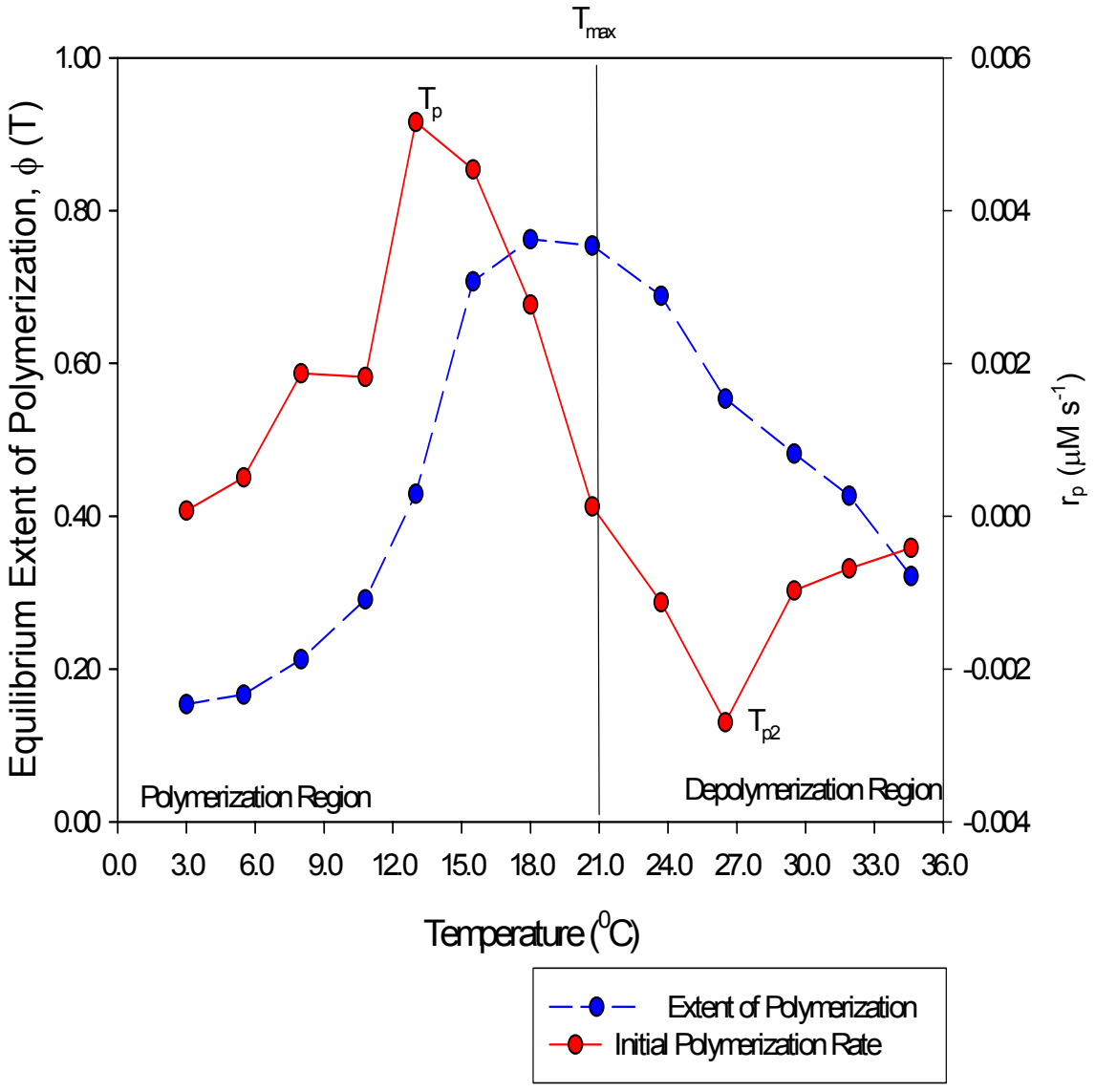

Figure 4.16. Initial rate of polymerization r_p (T) in the first region up to T_p: $[G]_0$ = 3.1 mg/mL, [KCl] = 15 mM, P = 0.1 MPa.

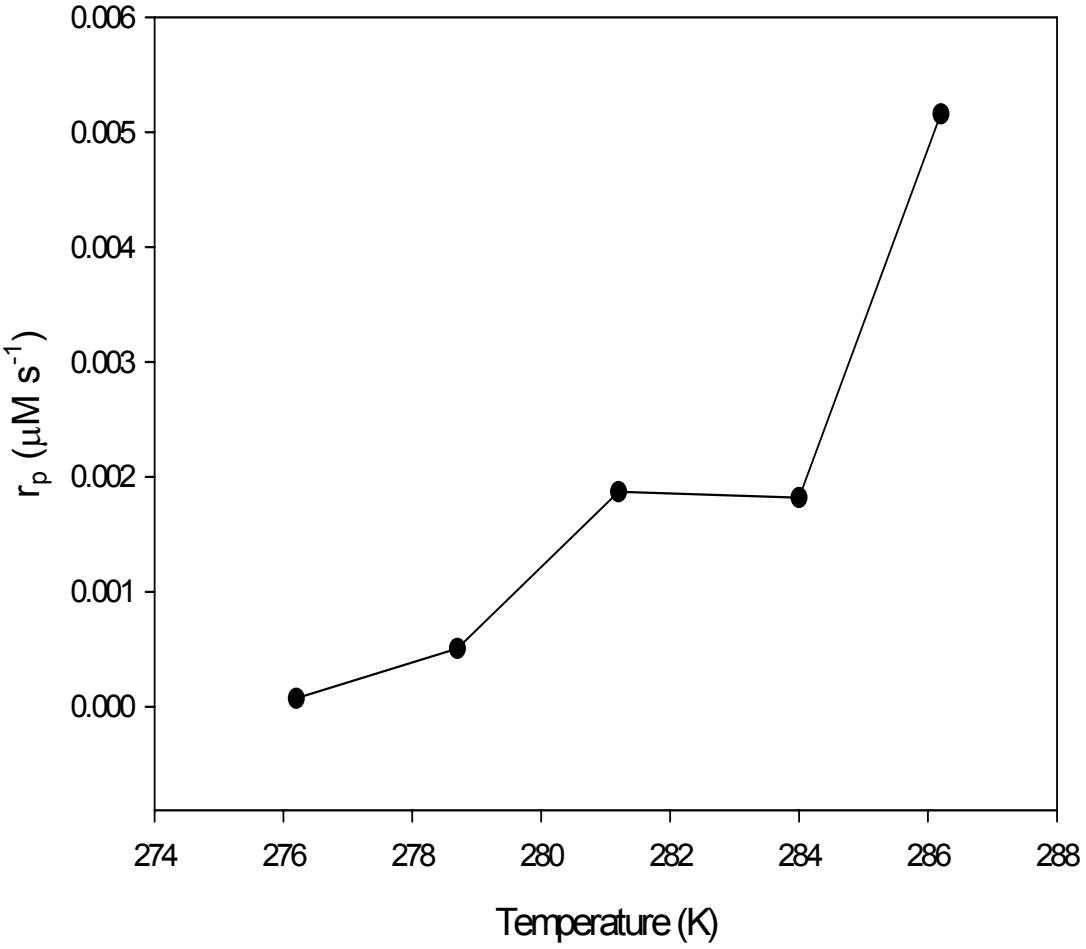

Figure 4.17. Initial rate of polymerization r_p (T) in the region from T_p to T_{p2}: $[G]_0$ = 3.1 mg/mL, [KCl] = 15 mM, P = 0.1 MPa.

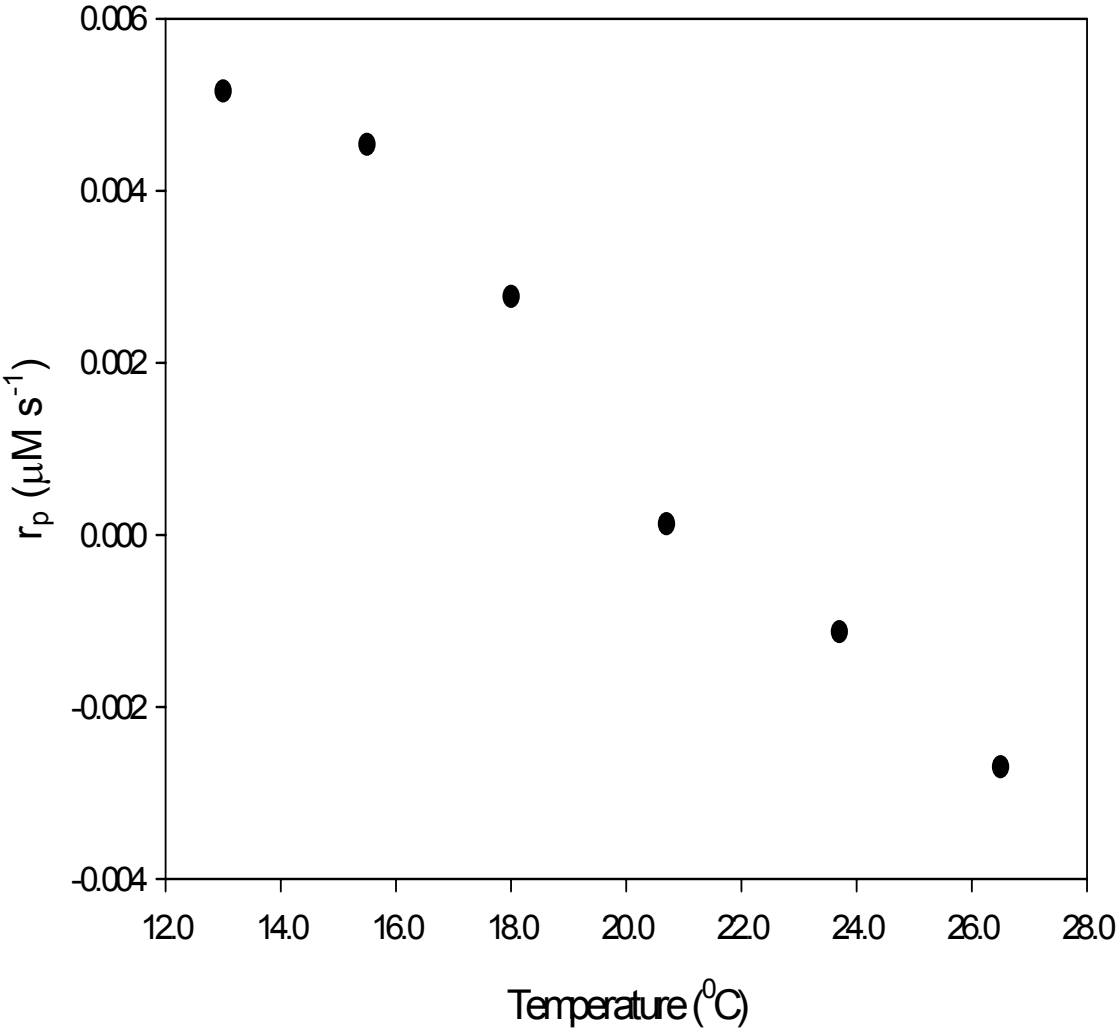

Figure 4.18. Initial rate of polymerization r_p (T) in the region from T_{p2} to the final temperature: $[G]_0$ = 3.1 mg/mL, [KCl] = 15 mM, P = 0.1 MPa.

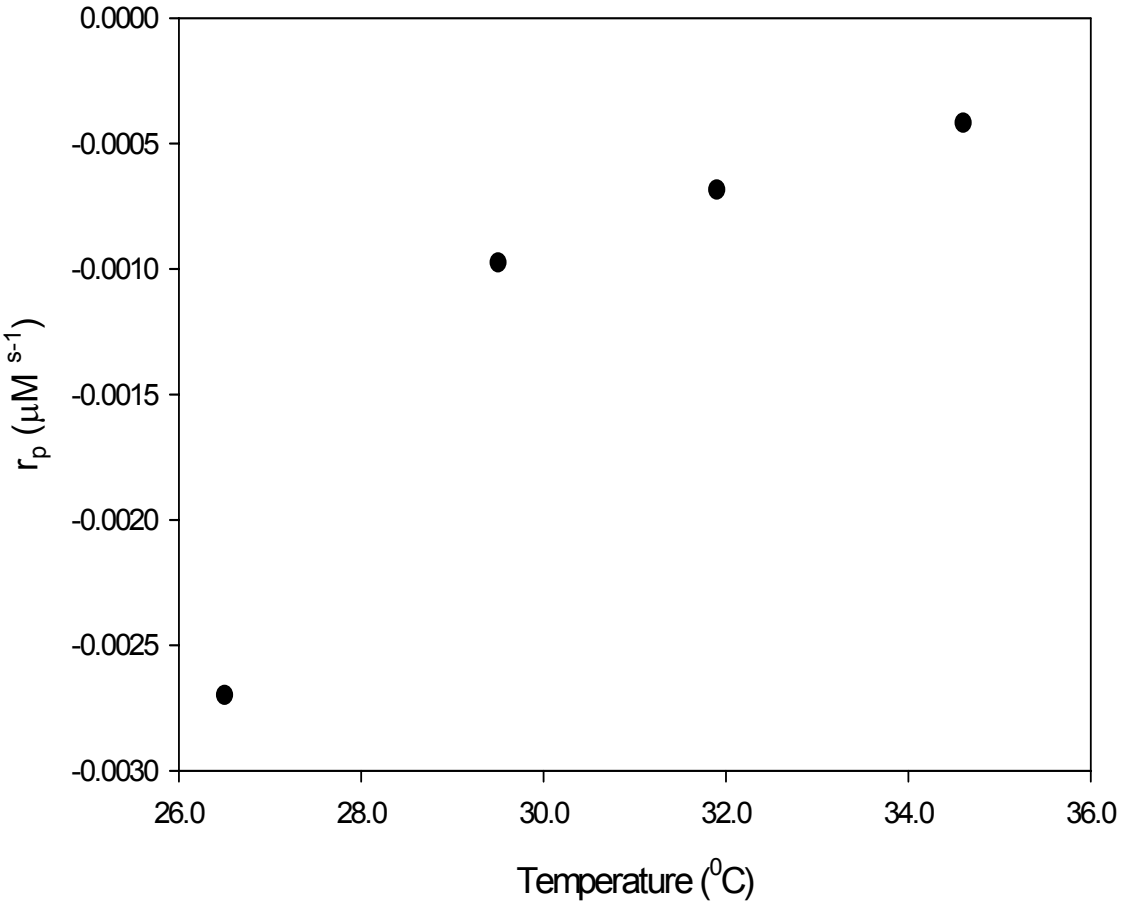

The results of these initial rate calculations also show a remarkable relationship to the extent of polymerization plot. At or very near both inflection points in the ϕ (T) plot, the plot of r_p (T) exhibits an extremum. Moreover, at or very near T_{max}, the initial rate approaches zero. As propagation sets in around 5 ^{0}C, the initial rate begins to increase rapidly and reaches a maximum at T_p (Figure 4.18). It is reasonable to expect an increase in the net polymerization rate with temperature as you approach T_p because more nucleated species are present and filaments are being formed as the temperature increases, making propagation much more favorable. At and above T_p, however, the initial rate decreases and approaches zero as T approaches T_{max}. It has been observed that the transport properties (i.e. viscosity) of a system drastically change above the phase transition. Although the viscosity of actin has not been studied near T_p, it has been experimentally shown that the viscosity of sulfur, which like actin, also has a floor temperature, dramatically increases above T_p.[43,44] Since actin propagation is a diffusion-limited reaction,[11] and diffusion is inversely proportional to viscosity, it may be that r_p is impeded by the drastic increase of viscosity. The rate likely begins to decrease above T_p as the viscosity increases and approaches zero near T_{max}, because the reverse reaction begins to occur and the net rate of polymerization becomes zero. Above T_{max}, depolymerization begins to set in so the viscosity begins to decrease. Going backwards from T_{p2} to T_{max} is analogous to going from T_p to T_{max} (see symmetry in Figure 4.19). Since T_{p2} is also defined as a phase transition temperature, the rate of depolymerization decreases and approaches zero upon re-entrance into the one-phase region (Figure 4.20). These arguments are supported by the initial rate plot and provide additional support to the existence of

T_{p2}, the ceiling temperature. We can therefore surmise that the transport properties of the monomer+polymer region control to a large degree the kinetics of actin polymerization.

4.1.5 Effect of Temperature Reversal

The impetus for reversing the temperature and repeating the extent of polymerization measurements came from a model designed to elucidate the effects of "thermal cycling" on the dynamics of "living" or reversible polymerization. Reversible polymers are reported to be ultrasensitive; that is, the length distribution is highly responsive to external changes such as temperature or pressure,[22] even exhibiting non-linear responses to linear perturbations. The goal was to understand how sensitive actin polymerization is to positive and negative temperature jumps in relation to both its thermodynamics and its kinetics.

In these experiments, the temperature was reversed in three regions: near T_p, T_{max}, and T_{p2}. These chosen points were a repeat of the points used for the experiment in chapter four. The effect of temperature reversals on $\phi(T)$ is shown in Figure 4.19. A comparison of ϕ (t) for each temperature at which reversals were performed are shown in Figures 4.20-4.25, and the effect of the reversals on the initial polymerization rate is shown in Figure 4.26. Table 4.4 below summarizes the results of the responses to the temperature reversals. In the discussion following, the temperature values are referenced by the "true" temperature followed by the letter A for original value or B for reverse or repeated value.

Table 4.4. Values of ϕ (T) and r_p (T) at points that were repeated and the percent deviation (% Dev.) from the original values. The letter following the temperatures correspond to A (original value) and B (repeated or reversed value): $[G]_0$ = 3.1 mg/mL, [KCl] = 15 mM, P = 0.1 MPa.

Bath Temperature (^{0}C)	**"True" Temperature (+/- 1 ^{0}C)**	**ϕ (T)**	**r_p (T)**	**% Dev. - ϕ (T)**	**% Dev. -r_p(T)**
9A	10.8A	0.291 (+/- 2 x 10^{-3})	1.82 x 10^{-3} (+/-1 x 10^{-5})	90%	97%
9B	10.8B	0.552 (+/- 1 x 10^{-3})	5.70 x 10^{-5} (+/-1 x 10^{-7})		
12A	13.0A	0.429 (+/- 6 x 10^{-3})	5.16 x 10^{-3} (+/-1 x 10^{-5})	36%	50%
12B	13.0B	0.584 (+/- 2 x 10^{-3})	2.64 x 10^{-3} (+/-1 x 10^{-3})		
21A	20.7A	0.754 (+/- 7 x 10^{-3})	1.29 x 10^{-4} (+/-1 x 10^{-6})	9%	1300%
21B	20.7B	0.683 (+/- 1 x 10^{-3})	-1.81 x 10^{-3} (+/-1 x 10^{-5})		
24A	23.7A	0.688 (+/- 1 x 10^{-3})	-1.13 x 10^{-3} (+/-1 x 10^{-5})	10%	39%
24B	23.7B	0.620 (+/- 1 x 10^{-3})	-6.89 x 10^{-4} (+/-1 x 10^{-6})		
30A	29.5A	0.482 (+/- 1 x 10^{-3})	-9.74 x 10^{-4} (+/-1 x 10^{-6})	16%	77%
30B	29.5B	0.407 (+/- 1 x 10^{-3})	-2.22 x 10^{-4} (+/-1 x 10^{-6})		
33A	31.9A	0.427 (+/- 1 x 10^{-3})	-6.84 x 10^{-4} (+/-1 x 10^{-6})	16%	12%
33B	31.9B	0.360 (+/- 1 x 10^{-3})	-7.69 x 10^{-4} (+/-1 x 10^{-6})		

Figure 4.19. Equilibrium extent of polymerization values, ϕ (T), for points where the temperature was reversed and repeated. The arrows indicate the order of measurements: $[G]_0$ = 3.1 mg/mL, [KCl] = 15 mM, P = 0.1 MPa.

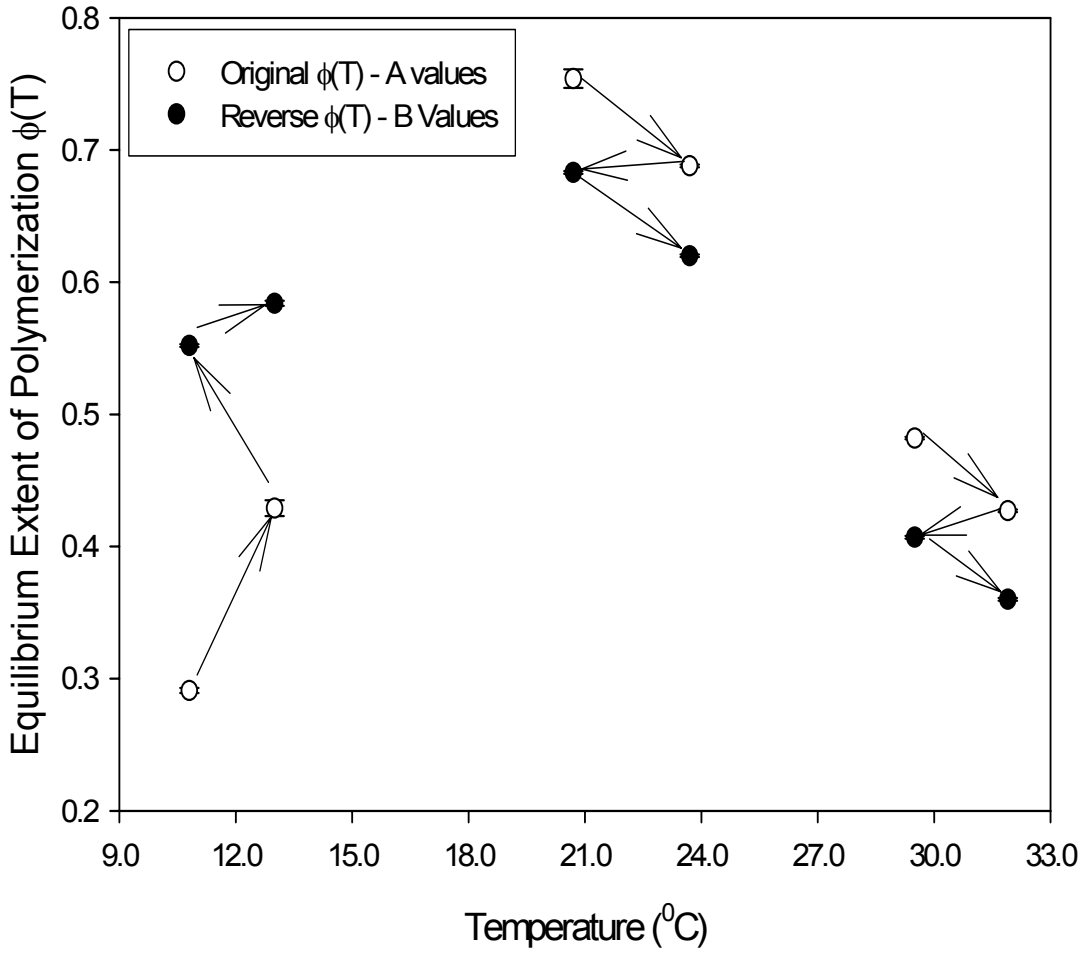

Figure 4.20. Extent of polymerization as a function of time at 10.8 ^{0}C: $[G]_0$ = 3.1 mg/mL, [KCl] = 15 mM, P = 0.1 MPa.

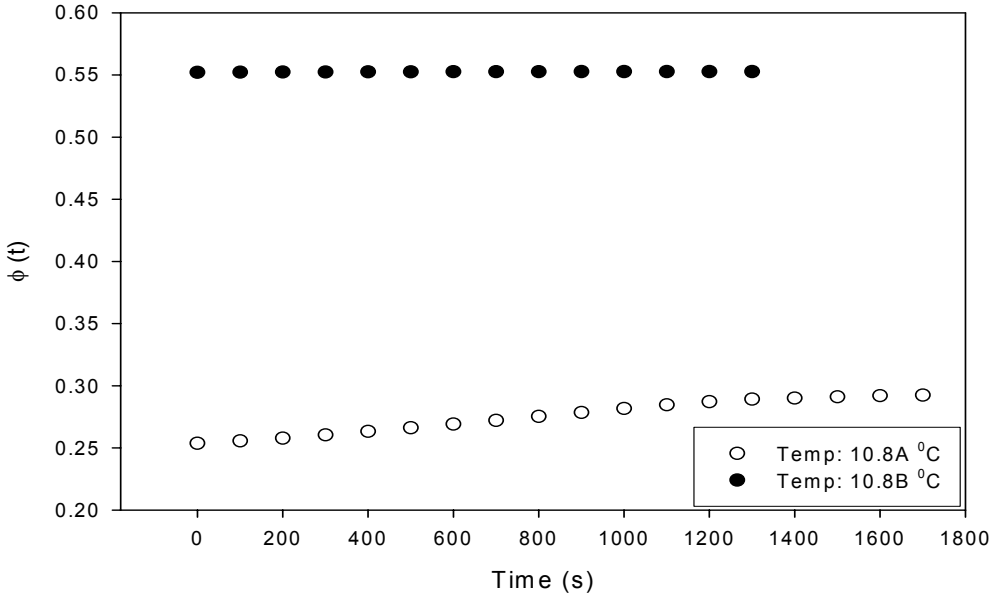

Figure 4.21. Extent of polymerization as a function of time at 13.0 ^{0}C: $[G]_0$ = 3.1 mg/mL, [KCl] = 15 mM, P = 0.1 MPa.

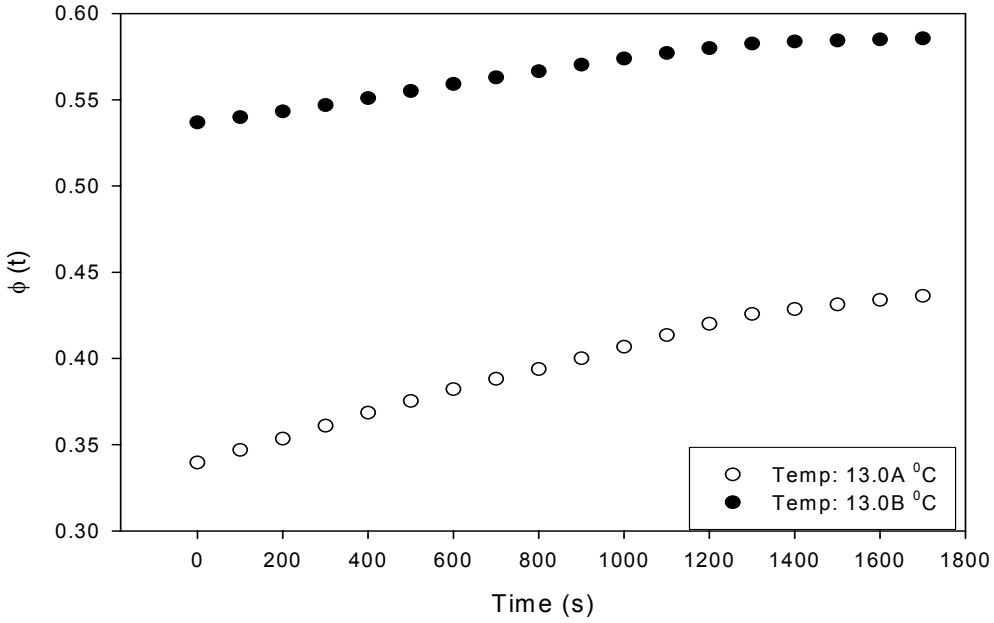

Figure 4.22. Extent of polymerization as a function of time at 20.7 ^{0}C: $[G]_0$ = 3.1 mg/mL, [KCl] = 15 mM, P = 0.1 MPa.

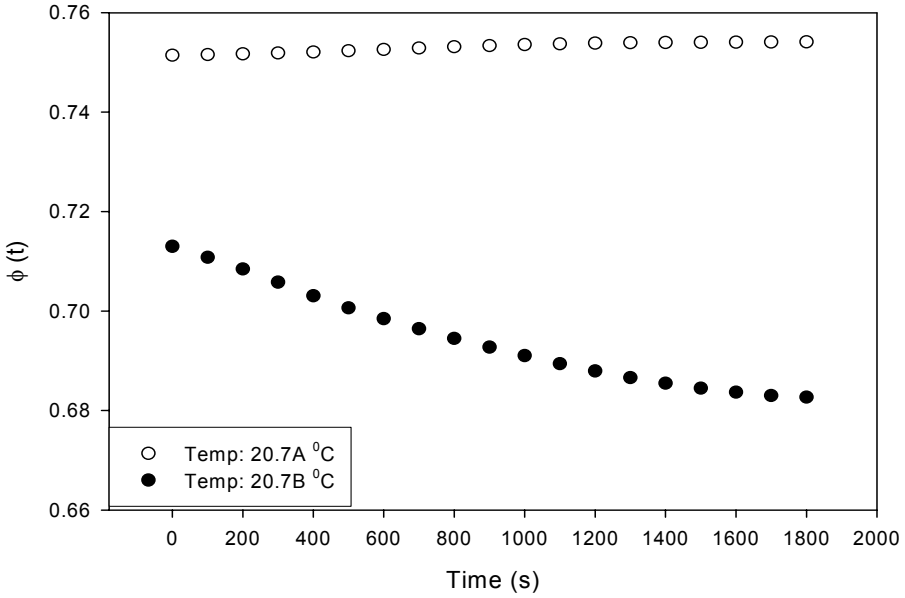

Figure 4.23. Extent of polymerization as a function of time at 23.7 ^{0}C: $[G]_0$ = 3.1 mg/mL, [KCl] = 15 mM, P = 0.1 MPa.

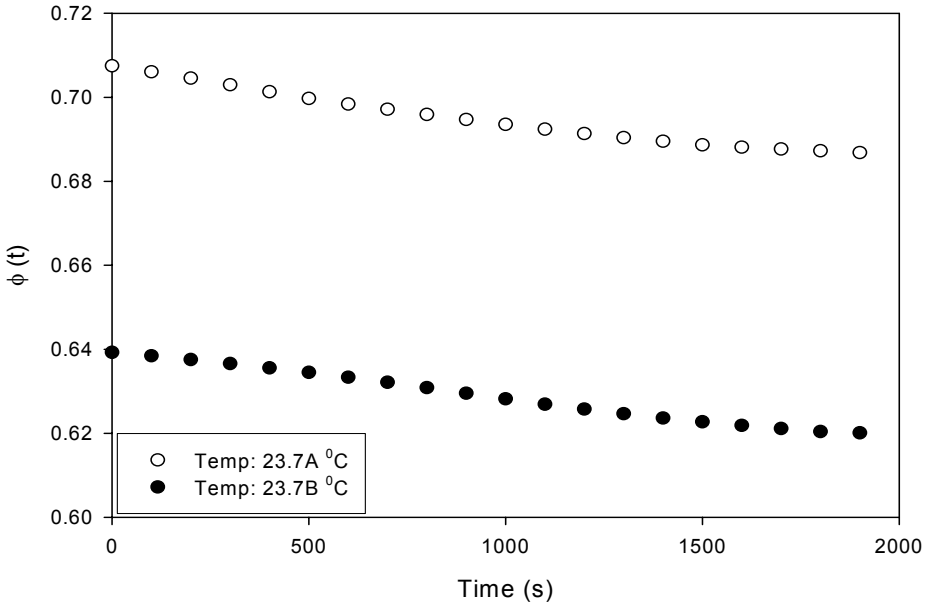

Figure 4.24. Extent of polymerization as a function of time at 29.5 ^{0}C: $[G]_0$ = 3.1 mg/mL, [KCl] = 15 mM, P = 0.1 MPa.

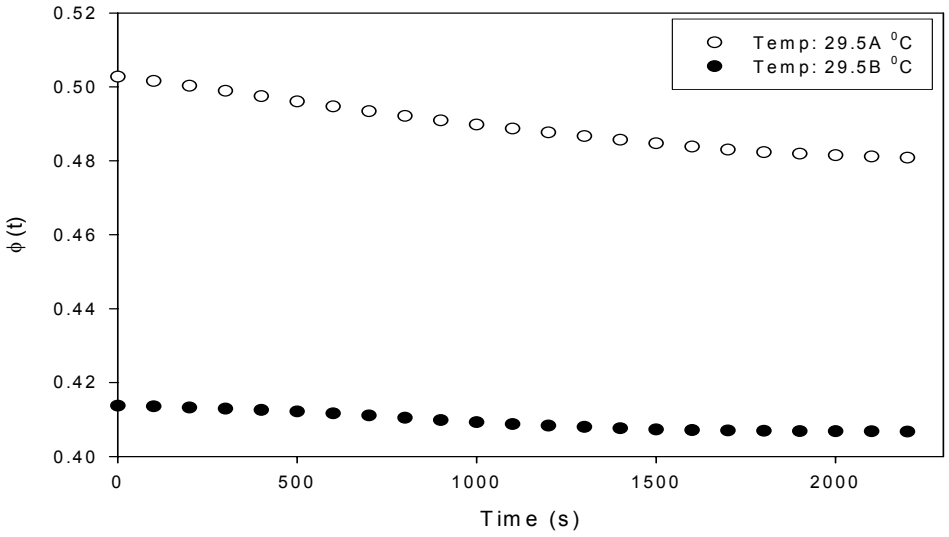

Figure 4.25. Extent of polymerization as a function of time at 31.9 ^{0}C: $[G]_0$ = 3.1 mg/mL, [KCl] = 15 mM, P = 0.1 MPa.

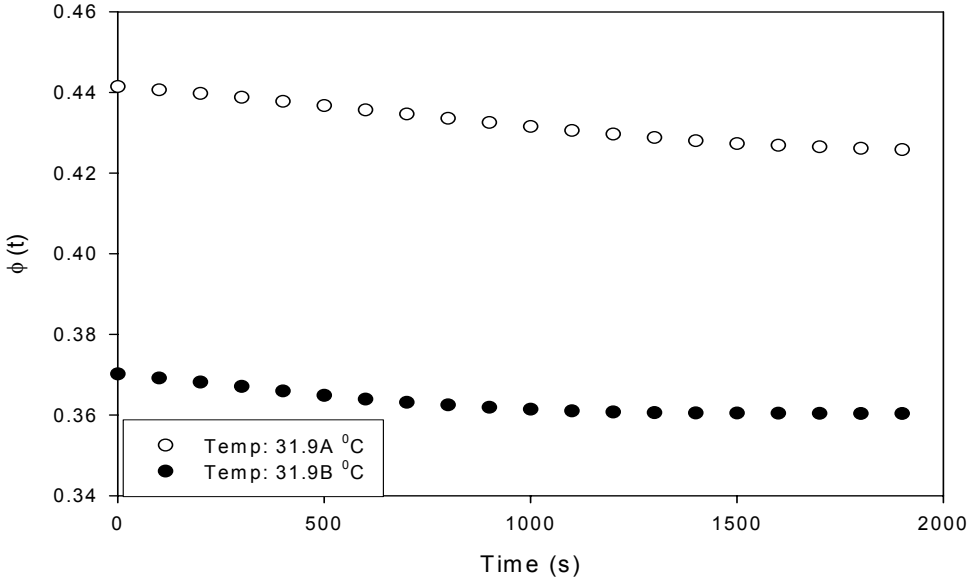

Figure 4.26. Initial values, $r_p(T)$, for points where the temperature was reversed and repeated. "A" values are original temperature values and "B" values are repeated temperature values. Below T_{max}, r_p represents initial polymerization rates and above T_{max}, r_p represents initial depolymerization rates: $[G]_0$ = 3.1 mg/mL, [KCl] = 15 mM, P = 0.1 MPa.

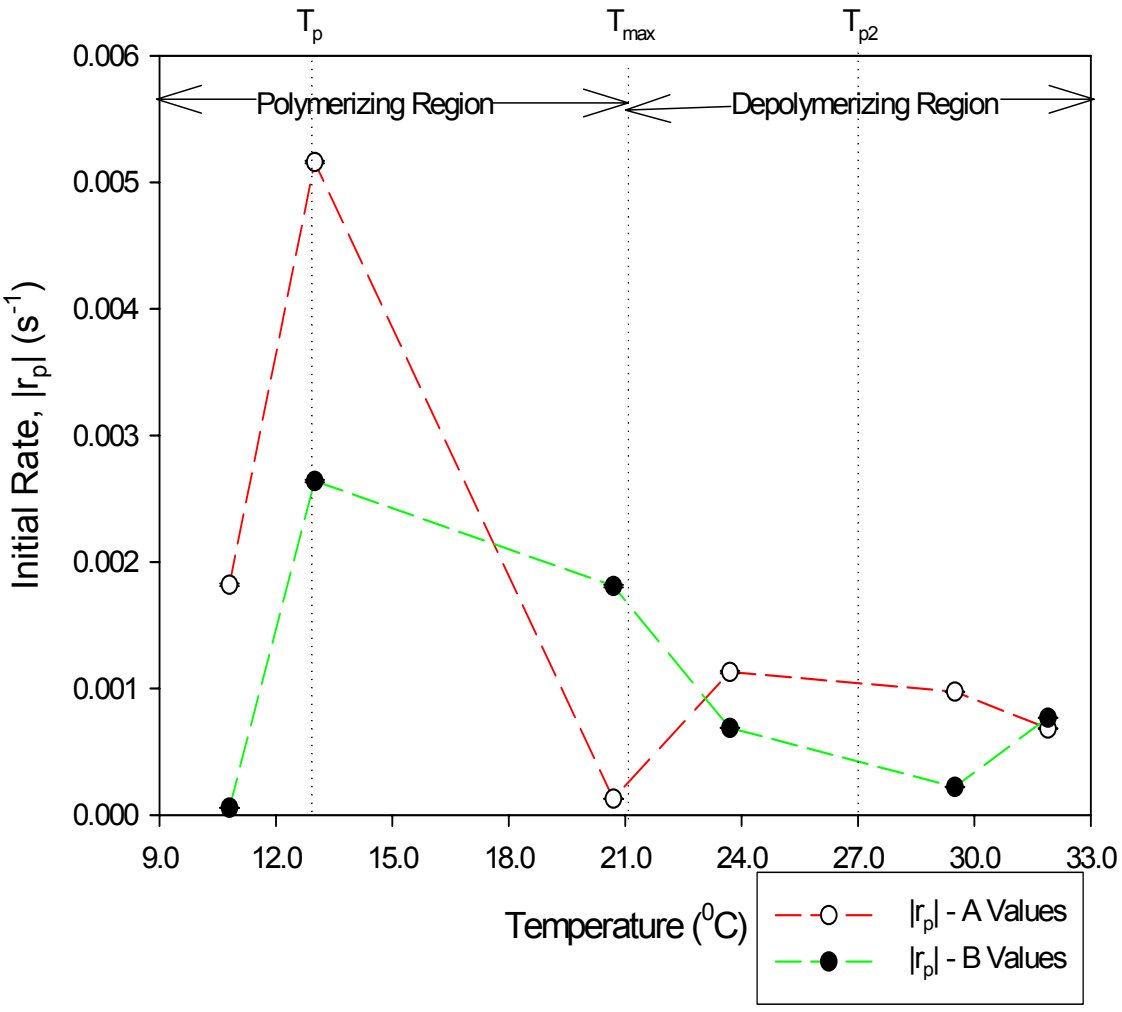

In every case, the actin polymerization system exhibited hysteresis upon a negative temperature jump. In the polymerization region, near T_p, the extent of polymerization increased even with a temperature decrease from 13.0A ^{0}C to 9B ^{0}C (Figure 4.19). The deviation from the original value was 90%. The divergence it took, however, indicated that it did not have the same effect as a positive temperature jump of the same magnitude, because it deviated from the path of the original ϕ (T). Upon return to 13.0B ^{0}C, the extent of polymerization was greater than at 13.0A ^{0}C. This signified that the extent had not recovered from the initial perturbation at 13.0A ^{0}C in the negative direction; though the deviation was slightly lower at 36%. At the subsequent temperature of 15.5 ^{0}C, the extent seemed to return to the original path of ϕ (T). Near but above T_{max}, the same trend was observed as the extent decreased with a negative temperature jump in the depolymerization region from 23.7A ^{0}C to 20.7B ^{0}C and back to 23.7B ^{0}C. Though the extent of polymerization simply decreased in both case, the deviations from the original values were significantly smaller than near T_p – 9% for 2 degrees and 10% for 23.7 degrees. Above T_p, there was also evidence of hysteresis as depolymerization was not reversed by the decrease in temperature from 31.9A ^{0}C to 29.5B ^{0}C. The deviations – 16% for both 29.5 and 31.9 degrees, were still much lower than near T_p and slightly larger than near T_{max}. The conclusion is that reversibility cannot be seen in the extent of polymerization on the time scale of one to two hours, and especially so near the transition temperatures.

The effect of negative perturbation on initial rates seemed to follow a different trend. The initial rate also never returned to the original value in the polymerization region for 10.8 and 13.0 degrees, although the reversal initial rates were lower by

97% and 50% respectively, indicating that the negative temperature may have had a "slowing down" effect on dynamics of polymerization. Slightly above T_{max}, the initial rate of depolymerization going from 23.7A ^{0}C to 20.7B ^{0}C drastically increased 1300% upon crossing back over into the polymerizing region. Traversing from 20.7B ^{0}C to 23.7B ^{0}C, the initial rate of depolymerization decreased by 39%. Above T_{p2}, the initial rate of depolymerization decreased by 77% upon reversal from 31.9A ^{0}C to 29.5B ^{0}C, and increased almost back to its original value upon return to 31.9B ^{0}C, showing only a 12% deviation. The conclusion is that the initial rate seems to be strongly affected by the temperature reversal. Also, below T_{max}, the initial polymerization rate decreased when the temperature was reversed and then increased at the next temperature. Above T_{max}, the initial depolymerization rate also decreased upon temperature reversal and then increased at the following temperature. The negative temperature therefore has a "slowing down" effect on the initial rate.

It can also be concluded that either the 2-3 degree temperature jumps utilized in these experiments cannot be considered "small" perturbations as defined by O'Shaughnessy and Vavylonis[22] for the actin system, or the sensitivity of the dynamics to perturbations in the opposite direction are not strong enough to override the large relaxation times required for full development of the molecular weight distribution of the filaments.[22,45,46]

Chapter 5: Results/Discussion of Actin Polymerization at 0.1 MPa in D_2O Buffer

5.1 Run #2: P = 0.1 MPa; [Actin] = 3.1 mg/ml in D_2O Buffer

The extent of polymerization was studied under conditions of atmospheric pressure (~0.1 MPa) in 99% D_2O Buffer, called Buffer D (see Experimental Methods in Chapter 3). This experiment was performed in the three-position chamber as described above in the Experimental Methods chapter and two samples were analyzed concurrently. The initial concentrations of monomer of the two samples were $[G_0]$ = 3.1 mg/mL (Run #2) and 1.0 mg/mL (Run #3). KCl, used as an initiating salt, was added to both samples at a concentration of [KCl] = 15 mM. The results of the 3.1 mg/mL sample are reported in this section and the results of the 1.0 mg/ml sample (Run #3) are reported in section 5.2. The actual temperatures, which differed slightly from the controlled temperature of the water bath, were measured with a thermocouple, attached near the sample cell and monitored by an electronic datalogger, and were used in all results and analysis. The effect of the temperature reversals on the thermodynamics and kinetics of Run #2 and Run #3 will be discussed in sections 5.1.5 and 5.2.5, respectively.

5.1.1. Extent of Polymerization Results

The fluorescence intensity was measured at a series of bath temperatures starting at 0 °C, as a function of time for approximately one hour at each temperature. The results of the equilibrium extent of polymerization as a function of temperature, ϕ (T), are presented in Table 5.1 and shown in Figure 5.1, where the various temperature ranges are represented by unique symbols. For the first bath temperature range, from 0 to 12 °C (see Figures 5.2, a and b), measurements were made as the bath temperature increased in three degree increments. After measurements at 12 °C were made, the bath temperature was lowered or reversed to 9 °C, in order to study the behavior due to temperature lowering or reversal; these results will be presented and discussed in section 5.1.5. Data were taken in the second bath temperature range (see Figure 5.3, a and b) from 9 to 24 °C by increments of three degrees. The third bath temperature range (see Figure 5.4, a and b) was from 21 to 33 °C, and the fourth and final bath temperature range (see Figure 5.5, a and b) was from 30 to 33 °C. The maximum intensity (complete polymerization) was measured at the final bath temperature of 33 °C upon addition of $MgCl_2$ to 15 mM. The intensity values over time divided by the equilibrium value of the maximum intensity yields the extent of polymerization, both ϕ (T) which is the equilibrium value and ϕ (t) at each temperature. Figure 5.6 is a comparison of the results of ϕ (T) with previous results from a similar experiment.[15] The tables of ϕ (t) can be found in Appendix A. Discussions of these results will be presented in sections 5.1.3.

Table 5.1. Extent of polymerization (ϕ (T)) values as a function of temperature. The "true" temperature was measured by a thermocouple at the sample cell: Solvent = D_2O $[G]_0$ = 3.1 mg/mL, [KCl] = 15 mM, P = 0.1 MPa.

Bath Temperature (^{0}C)	**"True" Temperature (+/- 0.1 ^{0}C)**	**"True" Temperature (+/- 0.1 K)**	**Extent of Polymerization ϕ (T)**	**Reverse Extent of Polymerization ϕ (T)**
0	8.0	281.2	0.4406 +/- 0.0001	
3	11.3	284.5	0.4418 +/- 0.0001	
6	12.8	286.0	0.4776 +/- 0.0001	
9	14.4	287.6	0.5332 +/- 0.0002	0.6616 +/- 0.0001
12	17.0	290.2	0.6143 +/- 0.0004	0.6729 +/- 0.0001
15	18.1	291.3	0.6916 +/- 0.0001	
18	20.0	293.2	0.7131 +/- 0.0001	
21	22.0	295.2	0.7155 +/- 0.0001	0.7082 +/- 0.0001
24	24.1	297.3	0.6922 +/- 0.0001	0.6554 +/- 0.0001
27	26.4	299.6	0.6045 +/- 0.0001	
30	29.0	302.2	0.5571 +/- 0.0001	0.5397 +/- 0.0001
33	31.6	304.8	0.5245 +/- 0.0001	0.4980 +/- 0.0001

Figure 5.1. Extent of polymerization as a function of temperature: Solvent = D_2O, $[G]_0$ = 3.1 mg/mL, [KCl] = 15 mM, P = 0.1 MPa. Symbols represent the various temperature ranges, as discussed in the text.

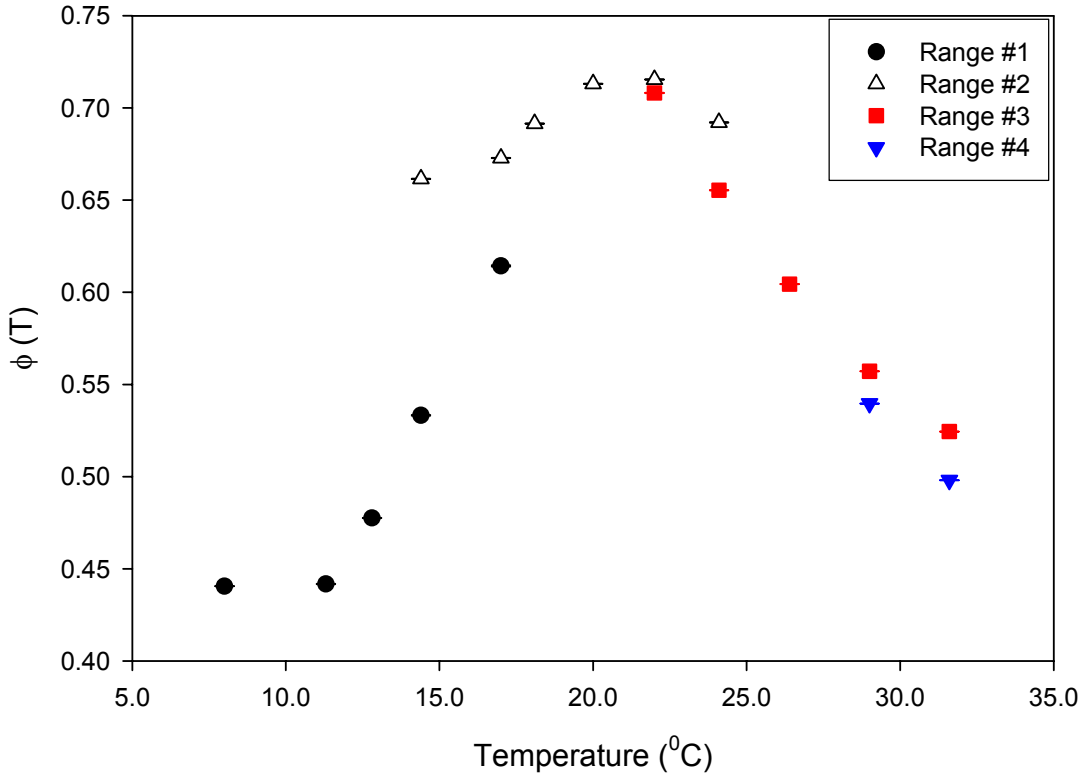

Figure 5.2a. Extent of polymerization as a function of time for temperature range #1: Solvent = D_2O, $[G]_0$ = 3.1 mg/mL, [KCl] = 15 mM, P = 0.1 MPa.

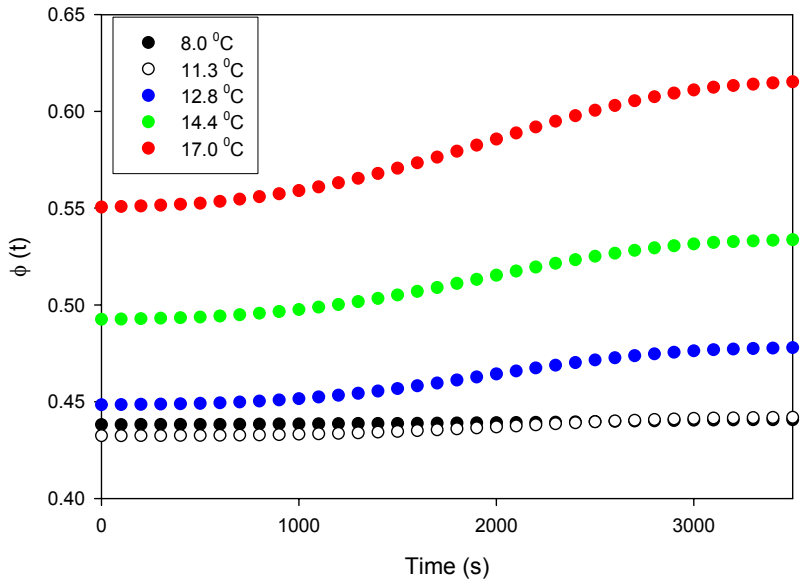

Figure 5.2b. Equilibrium extent of polymerization for temperature range #1: Solvent = D_2O, $[G]_0$ = 3.1 mg/mL, [KCl] = 15 mM, P = 0.1 MPa.

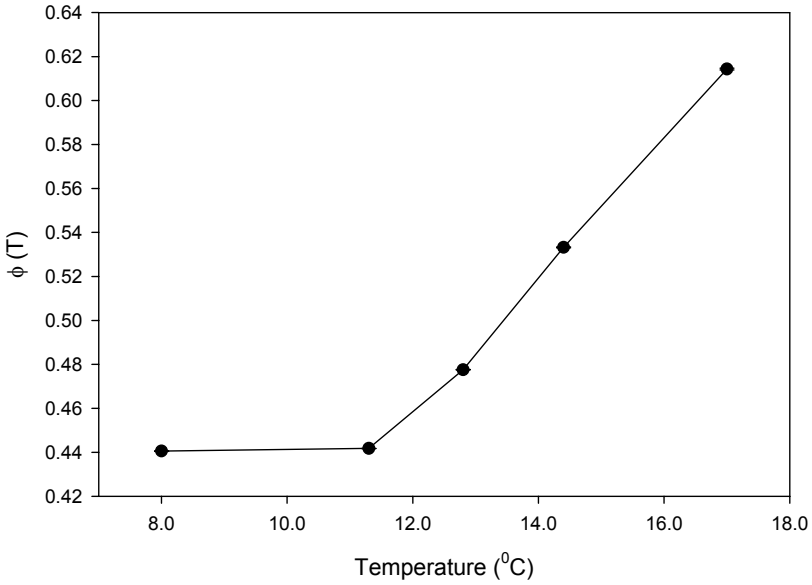

Figure 5.3a. Extent of polymerization as a function of time for temperature range #2: Solvent = D_2O, $[G]_0$ = 3.1 mg/mL, [KCl] = 15 mM, P = 0.1 MPa.

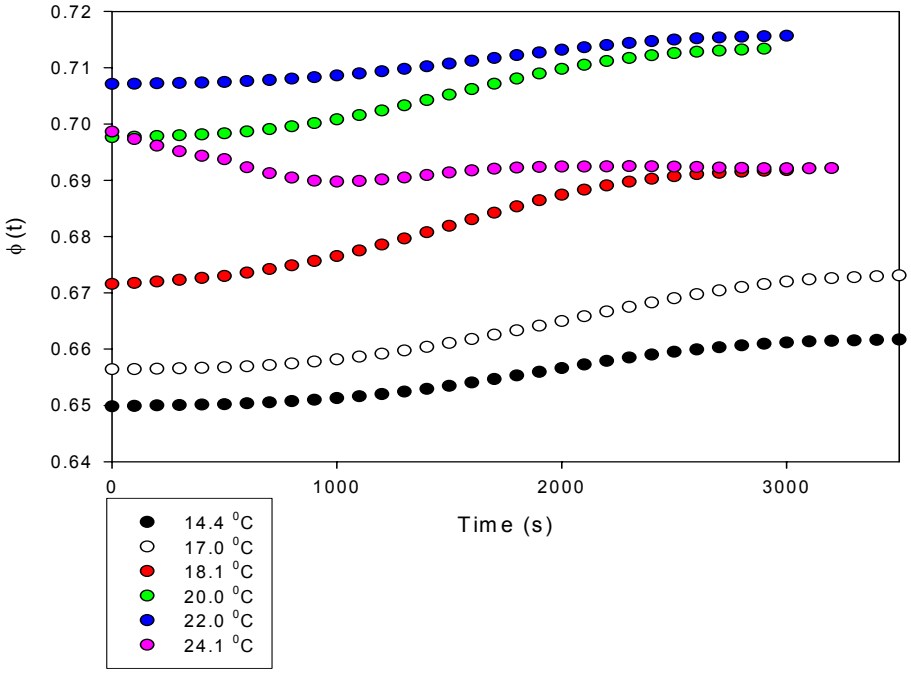

Figure 5.3b. Equilibrium extent of polymerization for temperature range #2: Solvent = D_2O, $[G]_0$ = 3.1 mg/mL, [KCl] = 15 mM, P = 0.1 MPa.

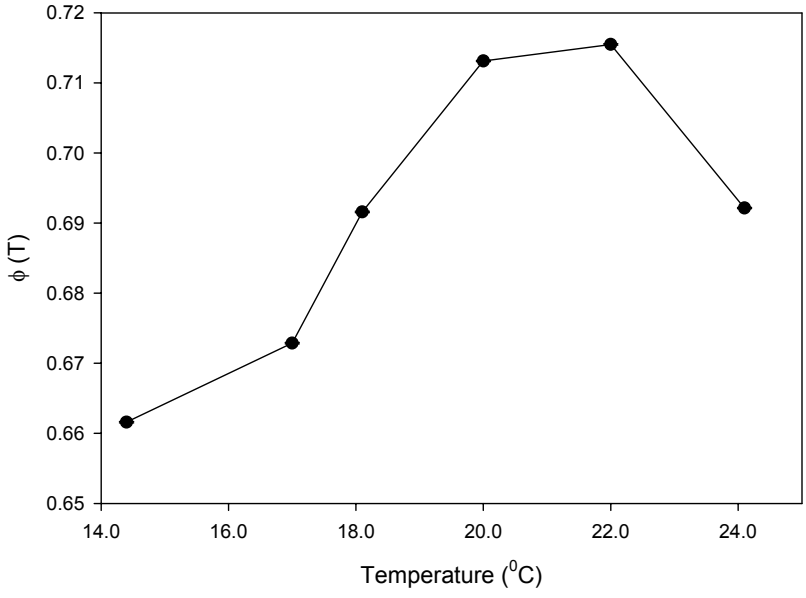

Figure 5.4a. Extent of polymerization as a function of time for temperature range #3: Solvent = D_2O, $[G]_0$ = 3.1 mg/mL, [KCl] = 15 mM, P = 0.1 MPa.

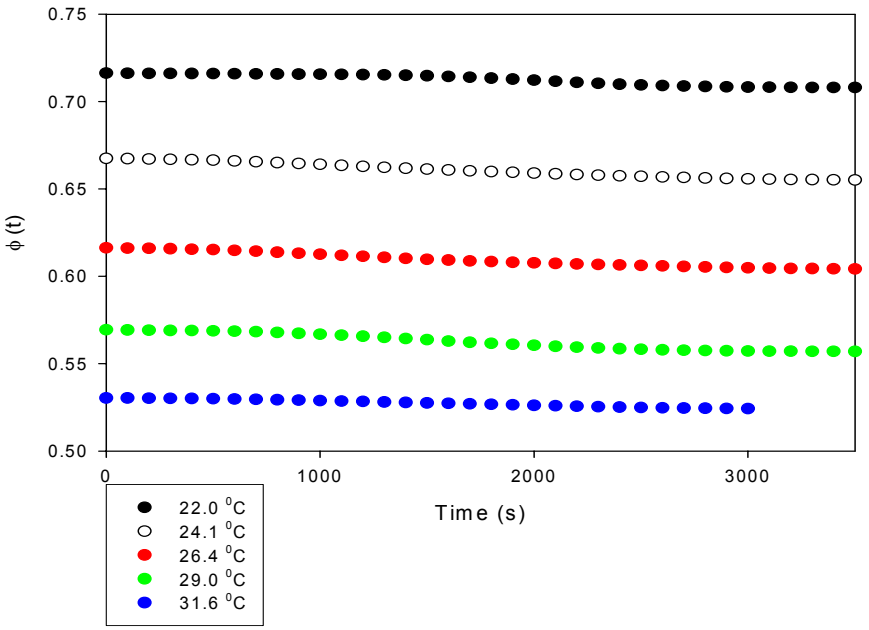

Figure 5.4b. Equilibrium extent of polymerization for temperature range #3: Solvent = D_2O, $[G]_0$ = 3.1 mg/mL, [KCl] = 15 mM, P = 0.1 MPa.

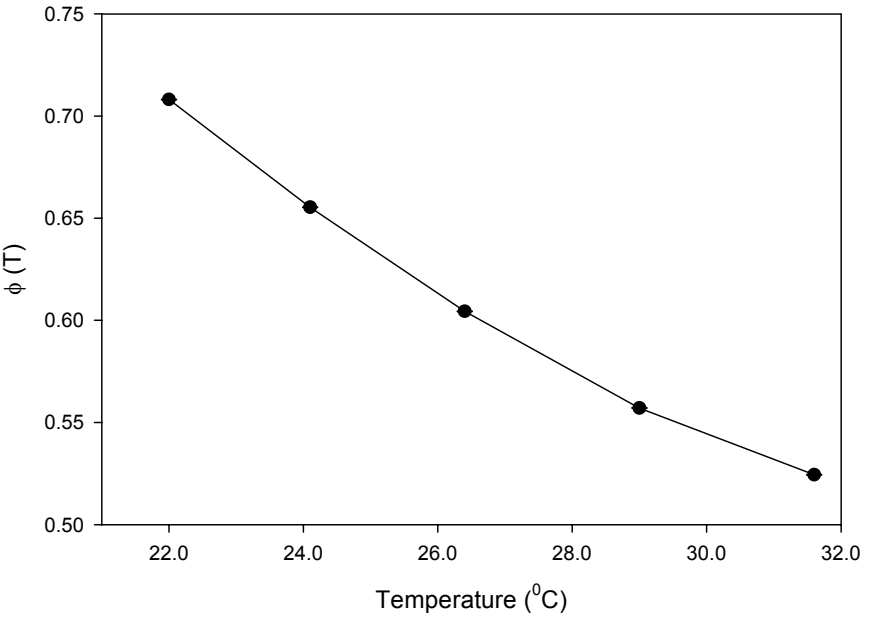

Figure 5.5a. Extent of polymerization as a function of time for temperature range #4: Solvent = D_2O, $[G]_0$ = 3.1 mg/mL, [KCl] = 15 mM, P = 0.1 MPa.

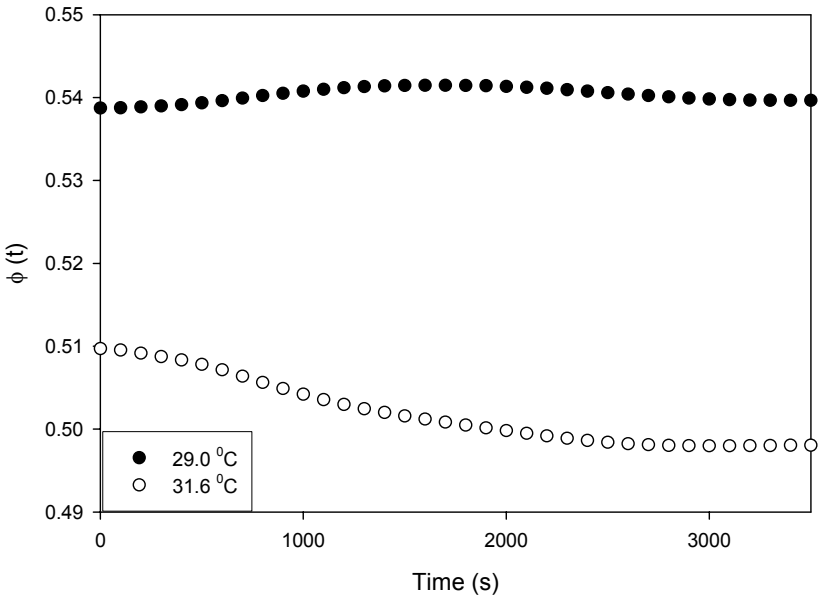

Figure 5.5b. Equilibrium extent of polymerization for temperature range #4: Solvent = D_2O, $[G]_0$ = 3.1 mg/mL, [KCl] = 15 mM, P = 0.1 MPa.

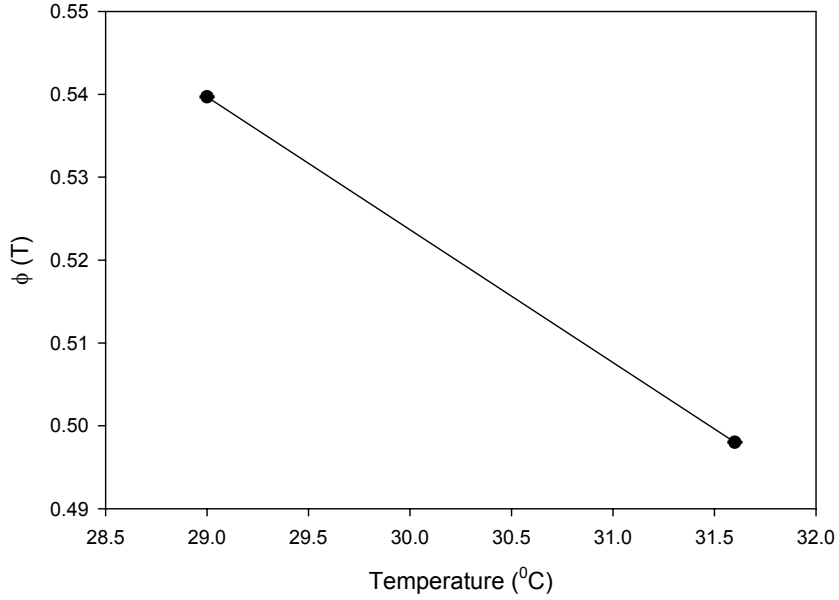

Figure 5.6. Extent of polymerization as a function of temperature in Buffer D: Solvent = D_2O, $[G]_0$ = 3.1 mg/mL, [KCl] = 15 mM, P = 0.1 MPa. The red circle represents current results, the green circles represent data from Niranjan et al.,[16] and the blue circles represent data from Yim et al.

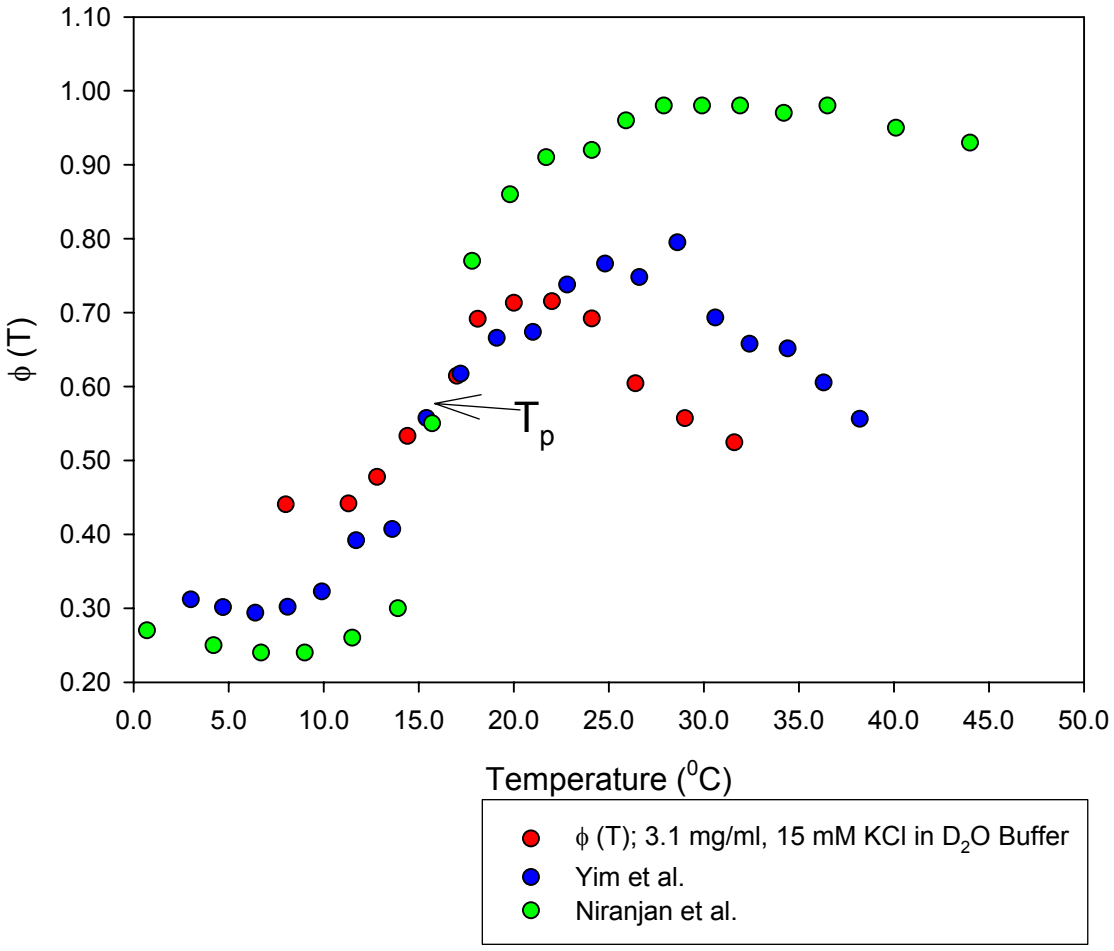

5.1.2 Initial Rates of Polymerization

As in the experiments from chapter four, the actual temperature near the cell as recorded by the datalogger required approximately 10 minutes to reach a steady value. A plot of temperature with time for this experiment is shown in Figure 5.7. The vertical line marks the time at which the temperature equilibrated. The transient regions can actually be observed in the kinetics plots (see Figure 4.2a, for example) between 0 and 600 seconds. After the transient region in the kinetic plot, the "reaction" region proceeds rapidly for about fifteen minutes.

In analyzing the kinetics of polymerization, the data of $M_f(t)$ between 0 and 600 seconds (the transient temperature region) is first truncated and the time is set to t = 0 at the temperature equilibration time of 600 seconds. A plot of the equilibrium values of $M_f(T)$ is shown in Figure 5.8. The results of r_p at all temperatures are shown in Table 5.2. Figure 5.9 depicts the initial rate as a function of temperature, $r_p(T)$, for the entire experiment. Discussions of these results are presented in sections 5.1.4.

Figure 5.7. Temperature near the cell in the three-position chamber as a function for time for a bath temperature of 0 ^{0}C: Solvent = D_2O, $[G]_0$ = 3.1 mg/mL, [KCl] = 15 mM, P = 0.1 MPa. The vertical line indicates the point beyond which the temperature is fairly constant.

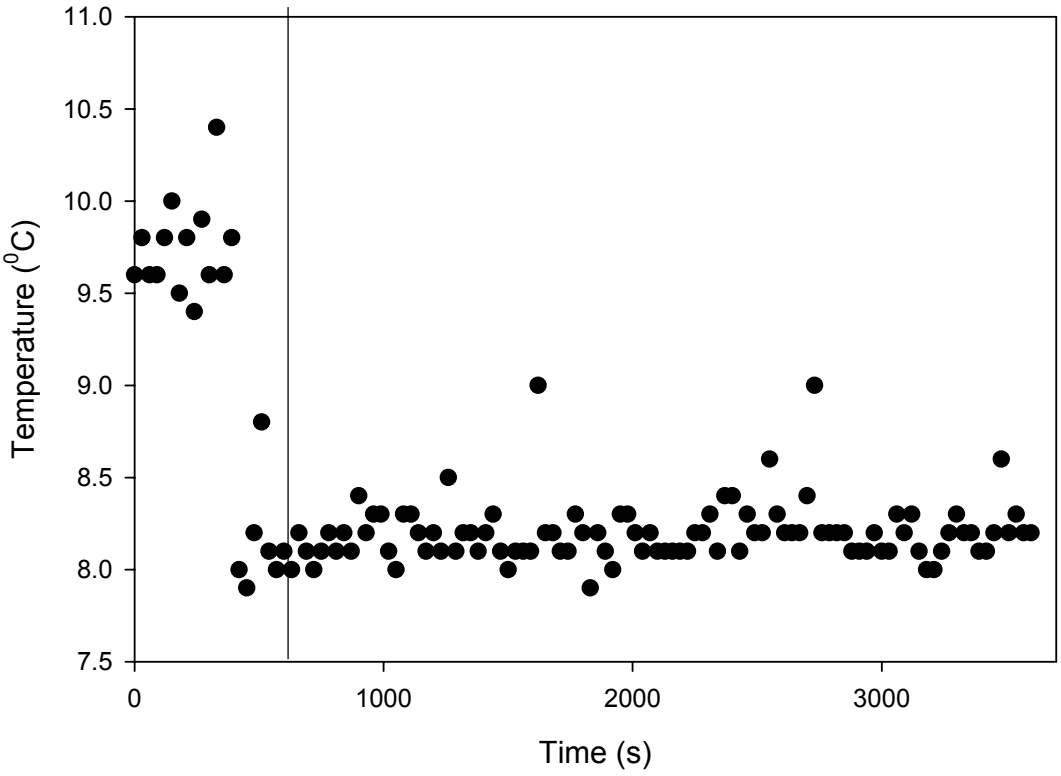

Figure 5.8. Equilibrium free monomer concentration, M_f, as a function of temperature: Solvent = D_2O, $[G]_0$ = 3.1 mg/mL, [KCl] = 15 mM, P = 0.1 MPa. Symbols represent the various temperature ranges.

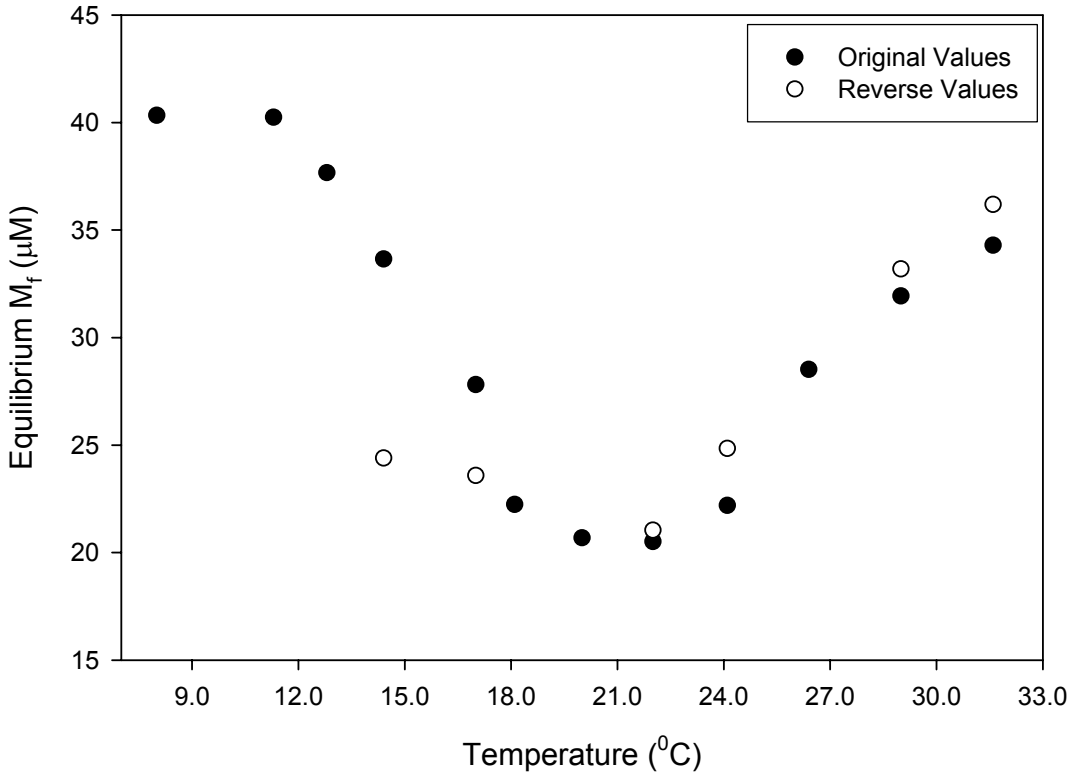

Table 5.2. Initial rate ($\mu M\ s^{-1}$) of polymerization as a function of temperature. The "true" temperature was measured by a thermocouple at the sample cell: Solvent = D_2O, $[G]_0$ = 3.1 mg/mL, [KCl] = 15 mM, P = 0.1 MPa.

Bath Temperature (^0C)	**"True" Temperature (+/- 1 ^0C)**	**Initial Rate, r_p ($\mu M\ s^{-1}$)**	**Reverse Initial Rate, r_p ($\mu M\ s^{-1}$)**
0	8.0	3.96×10^{-5} +/- 1×10^{-7}	
3	11.3	1.23×10^{-4} +/- 1×10^{-6}	
6	12.8	5.00×10^{-4} +/- 1×10^{-6}	
9	14.4	7.56×10^{-4} +/- 1×10^{-6}	2.11×10^{-4} +/- 0.0001
12	17.0	1.23×10^{-3} +/- 1×10^{-6}	2.91×10^{-4} +/- 0.0001
15	18.1	6.28×10^{-4} +/- 1×10^{-6}	
18	20.0	4.78×10^{-4} +/- 1×10^{-6}	
21	22.0	2.21×10^{-4} +/- 1×10^{-6}	-6.0×10^{-5} +/- 0.00001
24	24.1	-7.80×10^{-4} +/- 1×10^{-6}	-3.67×10^{-4} +/- 0.0001
27	26.4	-4.18×10^{-4} +/- 1×10^{-6}	
30	29.0	-3.42×10^{-4} +/- 1×10^{-6}	1.92×10^{-4} +/- 0.0001
33	31.6	-1.80×10^{-4} +/- 1×10^{-6}	-5.11×10^{-4} +/- 0.0001

Figure 5.9. Initial polymerization rate, r_p, as a function of temperature for each temperature range: Solvent = D_2O, $[G]_0$ = 3.1 mg/mL, [KCl] = 15 mM, P = 0.1 MPa.

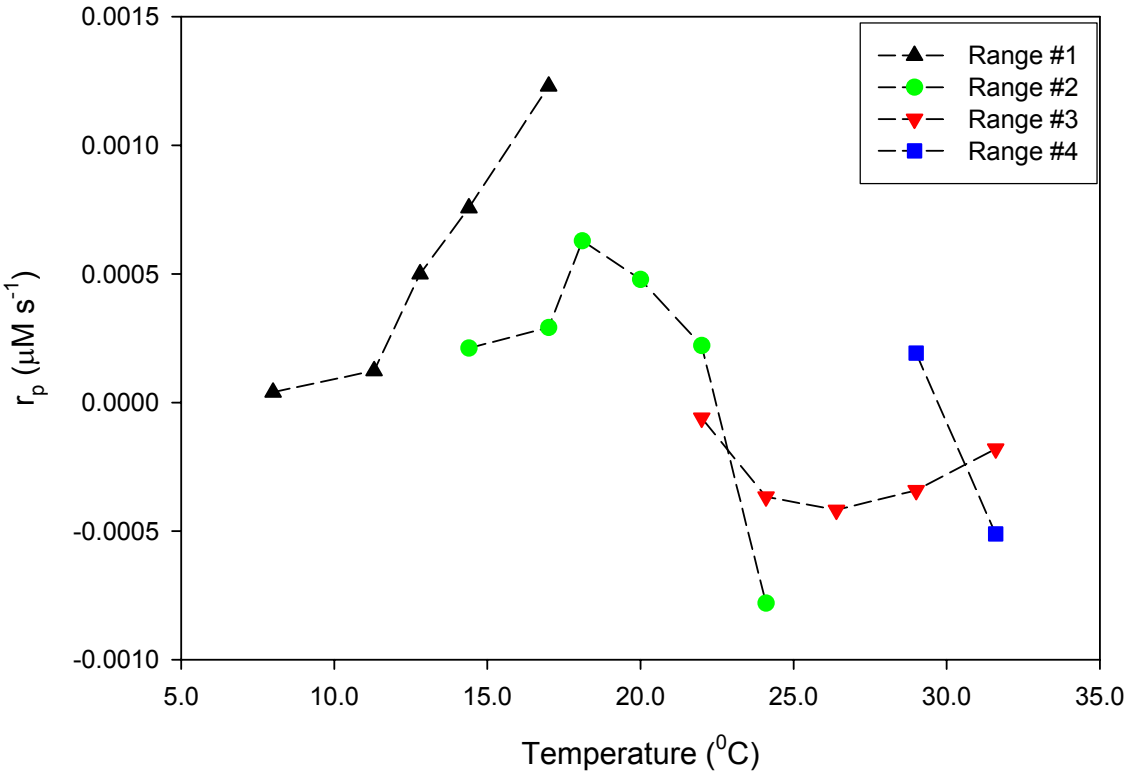

5.1.3 Discussion - Thermodynamics

The thermodynamic (extent of polymerization) data in this chapter were collected at conditions that mimic the conditions of a previous experiment performed at 3.00 mg/mL, atmospheric pressure (0.1 MPa) and 15.00 mM KCl.[16] This experiment was repeated for the same reasons as the previous experiment in H_2O – to confirm the prior results with a different source of actin and a new instrument, and to perform kinetic analysis with a larger volume of data.

The results of this study were compared with the results of Niranjan et al.[15,16] and unpublished results obtained by Yim et al, also using an ISS Koala instrument employed in the current work. The results are plotted in Figure 5.6 and summarized in Table 5.3. The appearance of an inflection point defined as the transition point T_p, is evident in all three plots, and the T_p values are in excellent agreement with each other. The maximum in the extent of polymerization was also exhibited in the three plots, but differed noticeably among them. The T_{max} for Yim was about 3 degrees higher than the current T_{max}. The Niranjan plot showed a T_{max} that was about 8 degrees higher than the current finding and did not seem to exhibit a significant depolymerization past T_{max}. It certainly did not give evidence of T_{p2}, the second inflection/transition point which is around 25-26 ^{0}C for the current work. It is not clear from the Yim plot where T_{p2} is because the point at 28.6 ^{0}C seems to be an outlier and obscures the anticipated trend in the data, but a noticeable inflection seems to occur at 33 ^{0}C, which deviates from the result obtained in the current work. In addition, the value for ϕ_{max} is nearly 1 for Niranjan but is about 0.7-0.8 for Yim and the current findings. An interesting observation is that the initial value of ϕ (T) varies

between these three experiments. In all the experiments with identical parameters that are compared in this work, a higher initial value of ϕ (T) seems to lower both the T_{max} and ϕ_{max} values, but does not affect the T_p value. There seems to be no logical explanation for the disparity in the findings forT_{p2}, but it is encouraging to find such good precision for T_p between all three experiments which were performed about two years apart.

Table 5.3. Comparison of results from current and prior work on actin polymerization: Solvent = D_2O, $[G]_0$ = 3.1 mg/mL, [KCl] = 15 mM, P = 0.1 MPa. Errors on T and ϕ are rough estimates based on visual extrapolation of the data in Figure 4.8.

Parameters	**Current Results**		**Niranjan Results**[16]		**Yim Results**	
$[G]_0$	3.01 (+/-0.01) mg/mL		3.00 (+/-0.01) mg/mL		3.00 (+/-0.01) mg/mL	
[KCl]	15.0 (+/- 0.1) mM		15.00 (+/- 0.01) mM		15.00 (+/- 0.01) mM	
T_p, ϕ_p	16 (+/-2) ^{0}C	0.58 (+/- 0.05)	16 (+/-2) ^{0}C	0.58 (+/- 0.05)	17 (+/-2) ^{0}C	0.60 (+/- 0.05)
T_{max}, ϕ_{max}	22 (+/-2) ^{0}C	0.71 (+/- 0.05)	33 (+/-2) ^{0}C	0.98 (+/- 0.05)	25 (+/-2) ^{0}C	0.77 (+/- 0.05)
T_{p2}, ϕ_{p2}	26 (+/-2) ^{0}C	0.62 (+/- 0.05)	None	None	33 ^{0}C?	0.65 (+/- 0.05)

The results of this experiment in buffer D are compared to the results of the experiment done in buffer A and a discussion of the effect of the H-/D- bonding are presented and summarized in section 5.3. The conclusion, however, can be made here that T_p and T_{max} exist for actin polymerization in D_2O, suggesting again that entropy is the driving force. These results are important because actin as well as other biomolecules are frequently introduced into D_2O for analysis with instruments

such as neutron scattering[14] or NMR and the effect of this environmental change on the thermodynamics of the system must be known if any comparison to H_2O is made. It has already been shown elsewhere[18] and here in chapter 7 that this effect is not trivial and that T_p is not monotonic with respect to the initial monomer concentration.[16]

5.10. Schematic phase diagram of the results of the actin polymerization: Solvent = D_2O, $[G]_0$ = 3.1 mg/mL, [KCl] = 15 mM, P = 0.1 MPa.

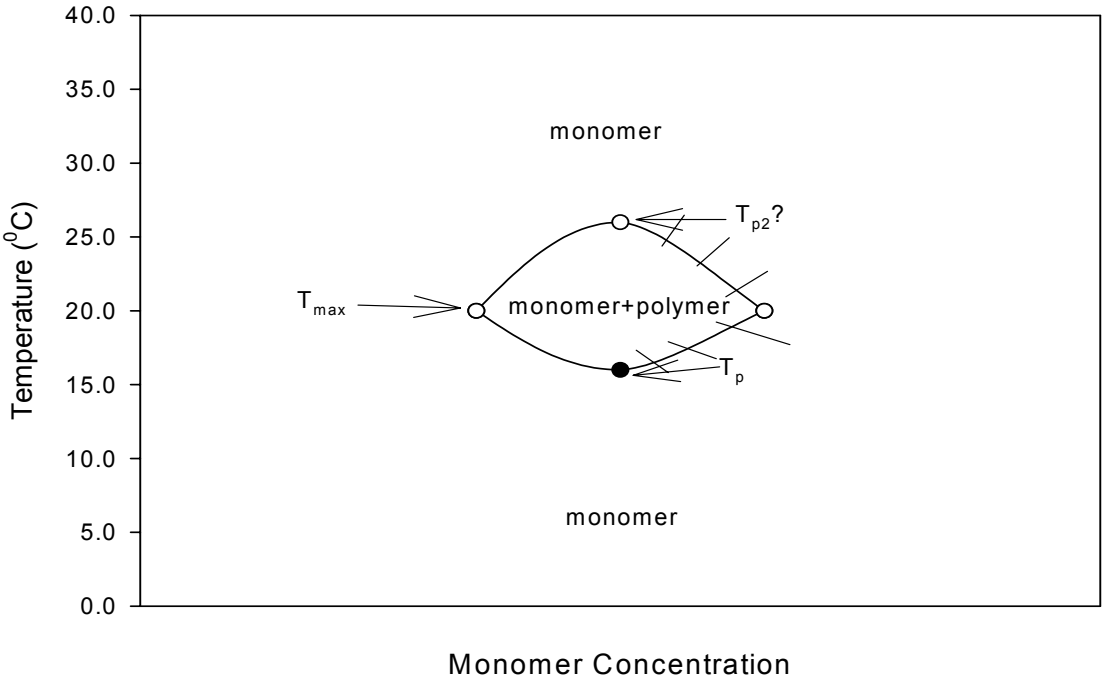

5.1.4 Discussion – Kinetics

The r_p, the initial polymerization rate is defined in chapter four as the fastest overall rate difference of the forward reaction and the reverse reaction of all species in solution – i.e. activated monomers, dimers, trimers, and the oligomers population having an exponential size distribution.[12] This definition is used here and a plot in Figure 5.11 shows r_p as a function of temperature compared to ϕ (T), both without the reversal points. Figures 5.12 – 5.14 show the three regions separated by the two critical points, T_p and T_{p2}, as well as further analysis and discussions following these plots.

Figure 5.11. Initial polymerization rate, r_p, and ϕ as a function of temperature excluding the reverse points: Solvent = D_2O, $[G]_0$ = 3.1 mg/mL, [KCl] = 15 mM, P = 0.1 MPa.

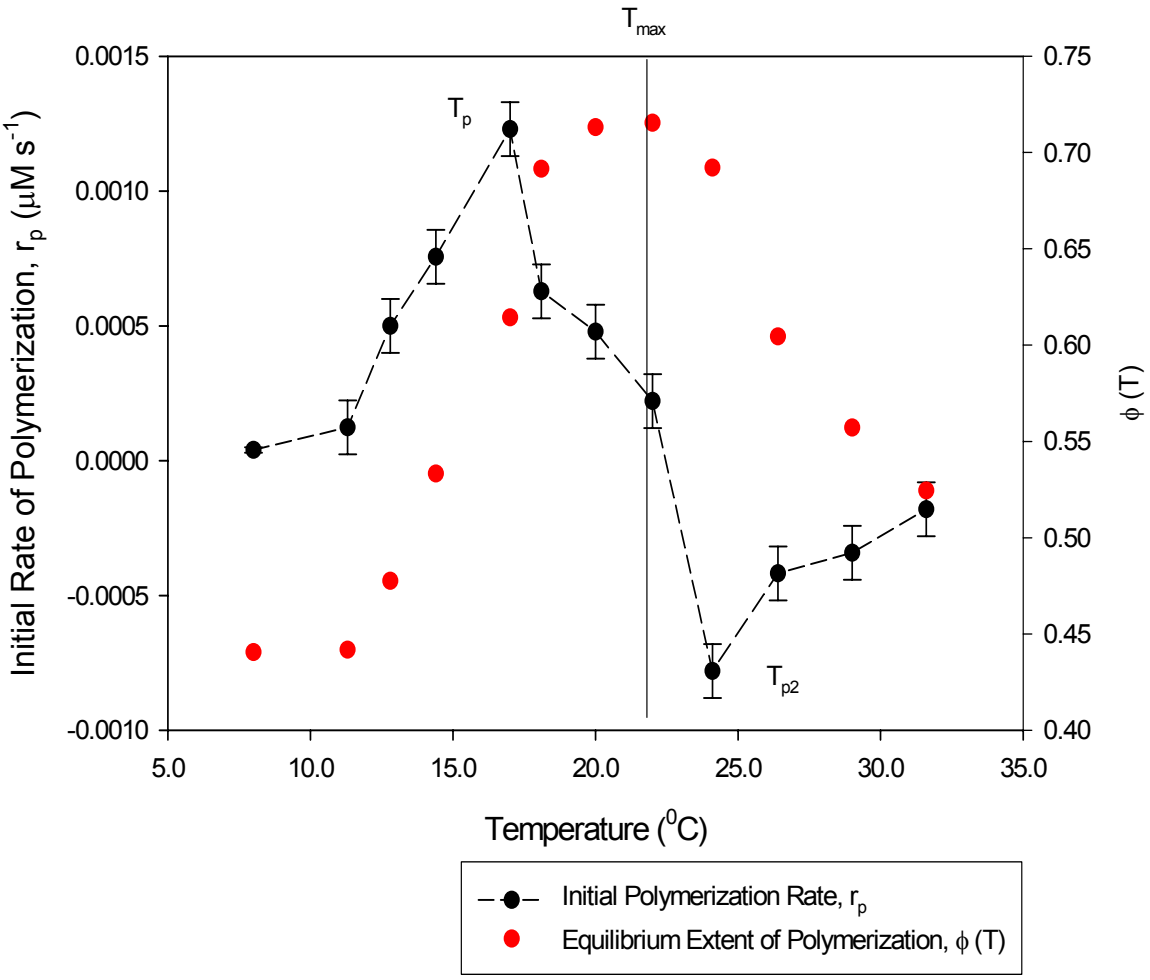

Figure 5.12. Initial rate of polymerization r_p (T) in the first region up to T_p: Solvent = D_2O, $[G]_0$ = 3.1 mg/mL, [KCl] = 15 mM, P = 0.1 MPa.

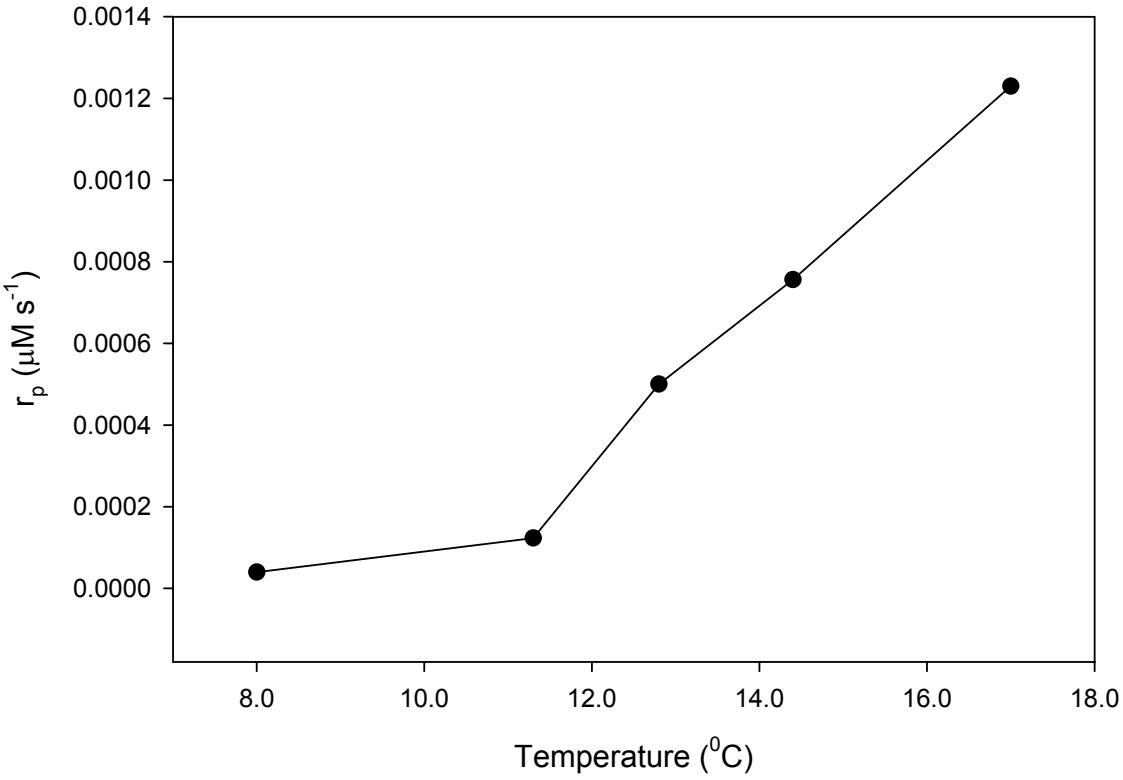

Figure 5.13. Initial rate of polymerization r_p (T) in the region from T_p to T_{p2}: Solvent = D_2O, $[G]_0$ = 3.1 mg/mL, [KCl] = 15 mM, P = 0.1 MPa.

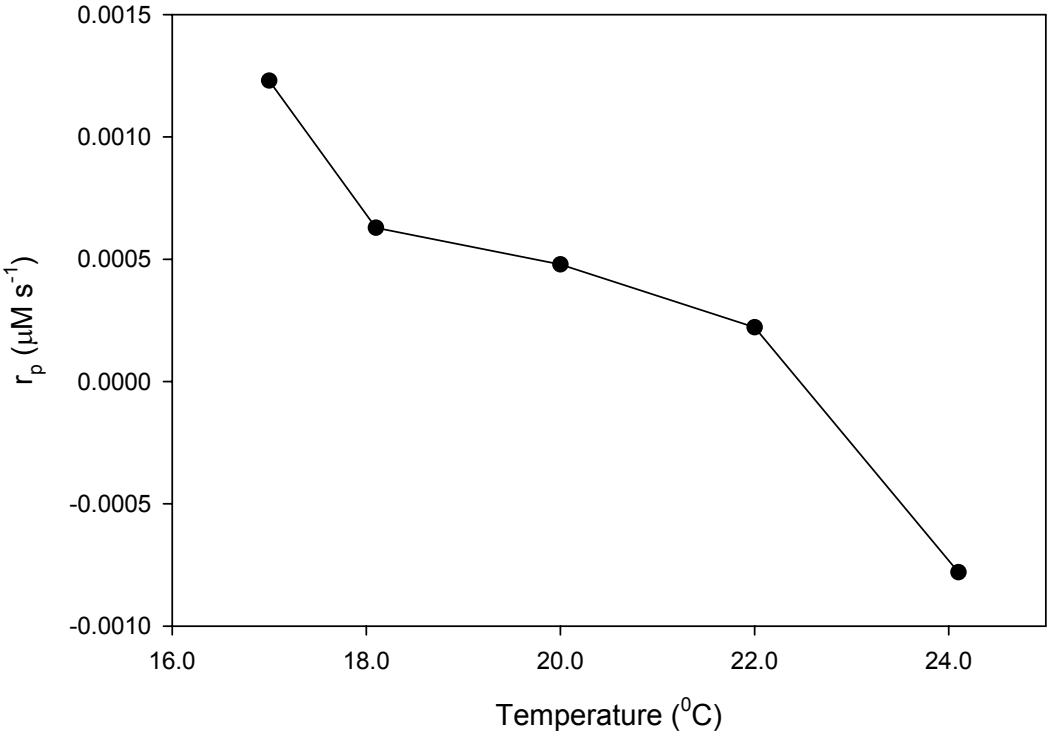

Figure 5.14. Initial rate of polymerization r_p (T) in the region from T_{p2} to the final temperature: Solvent = D_2O, $[G]_0$ = 3.1 mg/mL, [KCl] = 15 mM, P = 0.1 MPa.

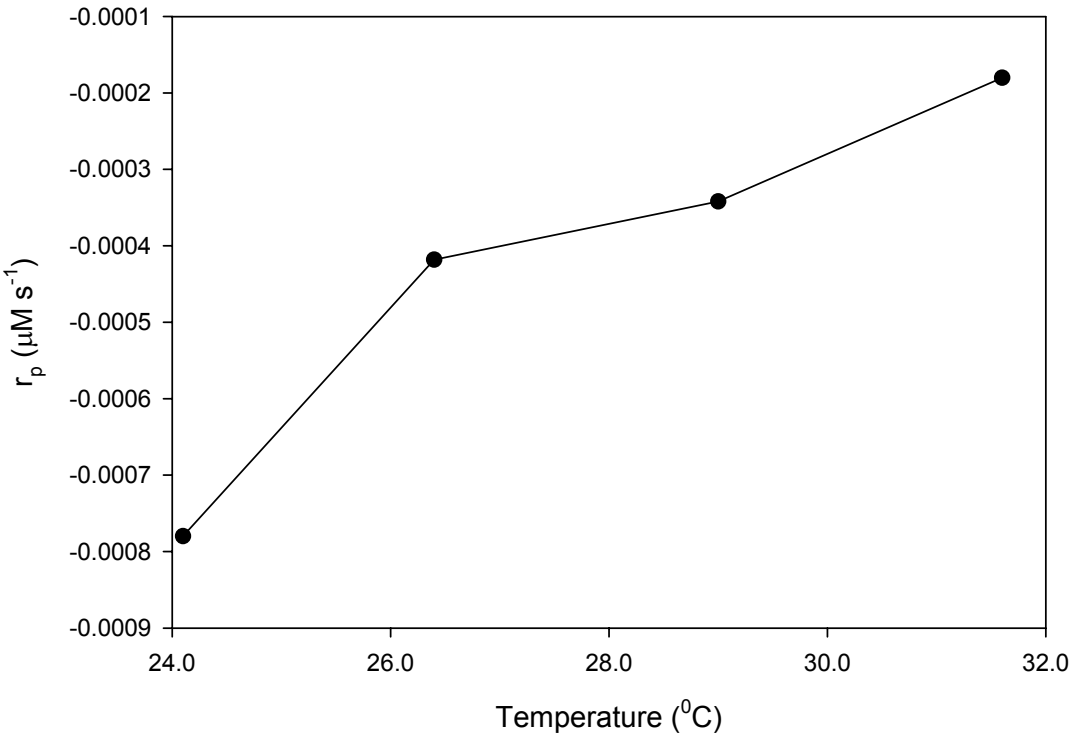

The results of these initial rate calculations also show a remarkable relationship to the extent of polymerization plot as seen in Figure 5.10. At or very near both inflection points in the ϕ (T) plot, the plot of r_p (T) exhibits extrema. The initial rate shows a maximum at T_p, passes through zero near T_{max}, and shows a minimum near T_{p2}. The arguments used in chapter four to explain the initial rate as it

relates to the extent of polymerization are assumed valid for this case. The effect of the solvent on the magnitude of r_p is discussed in chapter seven.

5.1.5 Effect of Temperature Reversal

In these experiments, the temperature was reversed in three regions: near T_p, T_{max}, and T_{p2}. These chosen points were a repeat of the points used for the experiment in chapter four. The effect of temperature reversals on ϕ (T) is shown in Figure 5.15. A comparison of ϕ (t) for each temperature at which reversals were performed are shown in Figures 5.16-5.21, and the effect of the reversals on the initial polymerization rate is shown in Figure 5.22. Table 5.4 below summarizes the results of the responses to the temperature reversals. In the discussion following, the temperature values are referenced by the "true" temperature followed by the letter A for original value or B for reverse or repeated value.

Table 5.4. Values of ϕ (T) and r_p (T) at points that were repeated and the percent deviation (% Dev.) from the original values. The letter following the temperatures correspond to A (original value) and B (repeated or reversed value): Solvent = D_2O, $[G]_0$ = 3.1 mg/mL, [KCl] = 15 mM, P = 0.1 MPa.

Bath Temperature (^{0}C)	**"True" Temperature (+/- 1 ^{0}C)**	**ϕ (T)**	**r_p (T)**	**% Dev. - ϕ (T)**	**% Dev. -r_p(T)**
9A	14.4A	0.5332 +/- 0.0002	7.56×10^{-4} +/- 0.0001	24%	72%
9B	14.4B	0.6616 +/- 0.0001	2.11×10^{-4} +/- 0.0001		
12A	17.0A	0.6143 +/- 0.0004	1.23×10^{-3} +/- 0.001	10%	76%
12B	17.0B	0.6729 +/- 0.0001	2.91×10^{-4} +/- 0.0001		
21A	22.0A	0.7155 +/- 0.0001	2.21×10^{-4} +/- 0.0001	1%	73%
21B	22.0B	0.7082 +/- 0.0001	-6.03×10^{-5} +/- 0.00001		
24A	24.1A	0.6922 +/- 0.0001	-7.80×10^{-4} +/- 0.0001	5%	53%
24B	24.1B	0.6554 +/- 0.0001	-3.67×10^{-4} +/- 0.0001		
30A	29.0A	0.5571 +/- 0.0001	-3.42×10^{-4} +/- 0.0001	3%	44%
30B	29.0B	0.5397 +/- 0.0001	1.92×10^{-4} +/- 0.0001		
33A	31.6A	0.5245 +/- 0.0001	-1.80×10^{-4} +/- 0.0001	5%	184%
33B	31.6B	0.4980 +/- 0.0001	-5.11×10^{-4} +/- 0.0001		

Figure 5.15. Equilibrium extent of polymerization values, ϕ (T), for points where the temperature was reversed and repeated. The arrows indicate the order of measurements: Solvent = D_2O, $[G]_0$ = 3.1 mg/mL, [KCl] = 15 mM, P = 0.1 MPa.

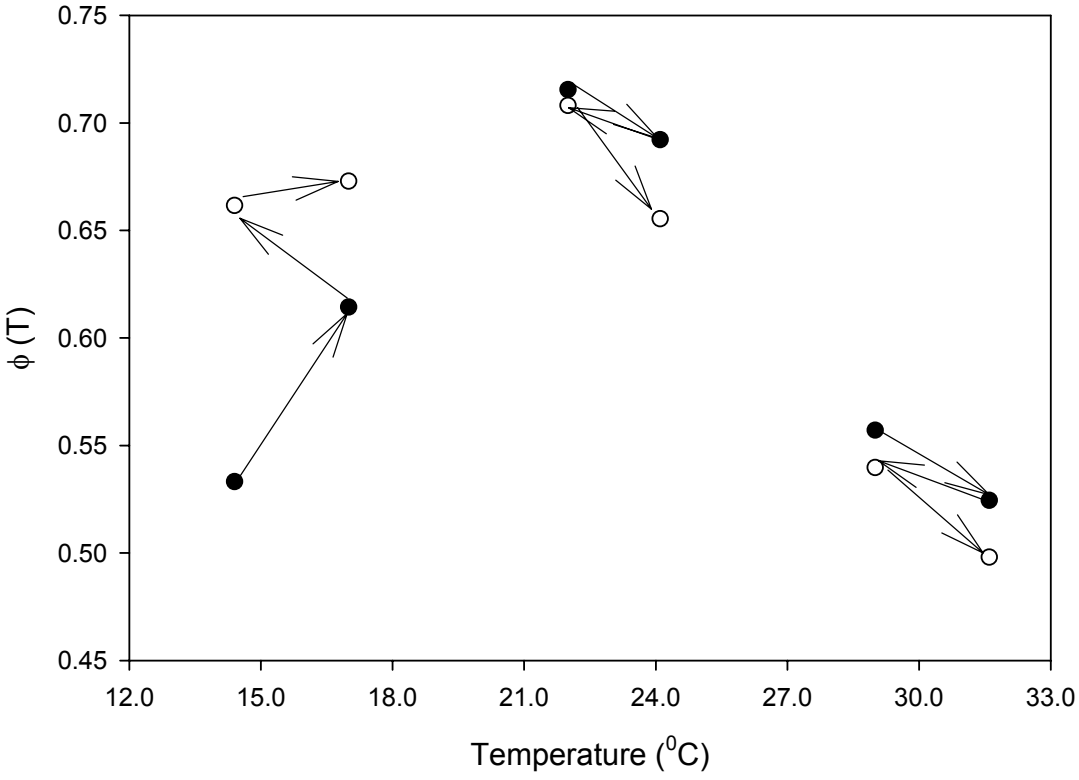

Figure 5.16. Extent of polymerization as a function of time at 14.4 ^{0}C for original (closed circle) and reversal (open circle) values: Solvent = D_2O, $[G]_0$ = 3.1 mg/mL, [KCl] = 15 mM, P = 0.1 MPa.

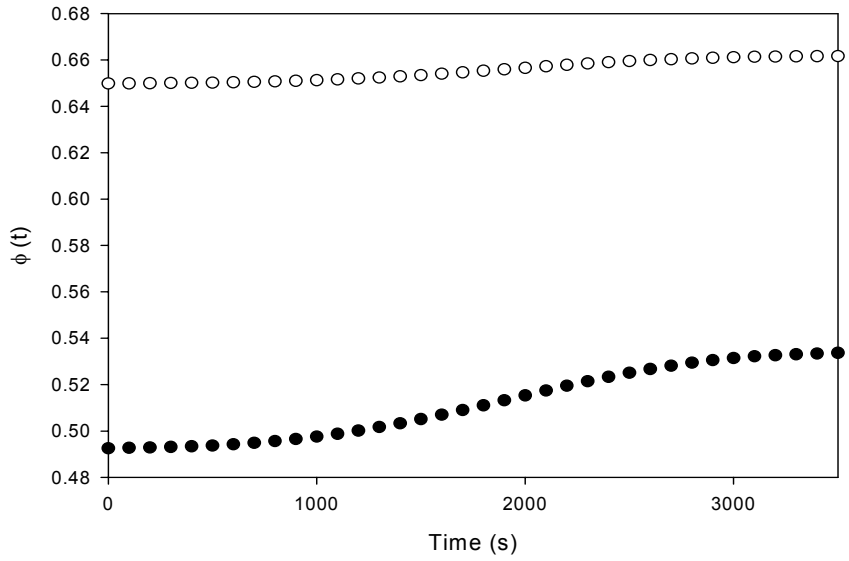

Figure 5.17. Extent of polymerization as a function of time at 17.0 ^{0}C for original (closed circle) and reversal (open circle) values: Solvent = D_2O, $[G]_0$ = 3.1 mg/mL, [KCl] = 15 mM, P = 0.1 MPa.

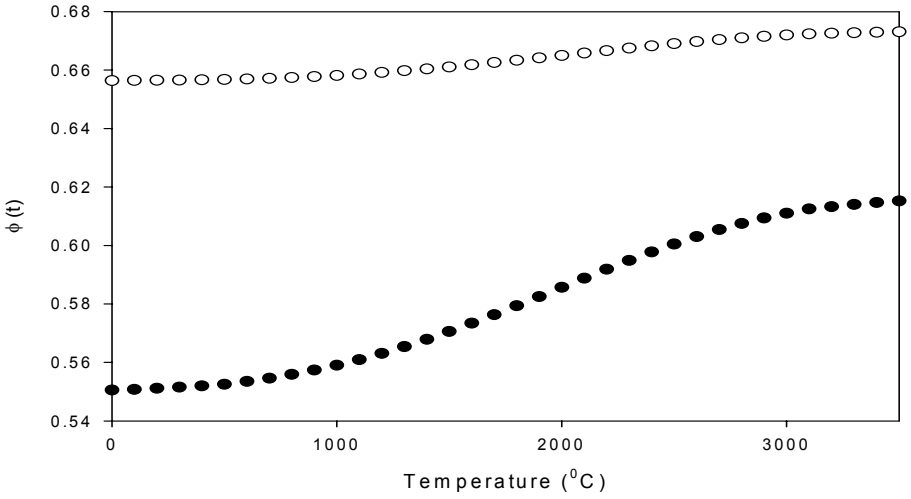

Figure 5.18. Extent of polymerization as a function of time at 22.0 ^{0}C for original (closed circle) and reversal (open circle) values: Solvent = D_2O, $[G]_0$ = 3.1 mg/mL, [KCl] = 15 mM, P = 0.1 MPa.

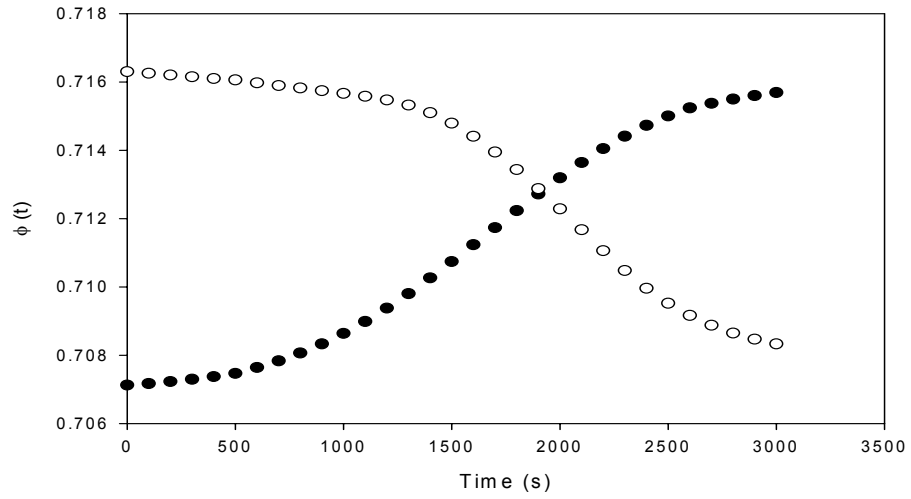

Figure 5.19. Extent of polymerization as a function of time at 24.1 ^{0}C for original (closed circle) and reversal (open circle) values: Solvent = D_2O, $[G]_0$ = 3.1 mg/mL, [KCl] = 15 mM, P = 0.1 MPa.

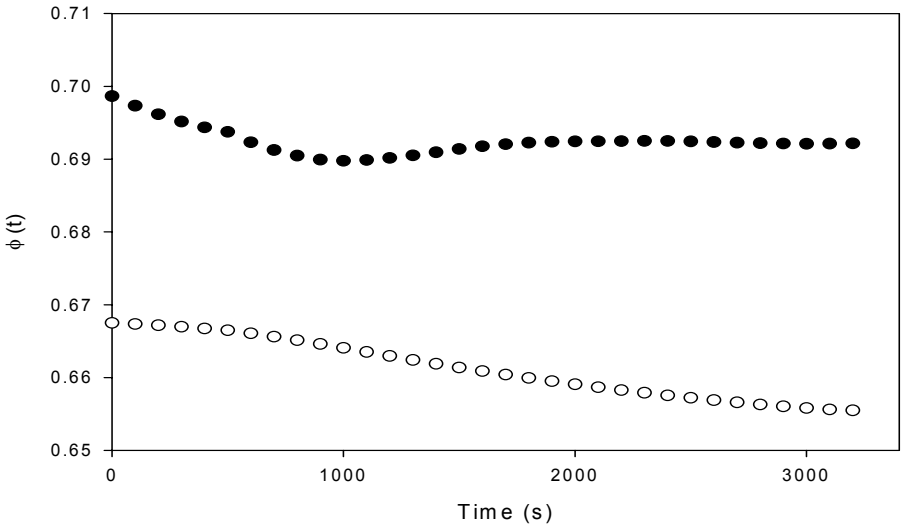

Figure 5.20. Extent of polymerization as a function of time at 29.0 ^{0}C for original (closed circle) and reversal (open circle) values: Solvent = D_2O, $[G]_0$ = 3.1 mg/mL, [KCl] = 15 mM, P = 0.1 MPa.

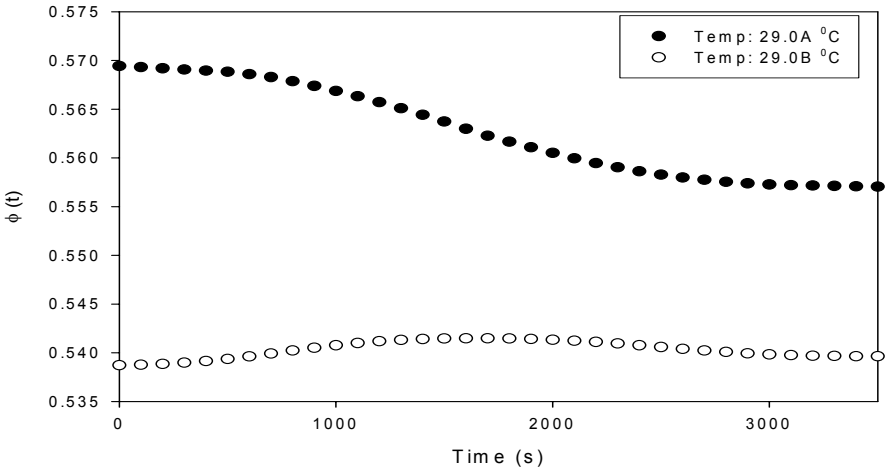

Figure 5.21. Extent of polymerization as a function of time at 31.6 ^{0}C for original (closed circle) and reversal (open circle) values: Solvent = D_2O, $[G]_0$ = 3.1 mg/mL, [KCl] = 15 mM, P = 0.1 MPa.

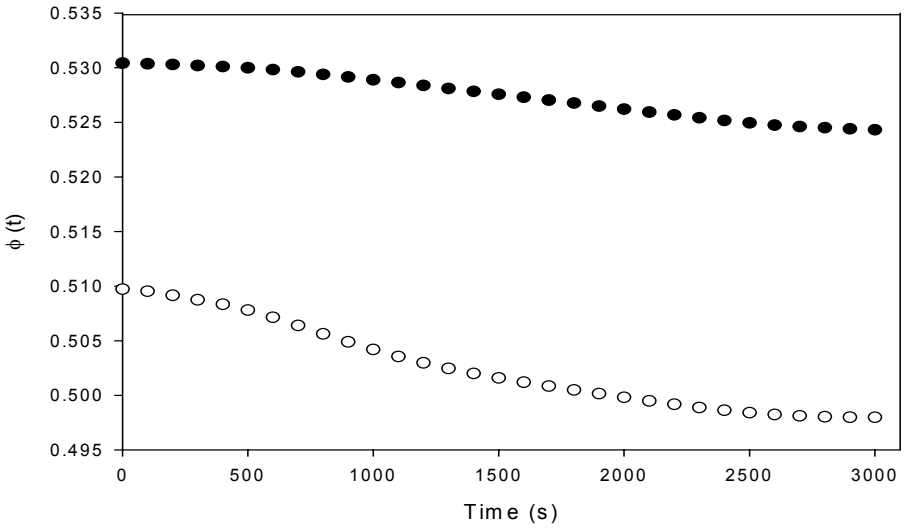

Figure 5.22. Initial values, $r_p(T)$, for points where the temperature was reversed and repeated. "A" values are original temperature values and "B" values are repeated temperature values. Below T_{max}, r_p represents initial polymerization rates and above T_{max}, r_p represents initial depolymerization rates: Solvent = D_2O, $[G]_0$ = 3.1 mg/mL, [KCl] = 15 mM, P = 0.1 MPa.

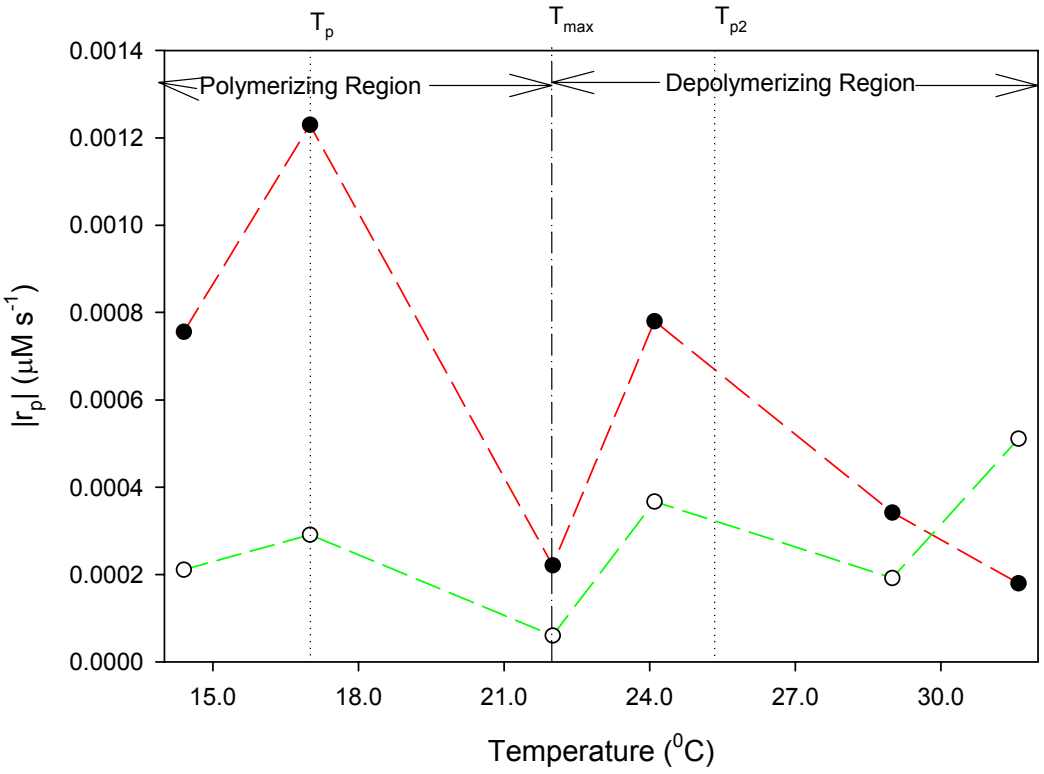

In the polymerizing region, near T_p, the extent of polymerization increased even with a temperature decrease from 17.0A ^{0}C to 14.1B ^{0}C. The deviation from the original value at 14.4A ^{0}C was 24%. The divergence it took, however, indicated that

it did not have the same effect as a positive temperature jump of the same magnitude, because it deviated from the path of the original ϕ (T). Upon return to 17.0B ^{0}C, the extent of polymerization was greater than at 13.0A ^{0}C, but the deviation was even lower at 10%. This suggests that there is significant hysteresis near the transition temperature for polymerization. Near T_{max}, the extent of polymerization actually increased upon a temperature decrease from 24.1A ^{0}C to 22.0B ^{0}C. The deviation was only 1% from the original value at 22.0A ^{0}C. Upon return to 24.1B ^{0}C, the extent of polymerization decreased to a value that was 5% lower than the original value at 24.1A ^{0}C. The small deviations near T_{max} may suggest that reversibility is better in the crossover region from polymerization to depolymerization. The extent also increased going from 31.6A ^{0}C to 29.0B ^{0}C, with a deviation of only 3% from the original value at 29.0A ^{0}C. Upon return from 29.0B ^{0}C to 31.6B ^{0}C, the extent decreased with a deviation of 5% from the original value. This region is analogous to T_{max}, where the extent seems to be approaching a minimum. The conclusion can therefore be made that reversibility can be seen in the extent of actin polymerization in D_2O, especially near the crossover regions.

The initial rate never returned to it original value. Rather, it deviated quite significantly from its original value, suggesting that the kinetics is sensitive to temperature reversals. There seems to be no obvious trend with regard to the magnitude of the deviations as the case might be for the extent of polymerization deviations. It was observed, however, that the initial rate "slowed down" when the temperature was reversed, then "sped up" when the temperature was returned in most cases.

5.2. Run #3: P = 0.1 MPa; [Actin] = 1.0 mg/ml in D_2O Buffer

The extent of polymerization was studied under conditions of atmospheric pressure (~0.1 MPa) in 99% Buffer D. This experiment was performed in the three-position chamber as described above and two samples were analyzed concurrently. The initial concentration of monomer was 1.0 mg/mL (Run #3) and KCl was added to a concentration of [KCl] = 15 mM. The results are reported in this section for Run #3. The effect of the temperature reversals on the thermodynamics and kinetics of Run #3 will be discussed in section 5.2.5.

5.2.1. Extent of Polymerization Results

The fluorescence intensity was measured at a series of bath temperatures starting around 0 °C, as a function of time for approximately one hour at each bath temperature. (See section 5.1.1 for a description of the temperature ranges that were analyzed. The results of the equilibrium extent of polymerization as a function of temperature, ϕ (T), are presented in Table 5.5 and shown in Figure 5.23, where the various temperature ranges are represented by unique symbols. The maximum intensity (complete polymerization) was measured at the final bath temperature of 33 °C upon addition of $MgCl_2$ to 15 mM. The intensity values over time divided by the equilibrium value of the maximum intensity yields the extent of polymerization, both ϕ (T) which is the equilibrium value and ϕ (t) at each temperature. Figure 5.24 is a comparison of the results of ϕ (T) with previous results from a similar experiment.[16] Discussions of these results will be presented in sections 5.1.3.

Table 5.5. Extent of polymerization (ϕ (T)) values as a function of temperature. The "true" temperature was measured by a thermocouple at the sample cell: Solvent = D_2O $[G]_0$ = 1.0 mg/mL, [KCl] = 15 mM, P = 0.1 MPa.

Bath Temperature (^{0}C)	**"True" Temperature (+/- 0.1 ^{0}C)**	**"True" Temperature (+/- 0.1 K)**	**Extent of Polymerization ϕ (T)**	**Reverse Extent of Polymerization ϕ (T)**
0	8.0	281.2	0.4216 +/- 0.0001	
3	11.3	284.5	0.4053 +/- 0.0001	
6	12.8	286.0	0.3987 +/- 0.0001	
9	14.4	287.6	0.4055 +/- 0.0001	0.4463 +/- 0.0002
12	17.0	290.2	0.4278 +/- 0.0003	0.4519 +/- 0.0001
15	18.1	291.3	0.4655 +/- 0.0001	
18	20.0	293.2	0.4970 +/- 0.0001	
21	22.0	295.2	0.5401 +/- 0.0003	0.6193 +/- 0.0001
24	24.1	297.3	0.5697 +/- 0.0003	0.6097 +/- 0.0001
27	26.4	299.6	0.6005 +/- 0.0001	
30	29.0	302.2	0.5782 +/- 0.0001	0.5717 +/- 0.0001
33	31.6	304.8	0.5515 +/- 0.0000	0.5204 +/- 0.0001

Figure 5.23. Extent of polymerization as a function of temperature: Solvent = D_2O, $[G]_0$ = 1.0 mg/mL, [KCl] = 15 mM, P = 0.1 MPa. Symbols represent the various temperature ranges, as discussed in the section 5.1.

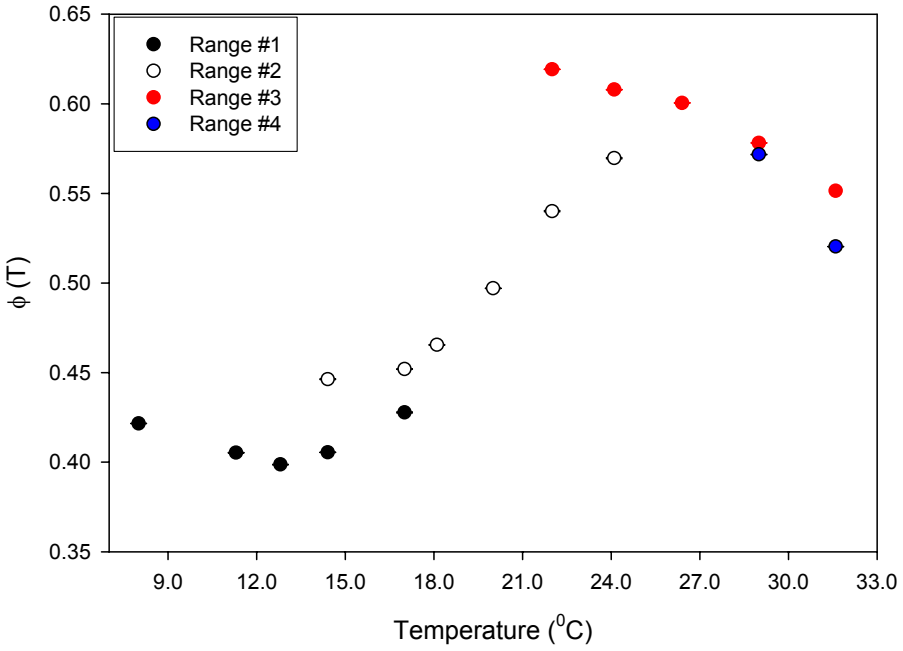

5.2.2. Initial Rates of Polymerization

In analyzing the kinetics of polymerization, the data of $M_f(t)$ between 0 and 600 seconds (see the transient temperature region in Figure 5.7) is first truncated and the time is set to t = 0 at the temperature equilibration time of 600 seconds. The results of r_p at all temperatures are shown in Table 5.6 below. Figure 5.24 depicts the initial rate as a function of temperature, r_p (T), for the entire experiment. Discussions of these results are presented in sections 5.2.4.

Figure 5.24. Initial polymerization rate, r_p, as a function of temperature for each temperature range: Solvent = D_2O, $[G]_0$ = 1.0 mg/mL, [KCl] = 15 mM, P = 0.1 MPa.

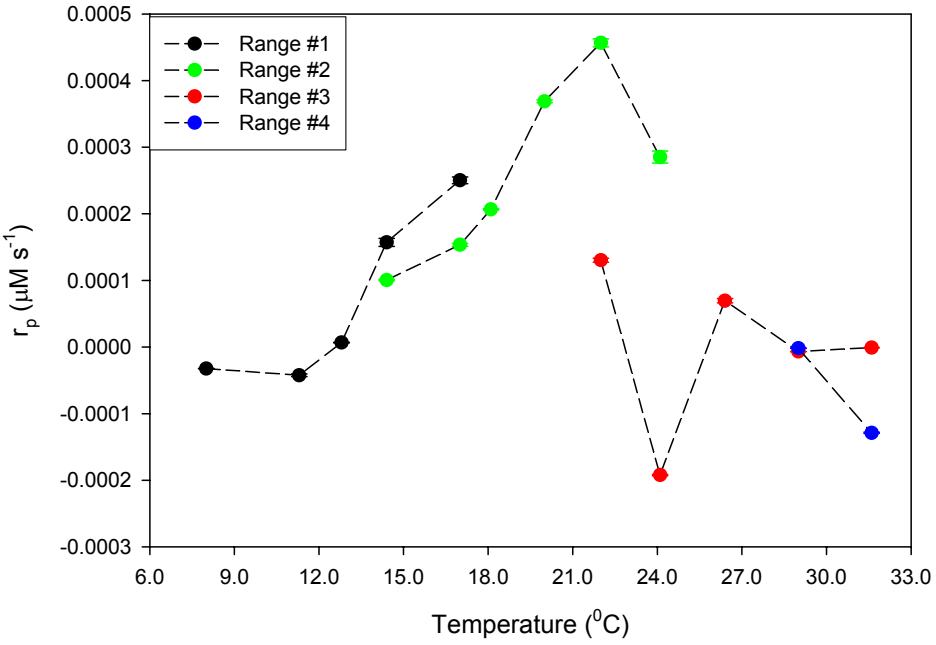

Table 5.6. Initial rate ($\mu M\ s^{-1}$) of polymerization as a function of temperature. The "true" temperature was measured by a thermocouple at the sample cell: Solvent = D_2O, $[G]_0$ = 1.0 mg/mL, [KCl] = 15 mM, P = 0.1 MPa.

Bath Temperature (^0C)	**"True" Temperature (+/- 1 ^0C)**	**Initial Rate, r_p ($\mu M\ s^{-1}$)**	**Reverse Initial Rate, r_p ($\mu M\ s^{-1}$)**
0	8.0	-3.24×10^{-5} +/- 3×10^{-7}	
3	11.3	-4.25×10^{-5} +/- 2.0×10^{-6}	
6	12.8	6.57×10^{-6} +/- 6×10^{-7}	
9	14.4	1.57×10^{-4} +/- 6×10^{-6}	1.00×10^{-4} +/- 1×10^{-6}
12	17.0	2.50×10^{-4} +/- 5×10^{-6}	1.53×10^{-4} +/- 2×10^{-6}
15	18.1	2.07×10^{-4} +/- 1×10^{-6}	
18	20.0	3.69×10^{-4} +/- 2×10^{-6}	
21	22.0	4.57×10^{-4} +/- 6×10^{-6}	1.30×10^{-4} +/- 3×10^{-6}
24	24.1	2.85×10^{-4} +/- 9×10^{-6}	-1.92×10^{-4} +/-1×10^{-6}
27	26.4	6.95×10^{-5} +/- 3.3×10^{-6}	
30	29.0	-6.95×10^{-6} +/- 1.3×10^{-7}	-1.79×10^{-6} +/- 1.7×10^{-7}
33	31.6	-8.30×10^{-4} +/- 4×10^{-8}	-1.29×10^{-4} +/- 1×10^{-6}

5.2.3. Discussion - Thermodynamics

The thermodynamic (extent of polymerization) data in this section were collected at conditions that mirror the conditions of a previous experiment performed at 1.0 mg/mL, atmospheric pressure (0.1 MPa) and 15.00 mM KCl.[16]

The results of this study were compared with the results of Niranjan et al.[15,16] The results are summarized in Table 5.7 and plotted in Figure 5.25. The appearance of an inflection point defined as the transition point T_p, is evident in both plots and the T_p values, both near 21 ^{0}C, are in excellent agreement with each other. The maximum in the extent of polymerization was also exhibited in both plots, but T_{max} for Niranjan et al. was about six degrees higher. The initial extent of polymerization for the current work is about four times that of Niranjan et al.[16] and may contribute to the lowering of T_{max} also seen in Figure 5.6. These studies have shown that for comparable experiments, T_p is not dependent on the initial extent of polymerization; but T_{max} and ϕ_{max} generally seem to be lowered if the initial extent is higher. Neither plot gave any evidence of a second inflection point beyond T_{max} and the existence of T_{p2}. This may be because the temperature ranges were not sufficient to exhibit this region.

Table 5.7. Comparison of results from current and prior work on actin polymerization: Solvent = D_2O, $[G]_0$ = 1.0 mg/mL, [KCl] = 15 mM, P = 0.1 MPa. Errors on T and ϕ are rough estimates based on visual extrapolation of the data in Figure 5.6.

Parameters	**Current Results**		**Niranjan Results[16]**	
$[G]_0$	1.00 (+/-0.01) mg/mL		1.00 (+/-0.01) mg/mL	
[KCl]	15.0 (+/- 0.1) mM		15.00 (+/- 0.01) mM	
T_p, ϕ_p	21 (+/-2) ^{0}C	0.58 (+/-0.05)	21 (+/-2) ^{0}C	0.58 (+/-0.05)
T_{max}, ϕ_{max}	27 (+/-2) ^{0}C	0.57 (+/-0.05)	35 (+/-2) ^{0}C	0.74 (+/-0.05)
T_{p2}, ϕ_{p2}	None in these temperature ranges.			

Figure 5.25. Extent of polymerization as a function of temperature in Buffer D: Solvent = D_2O, $[G]_0$ = 1.0 mg/mL, [KCl] = 15 mM, P = 0.1 MPa. The black circles represent current results and the open circles represent data from Niranjan et al.[16]

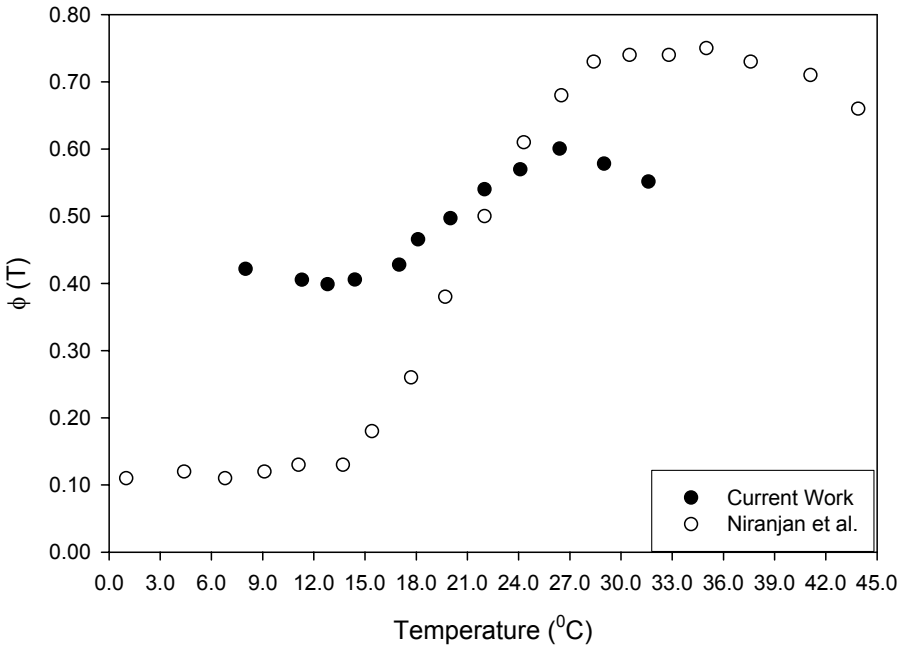

The effect of concentration on actin extent of polymerization in D_2O will be discussed in section 5.3 by comparing the results in this section. The conclusion, however, can be made here that T_p and T_{max} exist for actin polymerization in D_2O, suggesting again that entropy is the driving force. These results are important because actin as well as other biomolecules are frequently introduced into D_2O for analysis with instruments such as neutron scattering[14] or NMR, and the effect of this environmental change on the thermodynamics of the system must be known if any comparison to H_2O is made. It has already been shown elsewhere[18] that this effect is not trivial and that T_p is not monotonic with respect to the initial monomer concentration.[16]

5.2.4 Discussion – Kinetics

The r_p, the initial polymerization rate is defined in chapter four as the fastest overall rate difference of the forward reaction and the reverse reaction of all species in solution. This definition is again used here and a plot in Figure 5.26 shows r_p as a function of temperature compared to ϕ (T), both without the reversal points. Further analysis and discussions follow this plot.

Figure 5.26. Initial polymerization rate, r_p, and ϕ as functions of temperature excluding the reverse points: Solvent = D_2O, $[G]_0$ = 1.0 mg/mL, [KCl] = 15 mM, P = 0.1 MPa.

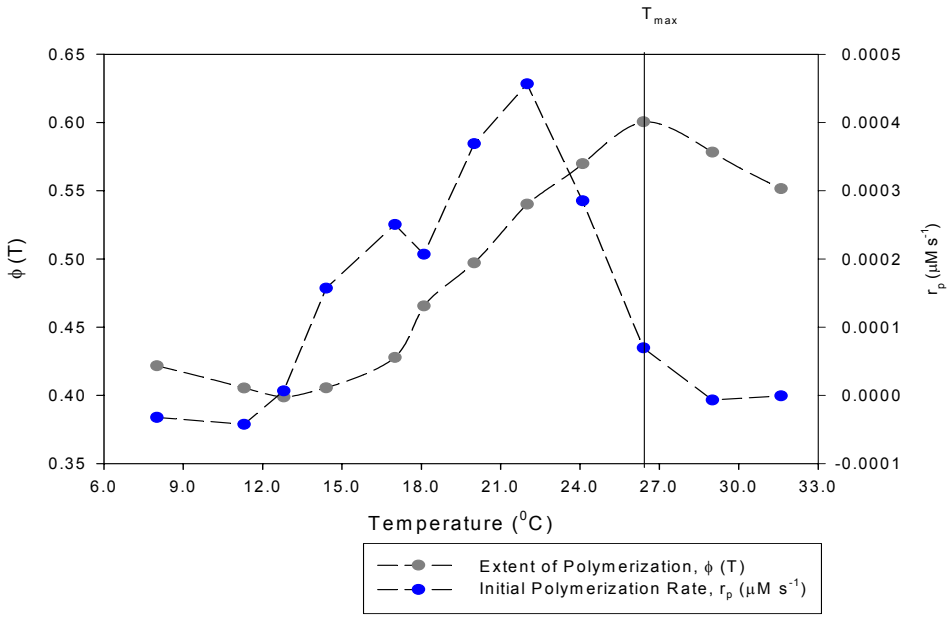

The results of these initial rate calculations again also show an unforeseen relationship to the extent of polymerization plot as seen in Figure 5.26. At or very near the inflection point, T_p, in the ϕ (T) plot, the plot of r_p (T) exhibits extrema. The initial rate shows a maximum at T_p and passes through zero near T_{max}. The arguments used in chapter four to explain the initial rate as it relates to the extent of polymerization are assumed valid for this case. The effect of the solvent on the magnitude of r_p is discussed in section 5.3.

5.2.5 Effect of Temperature Reversal

In these experiments, the temperature was reversed from 17.0 ^{0}C to 14.4 ^{0}C, from 24.1 ^{0}C to 22.0 ^{0}C, and from 31.6 ^{0}C to 29.0 ^{0}C. These chosen points were a repeat of the points used for the experiment in chapter four. The effect of temperature reversals on ϕ (T) is shown in Figure 5.27. A comparison of ϕ (t) for each temperature at which reversals were performed are shown in Figures 5.28-5.33, and the effect of the reversals on the initial polymerization rate is shown in Figure 5.34. Table 5.8 below summarizes the results of the responses to the temperature reversals. In the discussion following, the temperature values are referenced by the "true" temperature followed by the letter A for original value or B for reverse or repeated value.

Table 5.8. Values of ϕ (T) and r_p (T) at points that were repeated and the percent deviation (% Dev.). The letters correspond to A (original value) and B (repeated value): Solvent = D_2O, $[G]_0$ = 1.0 mg/mL, [KCl] = 15 mM, P = 0.1 MPa.

Bath Temperature (^{0}C)	**"True" Temperature (+/- 1 ^{0}C)**	**ϕ (T)**	**r_p (T)**	**% Dev. - ϕ (T)**	**% Dev. -r_p(T)**
9A	14.4A	0.4055 +/- 0.0001	1.57×10^{-4} +/- 6×10^{-6}	10%	36%
9B	14.4B	0.4463 +/- 0.0002	1.00×10^{-4} +/- 1×10^{-6}		
12A	17.0A	0.4278 +/- 0.0003	2.50×10^{-3} +/- 5×10^{-6}	6%	94%
12B	17.0B	0.4519 +/- 0.0001	1.53×10^{-4} +/- 2×10^{-6}		
21A	22.0A	0.5401 +/- 0.0003	4.57×10^{-4} +/- 6×10^{-6}	15%	72%
21B	22.0B	0.6193 +/- 0.0001	1.30×10^{-4} +/- 3×10^{-6}		
24A	24.1A	0.5697 +/- 0.0003	2.85×10^{-4} +/- 9×10^{-6}	7%	167%
24B	24.1B	0.6097 +/- 0.0001	-1.92×10^{-4} +/-1×10^{-6}		
30A	29.0A	0.5782 +/- 0.0001	-6.95×10^{-6} +/-1.3×10^{-7}	1%	74%
30B	29.0B	0.5717 +/- 0.0001	1.79×10^{-6} +/-1.7×10^{-7}		
33A	31.6A	0.5515 +/- 0.0000	-8.30×10^{-4} +/-4×10^{-8}	6%	84%
33B	31.6B	0.5204 +/- 0.0001	-1.29×10^{-4} +/-1×10^{-6}		

Figure 5.27. Equilibrium extent of polymerization values, ϕ (T), for points where the temperature was reversed and repeated. The arrows indicate the order of measurements and The letters in the legend correspond to A (original value) and B (repeated or reversed value): Solvent = D_2O, $[G]_0$ = 1.0 mg/mL, [KCl] = 15 mM, P = 0.1 MPa.

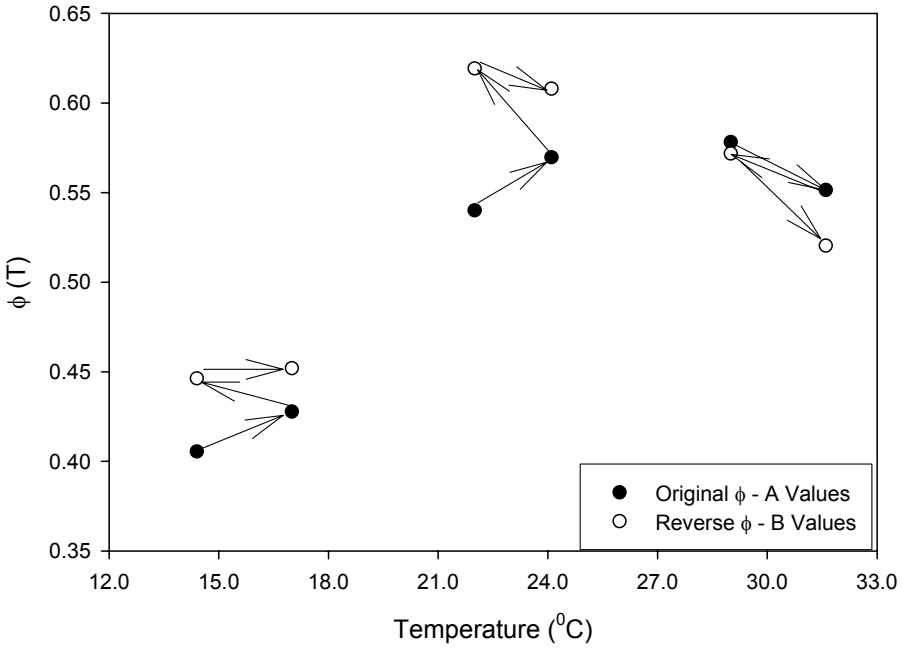

Figure 5.28. Extent of polymerization as a function of time at 14.4 ^{0}C for original (closed circle) and reversal (open circle) values: Solvent = D_2O, $[G]_0$ = 1.0 mg/mL, [KCl] = 15 mM, P = 0.1 MPa.

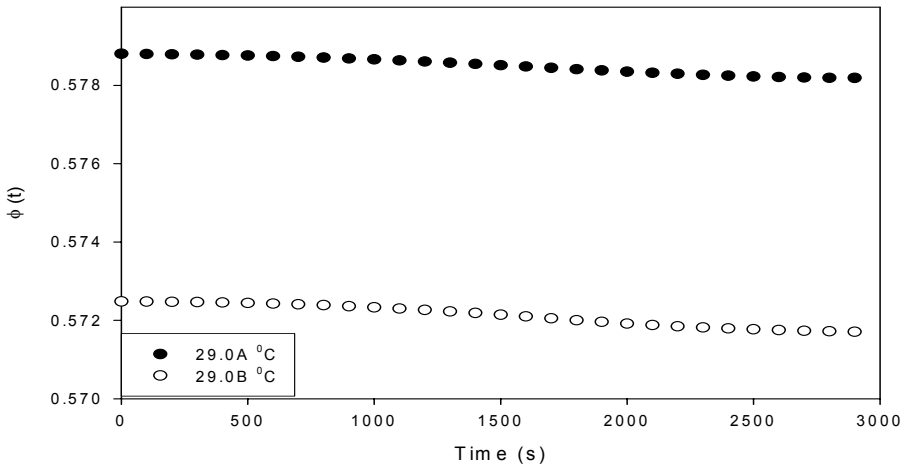

Figure 5.29. Extent of polymerization as a function of time at 17.0 ^{0}C for original (closed circle) and reversal (open circle) values: Solvent = D_2O, $[G]_0$ = 1.0 mg/mL, [KCl] = 15 mM, P = 0.1 MPa.

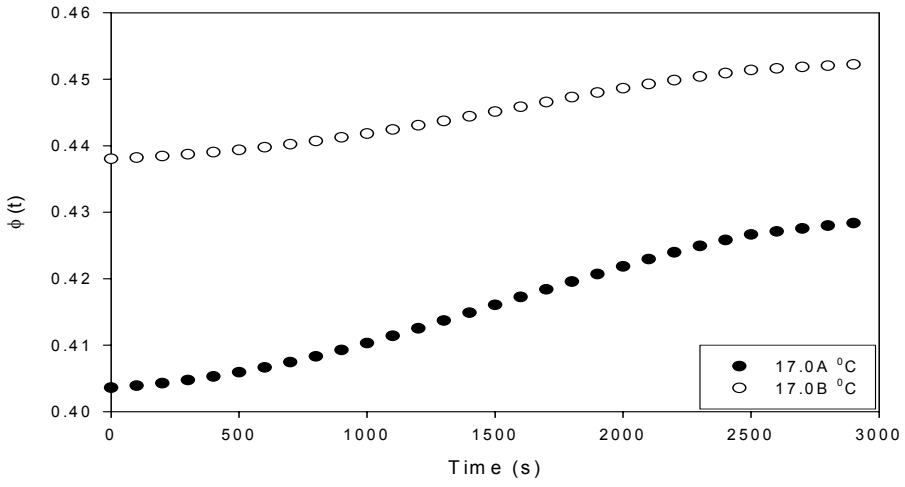

Figure 5.30. Extent of polymerization as a function of time at 22.0 ^{0}C for original (closed circle) and reversal (open circle) values: Solvent = D_2O, $[G]_0$ = 1.0 mg/mL, [KCl] = 15 mM, P = 0.1 MPa.

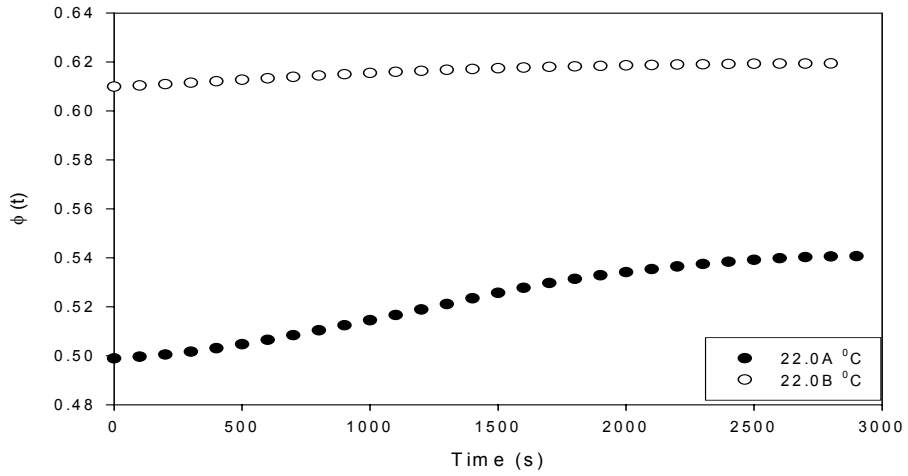

Figure 5.31. Extent of polymerization as a function of time at 24.1 ^{0}C for original (closed circle) and reversal (open circle) values: Solvent = D_2O, $[G]_0$ = 1.0 mg/mL, [KCl] = 15 mM, P = 0.1 MPa.

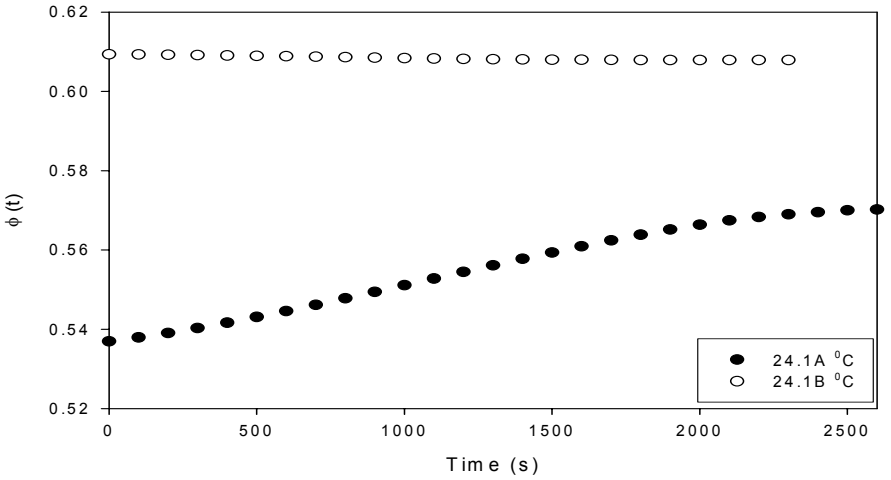

Figure 5.32. Extent of polymerization as a function of time at 29.0 ^{0}C for original (closed circle) and reversal (open circle) values: Solvent = D_2O, $[G]_0$ = 1.0 mg/mL, [KCl] = 15 mM, P = 0.1 MPa.

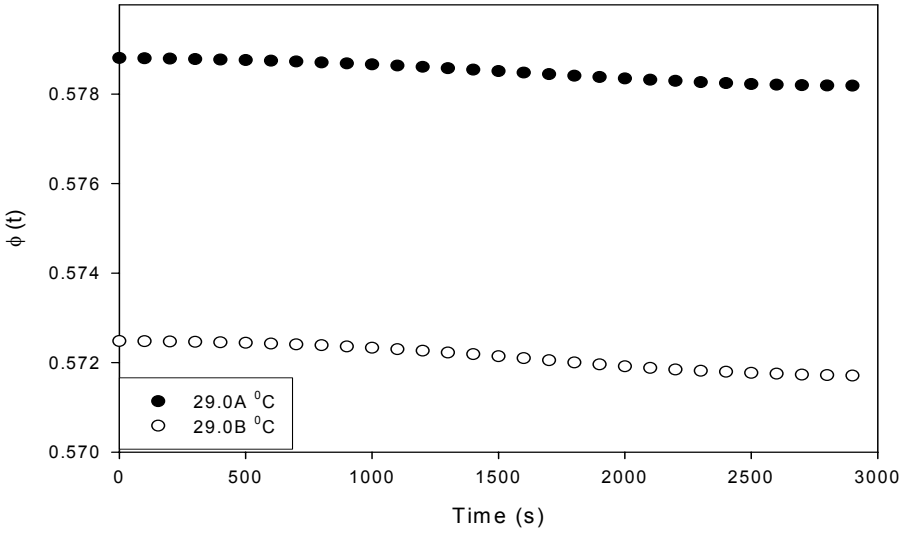

Figure 5.33. Extent of polymerization as a function of time at 31.6 ^{0}C for original (closed circle) and reversal (open circle) values: Solvent = D_2O, $[G]_0$ = 3.1 mg/mL, [KCl] = 15 mM, P = 0.1 MPa.

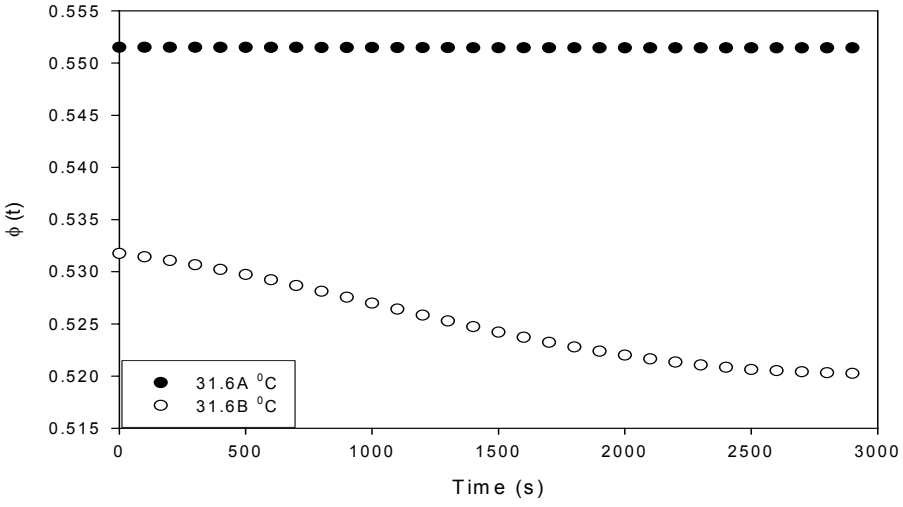

Figure 5.34. Initial values, $r_p(T)$, for points where the temperature was reversed and repeated. "A" values are original temperature values and "B" values are repeated temperature values. Below T_{max}, r_p represents initial polymerization rates and above T_{max}, r_p represents initial **de**polymerization rates: Solvent = D_2O, $[G]_0$ = 1.0 mg/mL, [KCl] = 15 mM, P = 0.1 MPa.

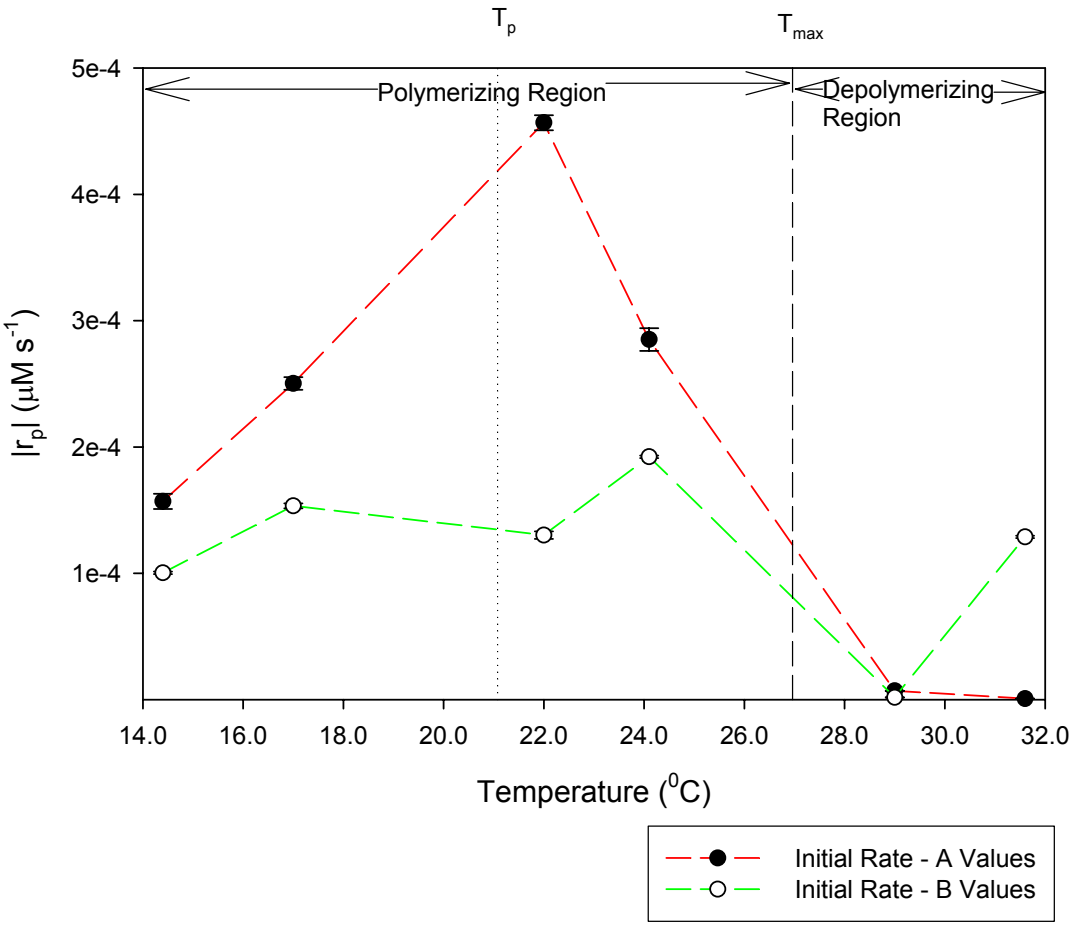

In the polymerizing region, near T_p, Figure 5.21 shows that ϕ increased with temperature decrease from 17.0A ^{0}C to 14.1B ^{0}C. Going back up to 17.0B ^{0}C, ϕ increased but not by much. At 24.1A ^{0}C, ϕ increased when the temperature was

lowered to 22.0B ^{0}C, but the temperature decreased back down towards 24.1B ^{0}C. The most telling point was for 29.0B ^{0}C, where ϕ actually returned to its original value for 29.0A ^{0}C coming from 31.6A ^{0}C, with a deviation of only 1%. The extent decreased upon temperature increase in the depolymerizing region from 29.0B ^{0}C to 31.6B ^{0}C. The calculation of the percent deviation of the reversed values from the original values showed that at every temperature that was repeated, the deviation was 15% or less for Run #3, suggesting that reversibility is more favorable for lower initial concentrations of G-actin. It was also seen that reversibility, as reflected in a small percent deviation value, is more favorable in the region near T_{max}, the crossover from polymerization to depolymerization.

The initial rate in every case before T_{max} was significantly lower than its initial value at a particular temperature, with the greatest deviation at 24.1 ^{0}C in the region past T_p, the region in which diffusion dominates the kinetics of polymerization. The initial rate "slows down" when the temperature is lowered, then "speeds up" when the temperature is returned in most cases. The magnitudes of the initial rates for the two depolymerization points are much lower than the initial rates in the polymerizing region.

5.3. The Solvent and Concentration Effect

Run #1 and Run#2 can be compared for 3 mg/ml and 15 mM of initiating KCl. For the solvent effect at 1.0 mg/ml, Run #3 can be compared with prior results of 1.0 mg/ml plus 15 mM KCl in H_2O; the major difference between the experiments is the nature of the solvent – H_2O versus D_2O based buffer. Figure 5.35 shows ϕ (T) for the

3 mg/ml runs, Figure 5.36 shows ϕ (T) for the 1 mg/ml runs, Figure 5.37 compares r_p (T) for Runs#1, 2, and 3. Figure 5.38 compares ϕ (T) for Run #2 and Run #3. At 3 mg/ml and 15 mM KCl, it seemed that both T_p and T_{p2} were increased by D_2O buffer. Quite the opposite happens at 1 mg/ml + 15 mM KCl as seen in Figure 5.24. $T_p(D_2O) - T_p(H_2O)$ is now -10, suggesting that the D_2O solvent lowers T_p below that for H_2O. Since this difference is positive for 3 mg/ml, it is necessary that it pass through zero as a function of initial monomer concentration.

The initial rate plot, Figure 5.37 shows that the magnitude in rate is greatest for the 3 mg/mL actin sample in H_2O, followed by the 3 mg/mL actin sample in D_2O – decreasing by a factor of 10, followed by the 1 mg/mL actin sample in D_2O. These results suggest that the solvent plays a stronger role on kinetics of polymerization than does initial actin concentration. The role of G-actin concentration in buffer D is the same as for buffer A – T_p increases as $[G_0]$ decreases as shown in Figure 5.26.

Figure 5.35. ϕ (T) 3 mg/ml: Comparing H_2O to D_2O solvents.

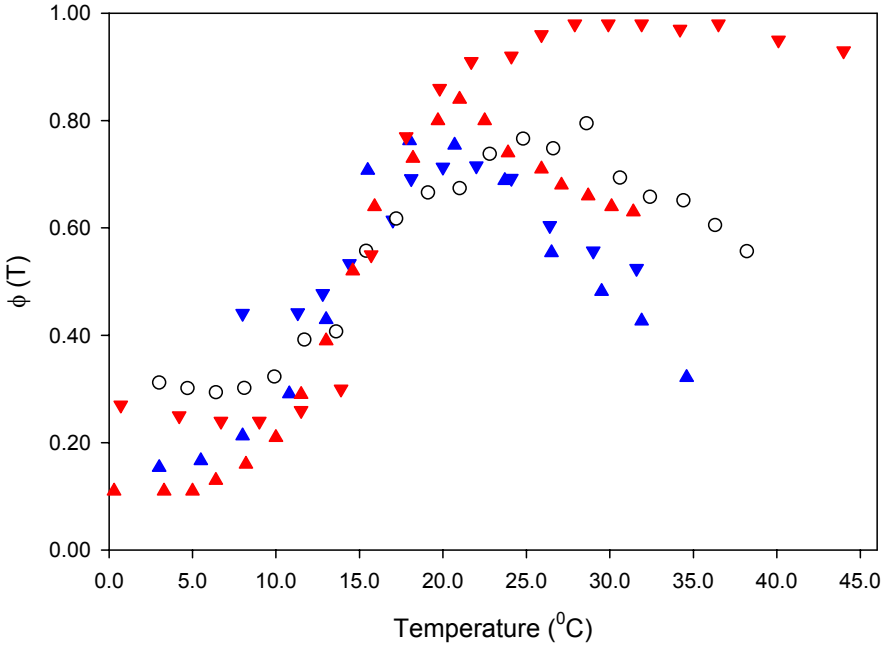

Figure 5.36. 1 mg/ml: Comparing H_2O to D_2O solvents.

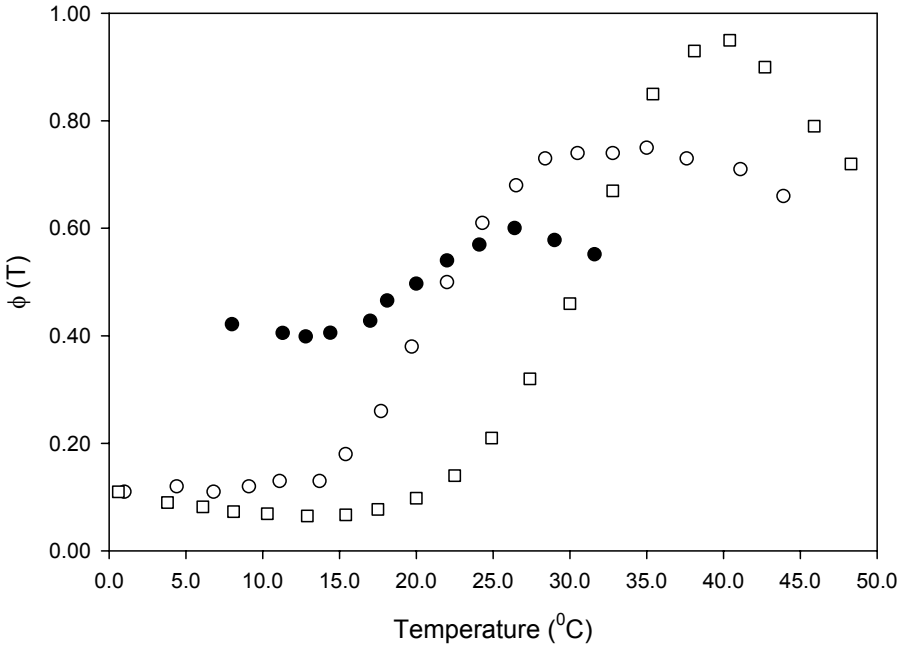

Figure 5.37. r_p (T) for 3 mg/ml: A comparison of solvents.

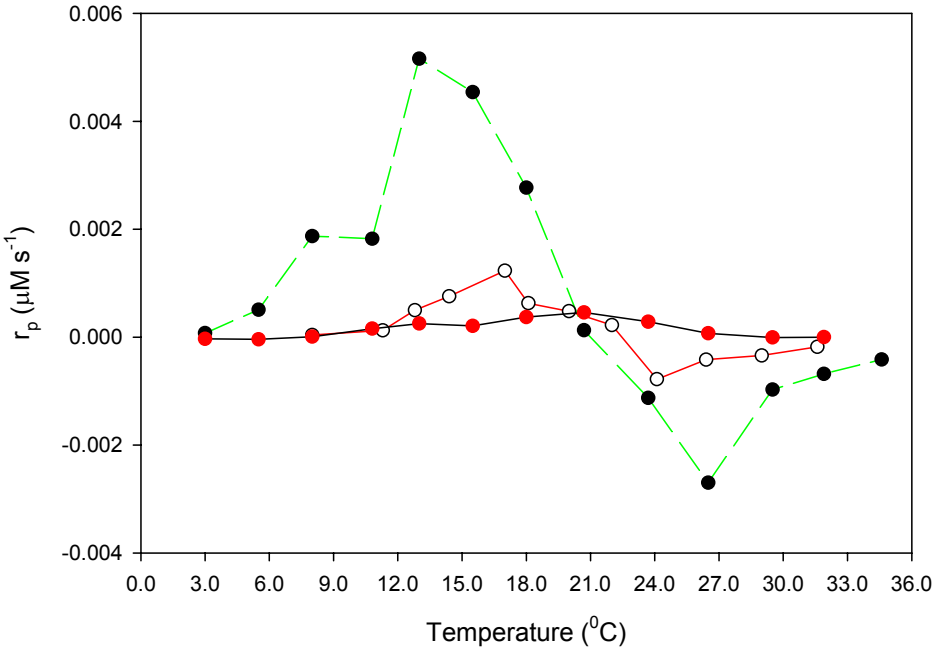

Figure 5.38. Initial actin concentration effect on ϕ (T) in D_2O.

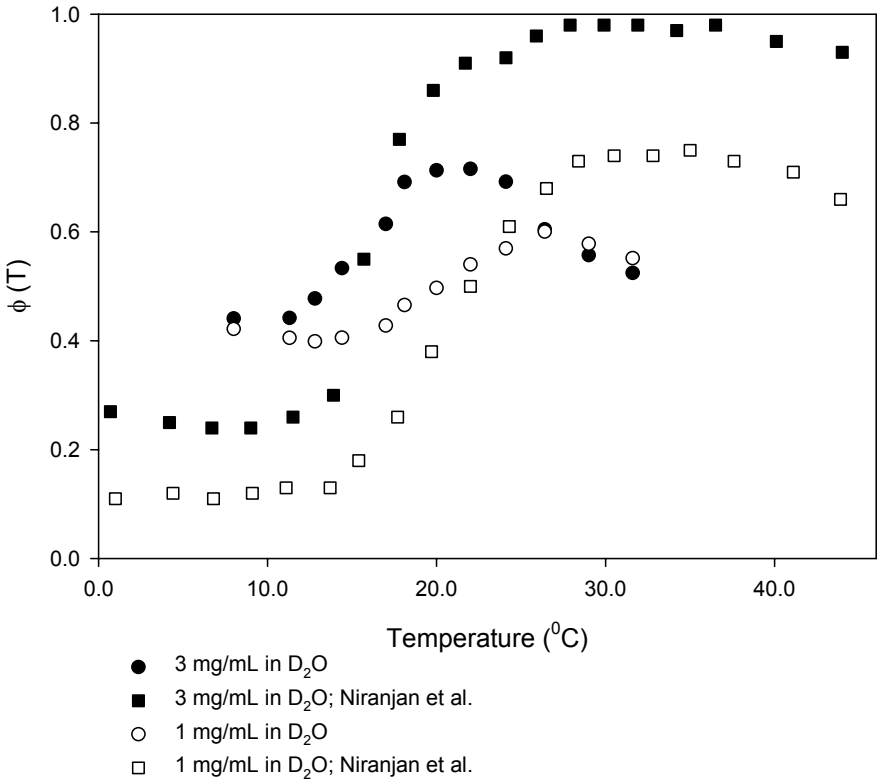

Chapter 6: Results/Discussion of Actin Polymerization under High Pressure

6.1. Run #4: P = 10 MPa; [Actin] = 2.93 mg/ml in H_2O Buffer

The extent of polymerization as a function of temperature was studied under constant hydrostatic pressures of 10 MPa (Run #4) and 20 MPa (Run #5). This experiment was performed in an ethanol-filled pressure chamber as described in chapter three. The initial concentrations of monomer of the two samples were $[G_0]$ = 2.93 mg/mL (Run #4) and 3.02 mg/mL (Run #5). Both samples were initiated by KCl at a concentration of 15 mM. The results of Run #4 are reported in this section and the results of Run #5 are reported in section 6.2 and both are compared with Run #1 in 6.3.

The temperature reversals were not done under high pressure because attempts to do so consistently resulted in aberrant data that could not be correlated or legitimately explained. The cause for this peculiar behavior could be attributed to the effect of temperature on pressure due to the thermal expansion of the hydrostatic fluid, ethanol. Increasing or decreasing temperature increases or decreases the fluid pressure, though possibly at different rates for each process. This naturally affects the polymerization properties. Although care was taken to re-adjust the pressure every ten to twenty minutes or whenever a noticeable change was observed, it is unknown how the relaxations of temperature, pressure, and polymer concentration due to a negative temperature perturbation affect the extent of polymerization.

6.1.1. Extent of Polymerization Results

The fluorescence intensity was measured in the bath temperature range of 0 – 36 ^{0}C, every 3 degrees as a function of time for approximately one hour at each temperature. The intensity values were divided by the maximum intensity, obtained by measuring the intensity after addition of 15 mM $MgCl_2$ after the last temperature reading, to yield the extent of polymerization as a function of time, ϕ (t). The average of ϕ (t) for the last ten minutes at a given temperature was taken the ϕ (T) for that temperature. Table 6.1 gives the results of ϕ (T) and figure 6.1 shows a plot of ϕ (T). Two plots are shown in figure 6.2 for ϕ (t) at different temperatures. Analysis and discussion of the extent of polymerization as a function of temperature will be presented in section 6.1.3.

Table 6.1. Extent of polymerization (ϕ (T)) values as a function of temperature: Solvent = H_2O $[G]_0$ = 2.93 mg/mL, [KCl] = 15 mM, P = 10 MPa.

Bath Temperature (^{0}C)	**"True" Temperature (+/- 0.5 ^{0}C)**	**"True" Temperature (+/- 0.5 K)**	**Extent of Polymerization ϕ (T)**	**Standard Error**
-2	5.2	278.4	0.6296	1 x 10^{-4}
0	6.2	279.4	0.6026	1 x 10^{-4}
3	8.0	281.2	0.5866	1 x 10^{-4}
6	10.1	283.3	0.5953	1 x 10^{-4}
9	11.8	285.2	0.6709	6 x 10^{-4}
12	14.2	287.4	0.7477	5 x 10^{-4}
15	16.7	289.9	0.8426	7 x 10^{-4}
18	19.0	292.2	0.9367	4 x 10^{-4}
21	21.5	294.7	0.9851	2 x 10^{-4}
24	24.0	297.2	0.9811	1 x 10^{-4}
27	26.7	299.9	0.9573	1 x 10^{-4}
30	29.1	302.3	0.9082	1 x 10^{-4}
33	31.8	305.0	0.8609	1 x 10^{-4}
36	34.3	307.5	0.8085	1 x 10^{-4}

Figure 6.1. Extent of polymerization as a function of temperature: Solvent = H_2O, $[G]_0$ = 2.93 mg/mL, [KCl] = 15 mM, P = 10 MPa.

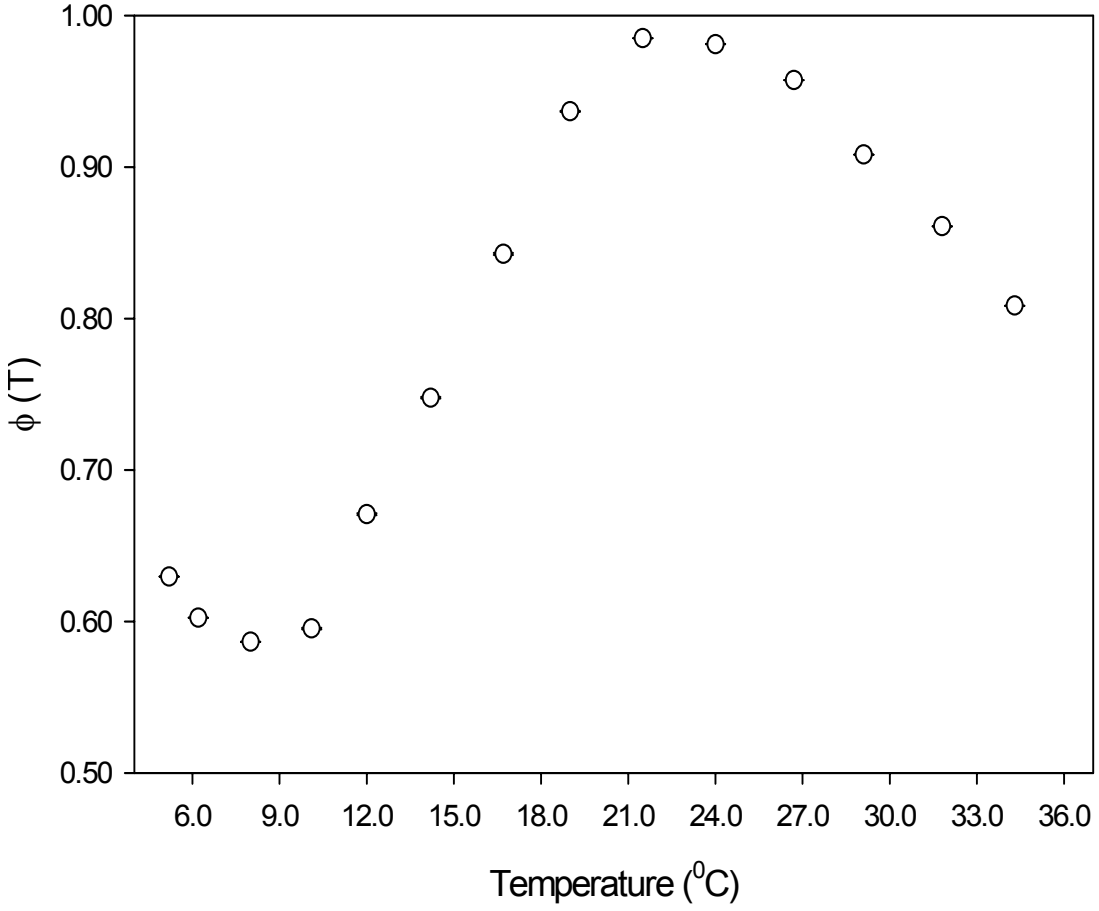

Figure 6.2. Extent of polymerization as a function of time for temperature below (16.7 ^{0}C) and above (29.1 ^{0}C) T_{max}: Solvent = H_2O, $[G]_0$ = 2.93 mg/mL, [KCl] = 15 mM, P = 10 MPa.

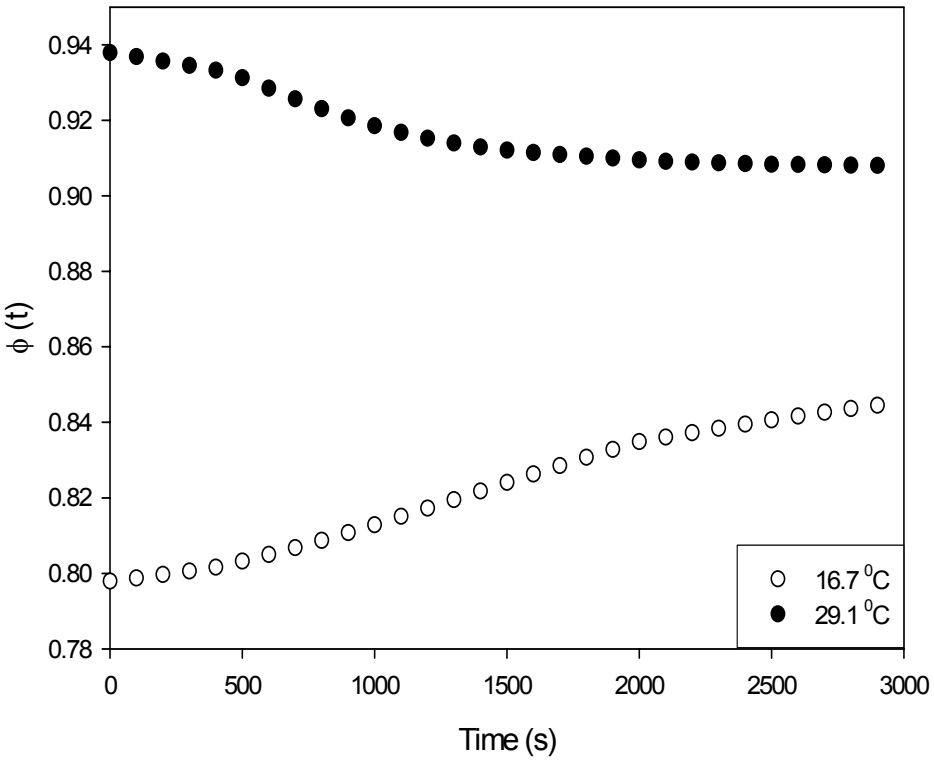

6.1.2 Initial Rates of Polymerization

As in the experiments from chapter four, the actual temperature near the cell as recorded by the datalogger required approximately 10 minutes to reach a steady value. A plot of temperature with time for this experiment is shown in Figure 6.3. The vertical line marks the time at which the temperature equilibrated. The transient regions can actually be observed in the kinetics plots (see Figure 4.2a for example) between 0 and 600 seconds. After the transient region in the kinetics plot, the "reaction", measured through the extent of polymerization, proceeds rapidly for about fifteen minutes.

In analyzing the kinetics of polymerization, the data of $M_f(t)$ (defined in chapter four as $[G_0]$ $(1- \phi)$) between 0 and 600 seconds (the transient temperature region) is first truncated and the time is set to $t = 0$ at the temperature equilibration time of 600 seconds. The results of r_p at all temperatures are shown in Table 6.2. Figure 6.4 depicts the initial rate as a function of temperature, r_p (T), for the entire experiment. Discussions of these results are presented in sections 6.1.4.

Figure 6.3. Temperature near the cell in the pressure chamber as a function for time for the "true" temperature of 11.8 ^{0}C: Solvent = H_2O, $[G]_0$ = 2.93 mg/mL, [KCl] = 15 mM, P = 10 MPa. The vertical line indicates the point beyond which the temperature is fairly constant to +/- 0.5 ^{0}C.

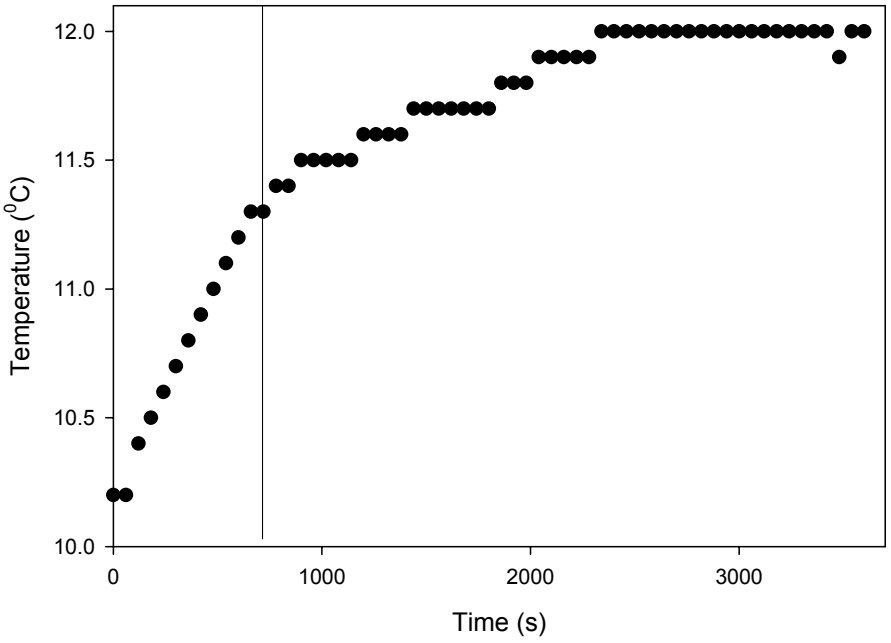

Table 6.2. Initial rate ($\mu M\ s^{-1}$) of polymerization as a function of temperature. The "true" temperature was measured by a thermocouple at the sample cell: Solvent = H_2O, $[G]_0$ = 2.93 mg/mL, [KCl] = 15 mM, P = 10 MPa.

Bath Temperature (^0C)	**"True" Temperature (+/- 0.5 ^0C)**	**Initial Rate, r_p ($\mu M\ s^{-1}$)**	**Standard Error**
-2	5.2	-2.9×10^{-4}	1×10^{-5}
0	6.2	-9.1×10^{-4}	2×10^{-5}
3	8.0	-3.0×10^{-4}	1×10^{-5}
6	10.1	-2.3×10^{-4}	1×10^{-5}
9	11.8	-1.9×10^{-5}	1×10^{-6}
12	14.2	7.9×10^{-4}	4×10^{-5}
15	16.7	7.2×10^{-4}	4×10^{-5}
18	19.0	7.6×10^{-4}	3×10^{-5}
21	21.5	5.6×10^{-5}	6×10^{-6}
24	24.0	-1.4×10^{-4}	1×10^{-5}
27	26.7	-1.0×10^{-3}	1×10^{-4}
30	29.1	-9.0×10^{-4}	5×10^{-5}
33	31.8	-4.7×10^{-4}	5×10^{-5}
36	34.3	-2.0×10^{-3}	1×10^{-4}

Figure 6.4. Initial polymerization rate, r_p, as a function of temperature: Solvent = H_2O, $[G]_0$ = 2.93 mg/mL, [KCl] = 15 mM, P = 10 MPa.

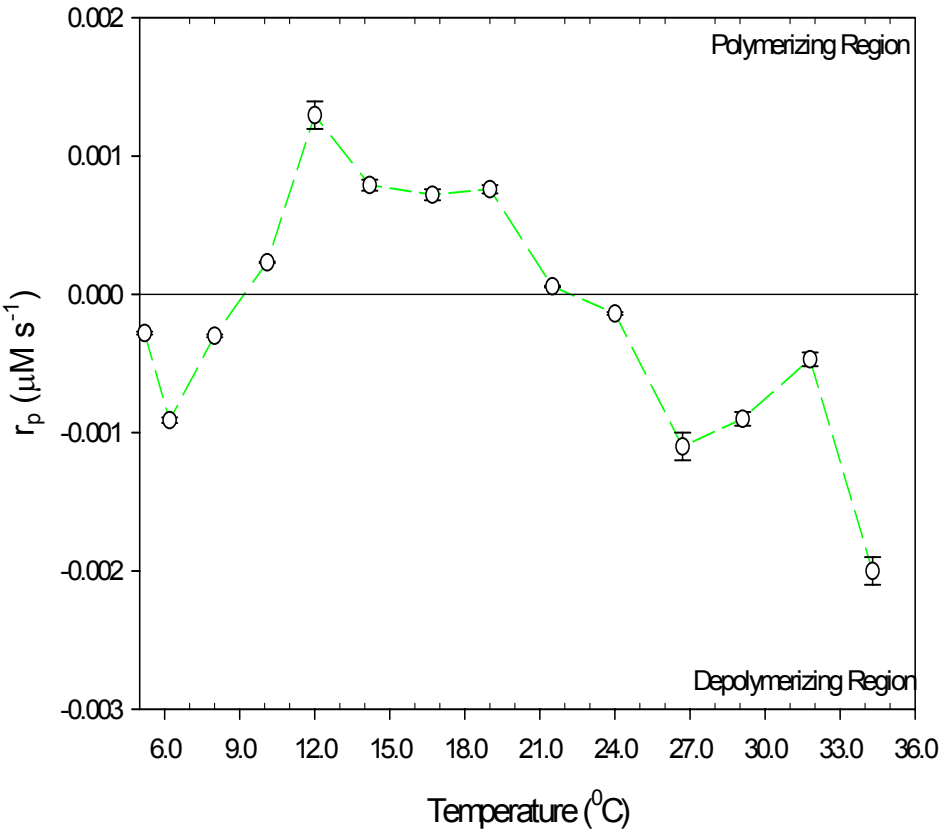

6.1.3 Discussion - Thermodynamics

The thermodynamic (extent of polymerization) data in this section were collected for a 2.93 mg/mL sample in buffer A at a pressure of 10 MPa and initiated by 15 mM KCl. This is the first time that the extent of polymerization with temperature under a constant high pressure is being reported. The experiments have been performed before in this lab but because of instrumental insufficiencies, the data did not have an acceptable degree of precision. The results of those previous experiments however, which are discussed briefly in chapter seven, suggested that

pressure had a significant effect on the transition temperature, T_p. It is expected that knowledge of the sign and the order of magnitude of the volume change upon polymerization as well as the effects of pressure on the extent of polymerization and the kinetics can be obtained from these experiments. This discussion is presented in chapter seven. A plot of ϕ (T) is reproduced in Figure 6.5 with the transition and crossover points indicated and Table 6.3 gives the values at these points.

Figure 6.5. Extent of polymerization as a function of temperature showing T_p, T_{max}, and T_{p2}: Solvent = H_2O, $[G]_0$ = 2.93 mg/mL, [KCl] = 15 mM, P = 10 MPa.

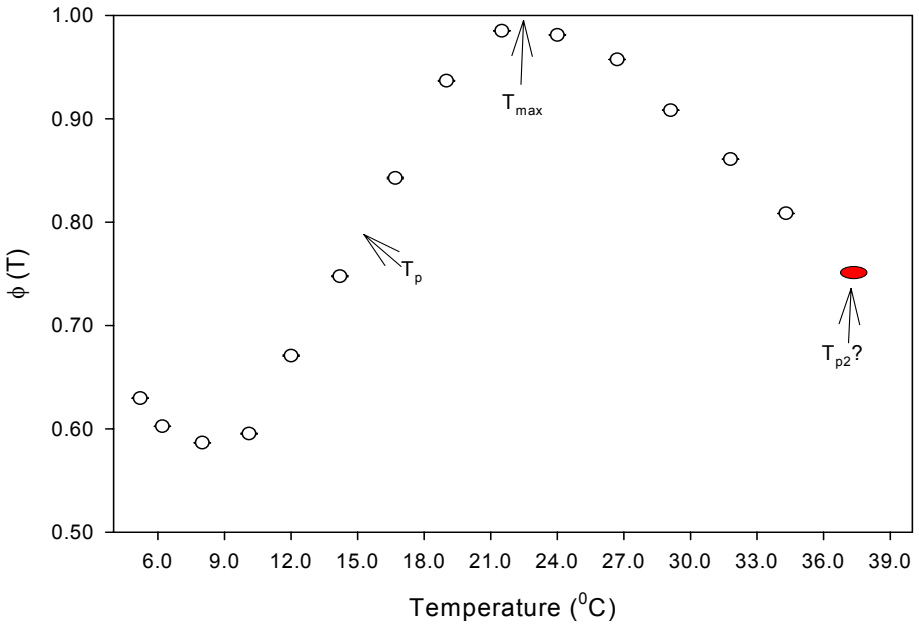

Table 6.3. Results from current work on actin polymerization: Solvent = H_2O, $[G]_0$ = 2.93 mg/mL, [KCl] = 15 mM, P = 10 MPa. Errors on T and ϕ are rough estimates based on visual extrapolation of the data in Figure 6.5.

Parameters	**Results**	
$[G]_0$	2.93 (+/-0.01) mg/mL	
[KCl]	15.0 (+/- 0.1) mM	
T_p, ϕ_p	16 (+/-2) ^{0}C	0.81 (+/-0.05)
T_{max}, ϕ_{max}	22 (+/-2) ^{0}C	0.99 (+/-0.05)
T_{p2}, ϕ_{p2}	39? ^{0}C	0.75?

The trend in Figure 6.2 is very similar to the trend observed for ϕ (T) at atmospheric pressure, suggesting that actin polymerization under pressure remains entropically driven – that is, ΔH and ΔS are both positive for polymerization. There are a few differences, however, that must be noted. It was first observed that the extent of polymerization starts at a rather high value, 0.62, even at this low temperature. This may be explained through Le Châtelier's Principle, which states that when stress is applied to a system at equilibrium, the reaction proceeds in the direction to neutralize the stress. Initially and at very low temperatures well below T_p, the sample is constituted of essentially monomers and the dimerization reaction, where two moles of monomers react to form one mole of dimers, can occur. Applying pressure or decreasing the sample volume at this stage favors dimers because the system wants to counteract the effective increase in moles per unit

volume according to Le Châtelier's Principle. Another observation of ϕ (T) at 10 MPa is that the extent initially decreases as temperature increases up to 8.0 ^{0}C. Since dimerization is an exothermic reaction,[16] an increase in temperature would push the equilibrium back towards monomers. This was not seen in experiments done for the 3 mg/ml samples in buffer A at 0.1 MPa because the experiments began at temperatures so close to the onset of polymerization where the entropy considerations dominate. It is generally observed for other atmospheric pressure experiments[18] where the initial temperature is more than ten degrees below the onset of polymerization.

The data becomes similar to atmospheric pressure experiments past 8 ^{0}C. In fact, an inflection point, T_p, is observed for Run #5 at or very near 16 ^{0}C – 3 degrees higher than the T_p for Run #1 at 0.1 MPa. The comparison is explored and analyzed later in chapter seven. There is also the presence of T_{max} which can be found near 22 ^{0}C. There is no strong evidence of a second inflection point, T_{p2}, past 22 ^{0}C and into the depolymerization region, as observed in atmospheric pressure experiments. This second inflection point may be outside the temperature range and visual extrapolation could very well put it near 38 ^{0}C. The data from Run #6 under 20 MPa do show stronger evidence of a T_{p2} near 34 ^{0}C (see Figure 6.13 in section 6.2). Figure 6.6 gives a schematic of the phase diagram of Run #5 with the observed floor temperature and the postulated ceiling temperature.

Figure 6.6. Schematic phase diagram of the results of the actin polymerization experiment reported in this section: Solvent = H_2O, $[G]_0$ = 2.93 mg/mL, [KCl] = 15 mM, P = 10 MPa.

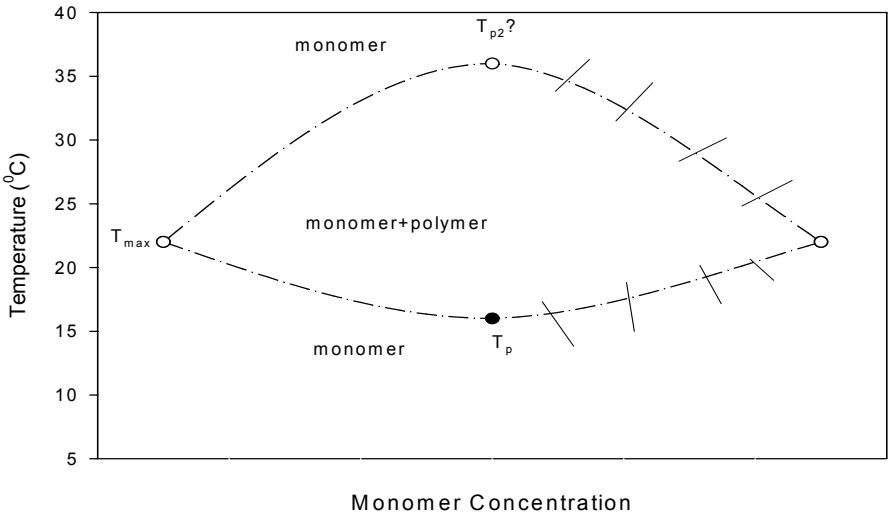

6.1.4 Discussion - Kinetics

The r_p, the initial polymerization rate is defined in chapter four as the fastest overall rate difference of the forward reaction and the reverse reaction of all species in solution. The plot in Figure 6.7 shows r_p as a function of temperature alongside ϕ (T). Figure 6.8 shows the regions separated by T_p.

The trend in the initial rate of polymerization for Run #4 shows remarkable correlation with the extent of polymerization plot. There is a minimum in r_p just before the onset of polymerization in the ϕ (T) plot. The plot of r_p (T) also bears some resemblance to the r_p plots for Runs #1-3 taken at atmospheric pressure. The

similarity is that there is a maximum in r_p near T_p. As suggested in chapters 4, this may result from the expected dramatic increase in viscosity near and above T_p. The highest value for r_p is actually a little before T_p and occurs near the onset of polymerization (11.8 ^{0}C) following the initial decrease in ϕ (T). It is not surprising that the initial rate is at a maximum nearer the onset of polymerization in this run because there are already many oligomers in solution as evidenced by the high extent in polymerization value of 0.6 or 60%.

T_{max} occurs somewhat near T_p and essentially reaches 100% polymerization, a value not achieved before for the extent of polymerization in buffer A either in this work or the prior work.[18] Beyond T_p, the initial rate decreases steadily into the depolymerization region. The local minimum at 26.7 ^{0}C does not correspond to any change in the ϕ (T) data and may be considered an outlier point. The final r_p value at 34.3 ^{0}C approaches zero as observed in the previous r_p plots near T_{p2} for Runs #1 - 3.

Figure 6.7. Initial polymerization rate, r_p, and ϕ as a function of temperature: Solvent = H_2O, $[G]_0$ = 2.93 mg/mL, [KCl] = 15 mM, P = 10 MPa.

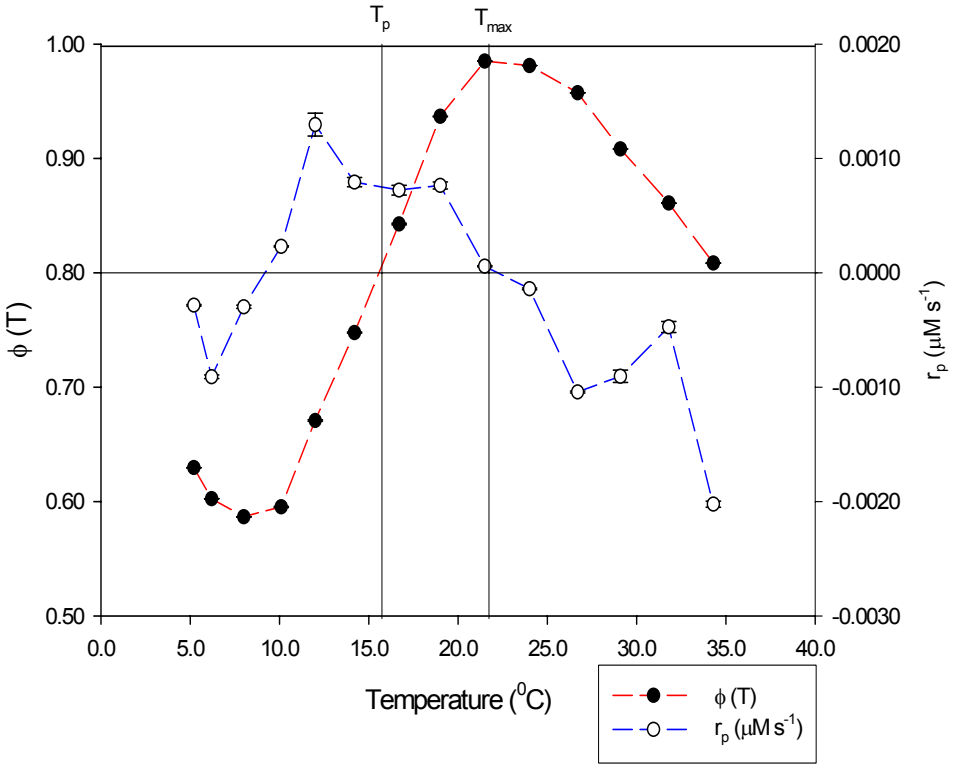

Figure 6.8. Initial rate of polymerization r_p (T) for the region up to (red line) and beyond (blue line) T_p: Solvent = H_2O, $[G]_0$ = 2.93 mg/mL, [KCl] = 15 mM, P = 10 MPa.

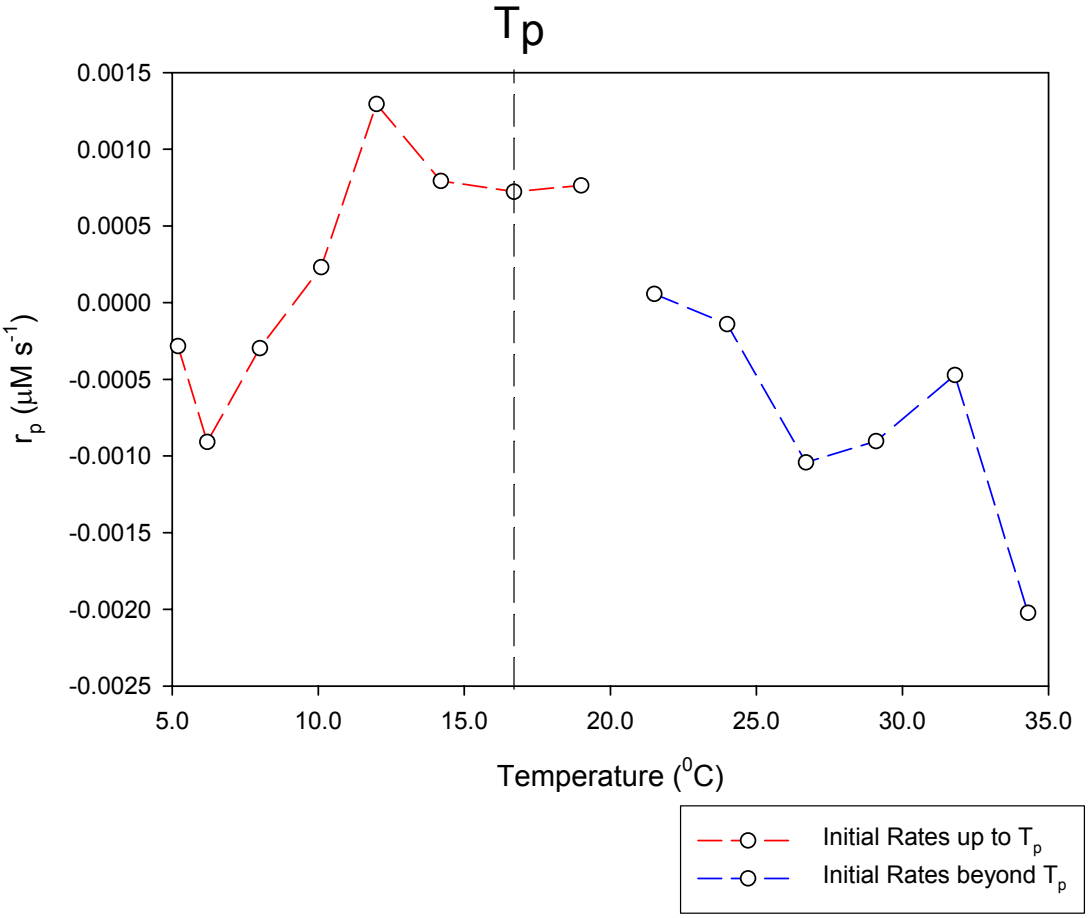

6.2. Run #5: P = 20 MPa; [Actin] = 3.00 mg/ml in Buffer A

The extent of polymerization as a function of temperature was studied under constant hydrostatic pressures of 20 MPa (Run #5). This experiment was performed in an ethanol filled pressure chamber as described in chapter three. The initial concentrations of monomer of this sample was $[G_0]$ = 3.02 mg/mL. The sample was initiated by KCl at a concentration of 15 mM. The peculiar random behavior observed under 10 MPa when temperature reversals were attempted, also occurred under 20 MPa.

6.2.1. Extent of Polymerization Results

The fluorescence intensity was measured in the bath temperature range of 0 – 42 ^{0}C, every 3 degrees as a function of time for approximately one hour at each temperature. The intensity values were divided by the maximum intensity, obtained by measuring the intensity after addition of 15 mM $MgCl_2$ after the last temperature reading, to yield the extent of polymerization as a function of time, $\phi(t)$, with the last ten minutes averaged to give ϕ for a particular temperature. Table 6.4 gives the results of $\phi(T)$ and Figure 6.9 shows a plot of $\phi(T)$. Two plots are shown in figure 6.10 for $\phi(t)$ at different temperatures. All the $\phi(t)$ plots can be found in Appendix A. Analysis and discussion of the extent of polymerization as a function of temperature will be presented in section 6.2.3.

Table 6.4. Extent of polymerization ($\phi(T)$) values as a function of temperature: Solvent = H_2O $[G]_0$ = 3.02 mg/mL, [KCl] = 15 mM, P = 20 MPa.

Bath Temperature (^{0}C)	"True" Temperature (+/- 0.5 ^{0}C)	"True" Temperature (+/- 0.5 K)	Extent of Polymerization ϕ (T)	Standard Error
0	2.6	275.8	0.5681	1×10^{-4}
3	5.6	278.8	0.5323	1×10^{-4}
6	7.5	280.7	0.5103	1×10^{-4}
9	8.8	282.0	0.4945	1×10^{-4}
12	11.0	284.2	0.5007	1×10^{-4}
15	14.2	287.4	0.5496	4×10^{-4}
18	16.5	289.7	0.6302	5×10^{-4}
21	18.8	292.0	0.7202	7×10^{-4}
24	22.0	295.2	0.8541	8×10^{-4}
27	24.5	297.7	0.9499	2×10^{-4}
30	27.3	300.5	0.9741	1×10^{-4}
33	30.0	303.2	0.9657	5×10^{-4}
36	33.5	306.7	0.9316	2×10^{-4}
39	35.5	308.7	0.7973	1×10^{-4}
42	37.4	310.6	0.7571	1×10^{-4}

Figure 6.9. Extent of polymerization as a function of temperature: Solvent = H_2O $[G]_0$ = 3.02 mg/mL, [KCl] = 15 mM, P = 20 MPa.

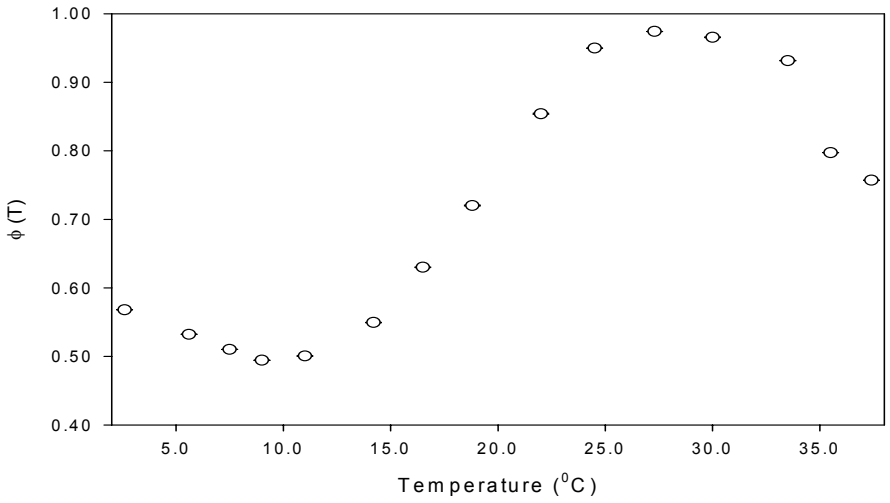

Figure 6.10. Extent of polymerization as a function of time for temperatures below (16.5 ^{0}C) and above (37.4 ^{0}C) T_{max}: Solvent = H_2O $[G]_0$ = 3.02 mg/mL, [KCl] = 15 mM, P = 20 MPa.

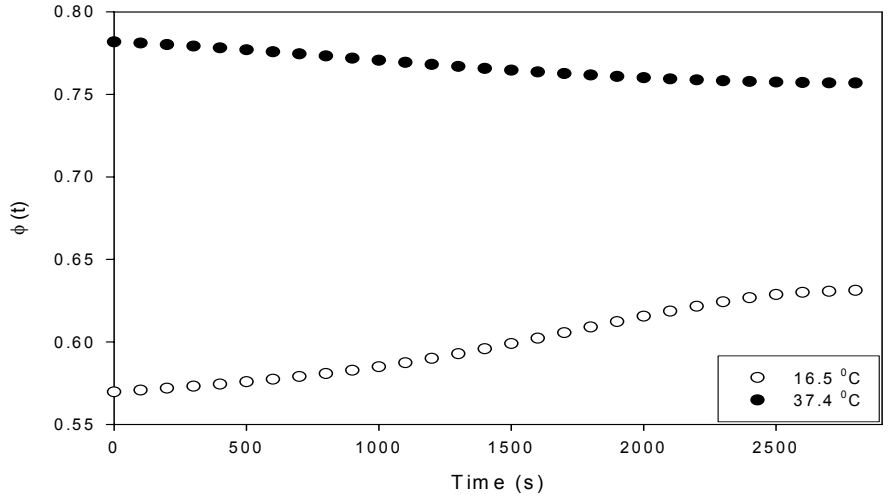

6.2.2. Initial Rates of Polymerization

As in the experiments from chapter four, the actual temperature near the cell as recorded by the datalogger required approximately 10 minutes to reach a steady value. A plot of temperature with time for this experiment is shown in Figure 6.11. The vertical line marks the time at which the temperature equilibrated. After the transient region in the kinetic plot, the "reaction" proceeds rapidly for about fifteen minutes before it begins to approach zero.

In analyzing the kinetics of polymerization, the data of $M_f(t)$, defined in chapter four as $[G_0]$ $(1- \phi)$, between 0 and 600 seconds (the transient temperature region) is first truncated and the time is set to $t = 0$ at the temperature equilibration time of 600 seconds. The results of r_p at all temperatures are shown in Table 6.5. Figure 6.12 depicts the initial rate as a function of temperature, r_p (T), for the entire experiment. Discussions of these results are presented in sections 6.2.4.

Figure 6.11. Temperature near the cell in the pressure chamber as a function for time (taken every two seconds) for the "true" temperature of 8.8 ^{0}C: Solvent = H_2O $[G]_0$ = 3.02 mg/mL, [KCl] = 15 mM, P = 20 MPa. The vertical line indicates the point beyond which the temperature is fairly constant to +/- 0.5 ^{0}C.

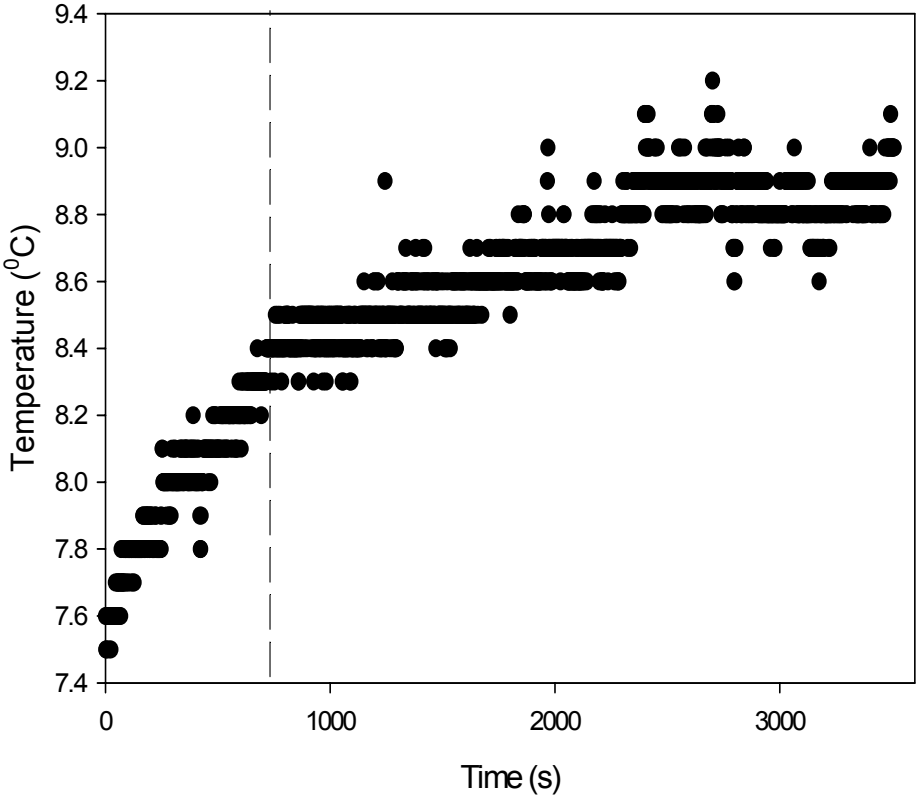

Table 6.5. Initial rate ($\mu M\ s^{-1}$) of polymerization as a function of temperature. The "true" temperature was measured by a thermocouple at the sample cell: Solvent = H_2O $[G]_0$ = 3.02 mg/mL, [KCl] = 15 mM, P = 20 MPa.

Bath Temperature (^0C)	**"True" Temperature (+/- 0.5 ^0C)**	**Initial Rate, r_p ($\mu M\ s^{-1}$)**	**Standard Error**
0	2.6	-2.2×10^{-4}	1×10^{-5}
3	5.6	-8.2×10^{-4}	2×10^{-5}
6	7.5	-6.5×10^{-4}	4×10^{-5}
9	8.8	-4.4×10^{-4}	1×10^{-5}
12	11.0	1.6×10^{-4}	1×10^{-5}
15	14.2	1.2×10^{-3}	1×10^{-4}
18	16.5	2.0×10^{-3}	1×10^{-4}
21	18.8	1.9×10^{-3}	1×10^{-4}
24	22.0	1.7×10^{-3}	1×10^{-4}
27	24.5	1.4×10^{-3}	1×10^{-4}
30	27.3	-8.6×10^{-4}	3×10^{-5}
33	30.0	-1.7×10^{-4}	1×10^{-4}
36	33.5	-1.4×10^{-4}	1×10^{-4}
39	35.5	-8.8×10^{-4}	3×10^{-5}
42	37.4	-8.9×10^{-4}	1×10^{-5}

Figure 6.12. Initial polymerization rate, r_p, as a function of temperature: Solvent = H_2O $[G]_0$ = 3.02 mg/mL, [KCl] = 15 mM, P = 20 MPa.

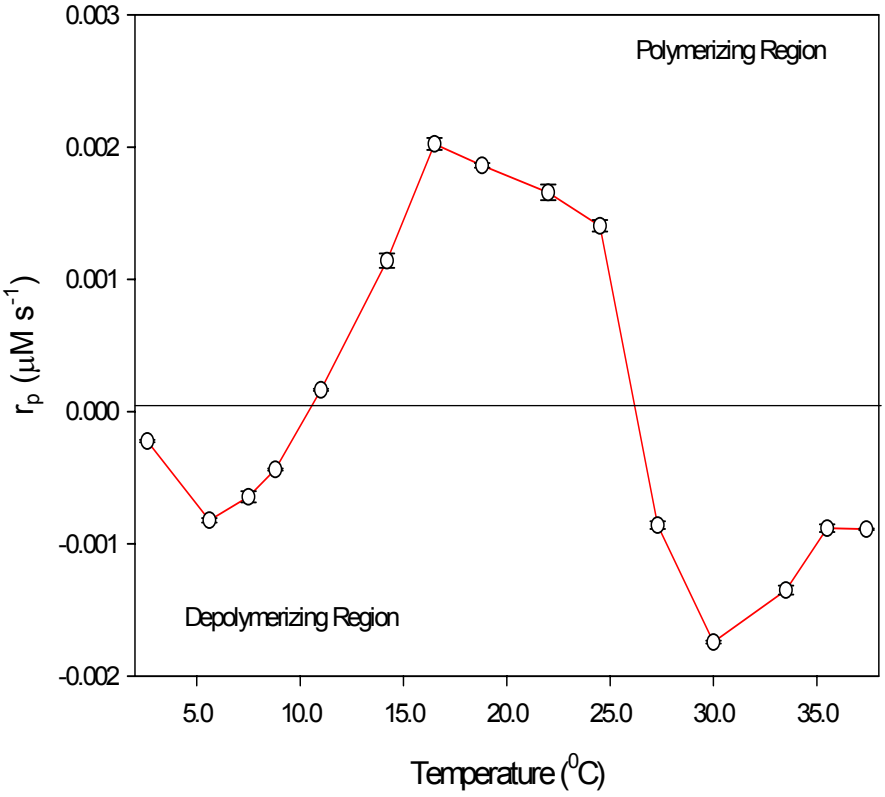

6.2.3 Discussion - Thermodynamics

The thermodynamic (extent of polymerization) data in this section were collected for a 3.02 mg/mL sample in buffer A at a pressure of 20 MPa and initiated by 15 mM KCl. Discussion of the data is presented in chapter seven. A plot of ϕ (T) is reproduced again in Figure 6.13 with the transition and crossover points indicated and Table 6.6 gives the values at these points.

Figure 6.13. Extent of polymerization as a function of temperature showing T_p, T_{max}, and T_{p2}: Solvent = H_2O $[G]_0$ = 3.02 mg/mL, [KCl] = 15 mM, P = 20 MPa.

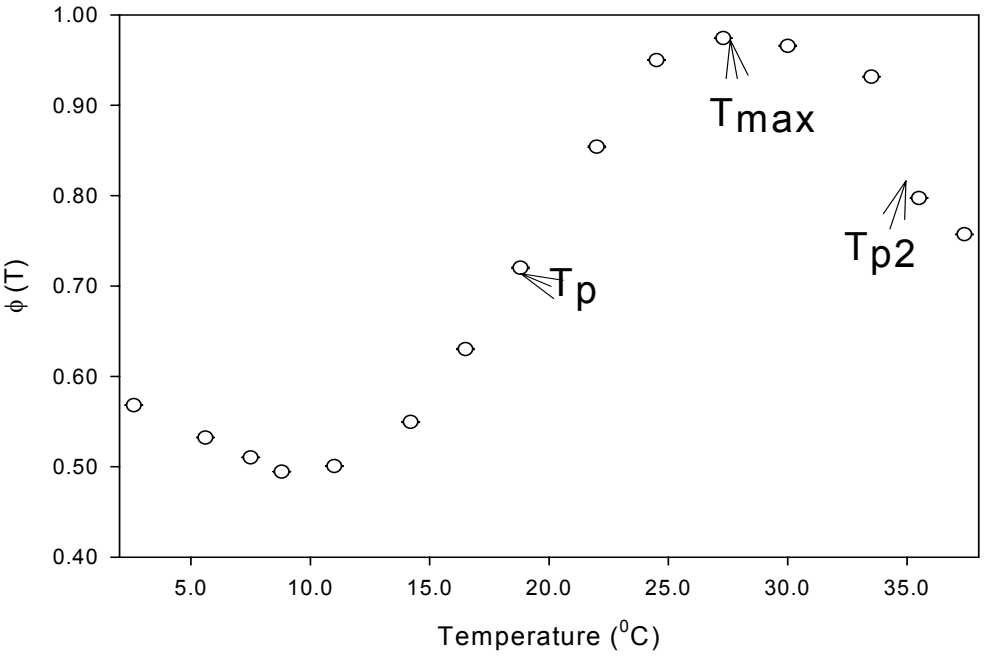

Table 6.6. Comparison of results from current work on actin polymerization: Solvent = H_2O $[G]_0$ = 3.00 mg/mL, [KCl] = 15 mM, P = 20 MPa. Errors for T and ϕ are rough estimates based on visual extrapolation of the data in Figure 6.9.

Parameters	**Results**	
$[G]_0$	3.02 (+/-0.01) mg/mL	
[KCl]	15.0 (+/- 0.1) mM	
T_p, ϕ_p	19 (+/-2) ^{0}C	0.70 (+/-0.05)
T_{max}, ϕ_{max}	28 (+/-2) ^{0}C	0.99 (+/-0.05)
T_{p2}, ϕ_{p2}	34 ^{0}C	0.85 (+/-0.05)

The trend in Figure 6.2 is very similar to the trend observed for ϕ (T) at atmospheric pressure, and at 10 MPa. The trend of ϕ (T) at 20 MPa initially decreases as temperature increases, as observed at 10 MPa but not at 0.1 MPa. The initial extent of polymerization started at a rather high value of 0.58. See section 6.1.3 for a discussion of this observation.

An inflection point, T_p, is observed for Run #5 near 19 ^{0}C – 6 degrees higher than the T_p for Run #1 at 0.1 MPa and 3 degrees higher than the T_p for Run #4 at 10 MPa, all in buffer A solvent. The comparisons are explored and analyzed in chapter seven. There is also the presence of the T_{max} at 28 ^{0}C. The second inflection point appears in the depolymerization region T_{p2} near 34 ^{0}C. Figure 6.14 gives a schematic of the phase diagram of Run #5 with the observed floor temperature and the postulated ceiling temperature.

Figure 6.14. Schematic phase diagram of the results of the actin polymerization experiment Run #5: Solvent = H_2O $[G]_0$ = 3.02 mg/mL, [KCl] = 15 mM, P = 20 MPa.

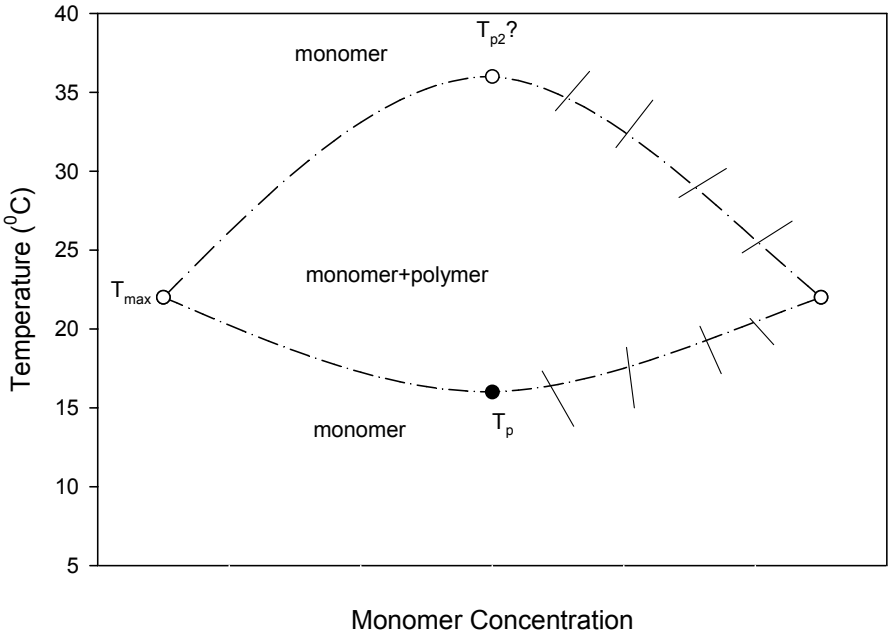

6.2.4. Discussion - Kinetics

The plot in Figure 6.15 shows r_p as a function of temperature alongside ϕ (T). Figure 6.16 show the three regions separated by T_p and T_{p2}. The trend in the initial rate of polymerization for Run #5 again shows remarkable correlation with the extent of polymerization plot. There is a minimum in r_p just before the onset of

polymerization in the ϕ (T) plot. The plot of r_p (T) bears resemblance to the previous r_p plot for Run #4 taken at 10 MPa, except the anomaly in the depolymerization region near or approaching T_{p2} (when judged against the atmospheric pressure plots) does not exist here. There is one minimum in the depolymerization and it is near T_{p2}. The maximum in r_p is near T_p, which may be attributed to an expected dramatic increase in viscosity near and above T_p. The highest value for r_p is actually a little below $T_{p,}$ as was the case for Run #4, and occurs near the onset of polymerization (11.0 ^{0}C) following the initial decrease in ϕ (T).

T_{max} occurs further from T_p than in Run #4 and essentially reaches 100% polymerization. The application of pressure seems to favor full polymerization of the sample in the polymerization region.

Figure 6.15. Initial polymerization rate, r_p, and ϕ as a function of temperature: Solvent = H_2O $[G]_0$ = 3.02 mg/mL, [KCl] = 15 mM, P = 20 MPa.

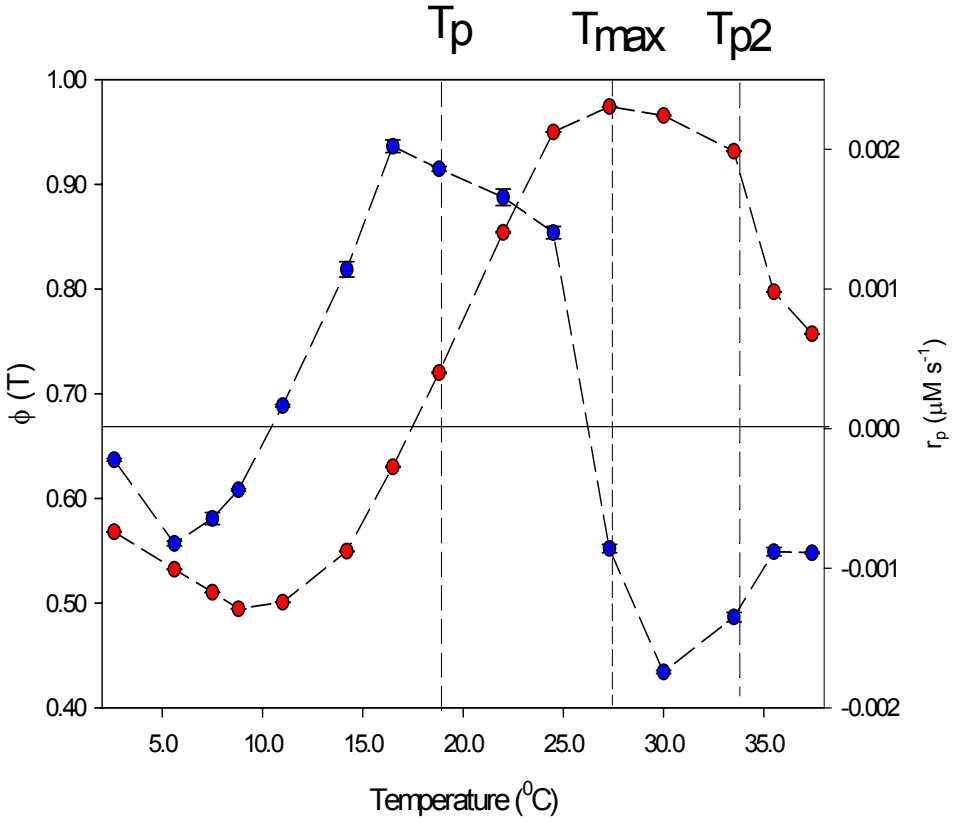

Figure 6.16. Initial rate of polymerization r_p (T) for the region up to T_p (red dot), between T_p and T_{p2} (green circle) and beyond T_{p2} (blue circle): Solvent = H_2O $[G]_0$ = 3.02 mg/mL, [KCl] = 15 mM, P = 20 MPa.

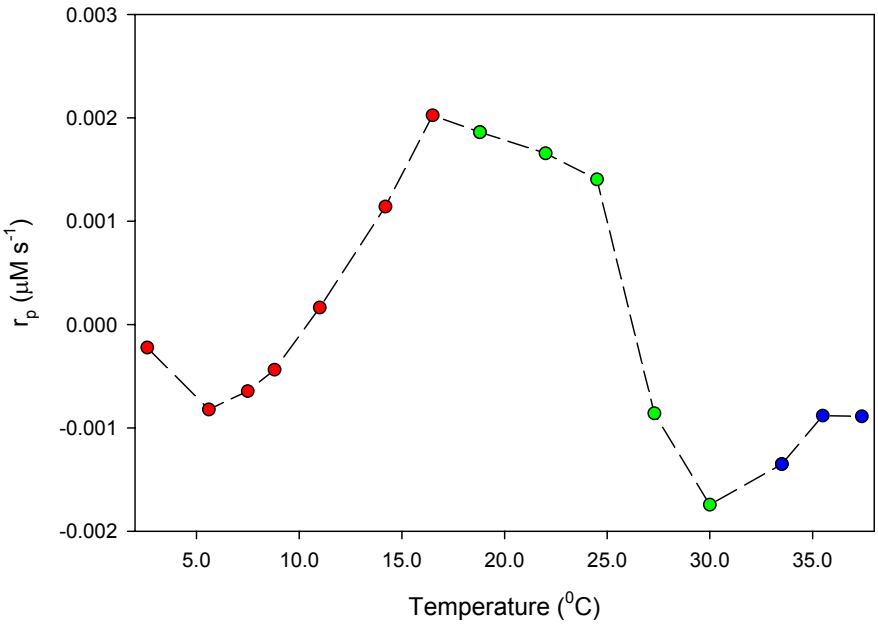

6.3. The Volume Change of Polymerization

Previous measurements of the volume change in a polymerizing system of actin were discussed in chapter two of this text and have been given a comprehensive treatment elsewhere.[47] The present work, for the first time, attempts to find ΔV from a comparison of $\phi(T)$ data taken at different static pressures: Run #1, Run #4, and Run #5 (see Figure 6.17). The relationship for ΔV is found in Equation 2.2 is $(\partial \ln K_x/\partial P)_{T,x} = -\Delta V/RT$. This equation can be exploited by the experimental methods used in this work because every component in solution between the three runs is essentially held constant. Also the value of K_x can be calculated from the extent of polymerization according to the following calculation in Equation 6.1 below:

$$K_x (T) = 1/[G_0] \text{ x } (1-\phi_{eq}(T)) \qquad (6.1)$$

So for a given temperature, the extent of polymerization is estimated from each pressure curve in Figure 6.17 below, K_x is determined, and the slope of $\ln K_x$ with pressure is determined by non-linear regression analysis using Sigma Plot software. The results are presented in Table 6.7 below for three different temperatures in the depolymerization region (shown in Figure 6.17) and the plot of $\ln K_x$ versus pressure is shown in Figures 6.18-6.20. The depolymerization was chosen because the data are more distinguishable in that region; also because ϕ is not linear with respect to pressure for the current data below 27 ^{0}C (Figure 6.21). The cause of this is presently unknown. The results from the depolymerization region are used to construct synopses about the volume change of polymerization.

Figure 6.17 The extent of polymerization, ϕ(T), at different pressures. The solid lines represent temperatures where the volume change was calculated: Solvent = H_2O $[G]_0$ = 3 mg/mL, [KCl] = 15 mM.

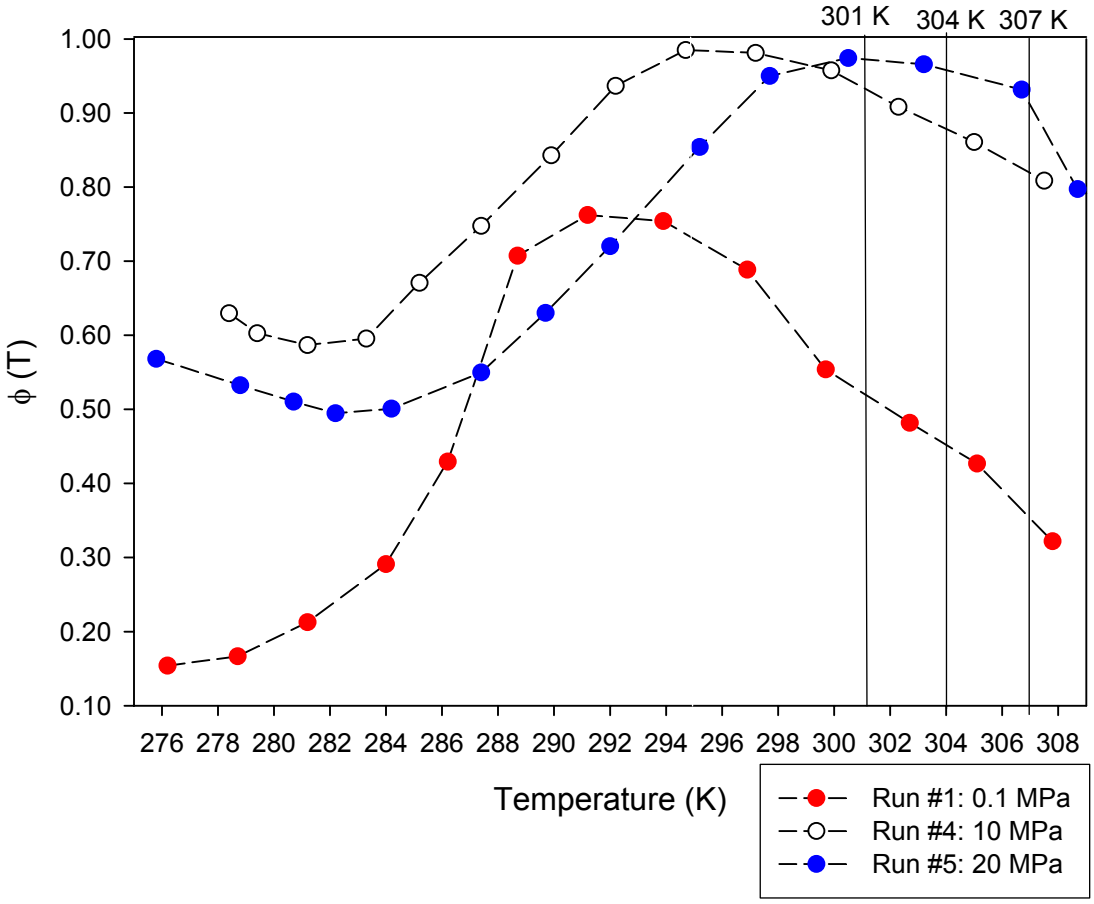

Table 6.7 Values of T_p and T_{p2} at each pressure and ΔV values at three different temperatures: Solvent = H_2O $[G]_0$ = 3 mg/mL, [KCl] = 15 mM.

Run #	**Pressure (MPa)**	**T = 295 (+/- 2) K**	**T = 301 (+/- 2) K**	**T = 304 (+/- 2) K**	**T = 307 (+/- 2) K**	**T_p (+/- 2) K**	**T_{p2} (+/- 2) K**
1	0.1 (+/- 0.01)	0.72 (+/- 0.05)	0.52 (+/- 0.05)	0.47 (+/- 0.05)	0.39 (+/- 0.05)	285	300
4	10 (+/- 2)	0.98 (+/- 0.05)	0.93 (+/- 0.05)	0.89 (+/- 0.05)	0.83 (+/- 0.05)	289	312?
5	20 (+/- 2)	0.82 (+/- 0.05)	0.99 (+/- 0.05)	0.98 (+/- 0.05)	0.95 (+/- 0.05)	292	307?
d ln K_x/dP		N/A	1.96 x 10^{-4} (+/- 2 x 10^{-6})	1.66 x 10^{-4} (+/- 2 x 10^{-6})	1.27 x 10^{-4} (+/- 4 x 10^{-6})		
ΔV (depolymerization)		N/A	-484 (+/- 63) cm^3/mol	-415 (+/- 57) cm^3/mol	-324 (+/- 63) cm^3/mol		

Figure 6.18 ln K_x versus pressure at 301 K. The slope is used to calculate ΔV according to equation 2.2: Solvent = H_2O $[G]_0$ = 3 mg/mL, [KCl] = 15 mM.

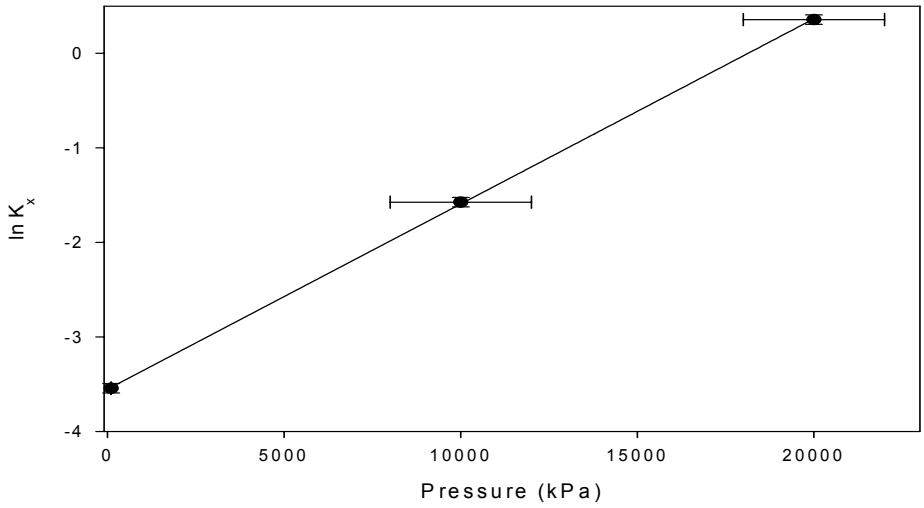

Figure 6.19 ln K_x versus pressure at 304 K. The slope is used to calculate ΔV according to equation 2.2: Solvent = H_2O $[G]_0$ = 3 mg/mL, [KCl] = 15 mM.

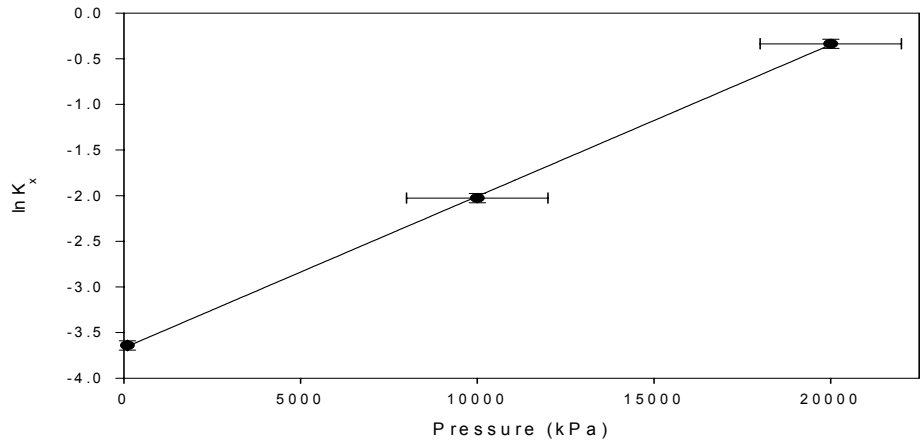

Figure 6.20 ln K_x versus pressure at 307 K. The slope is used to calculate ΔV according to equation 2.2: Solvent = H_2O $[G]_0$ = 3 mg/mL, [KCl] = 15 mM.

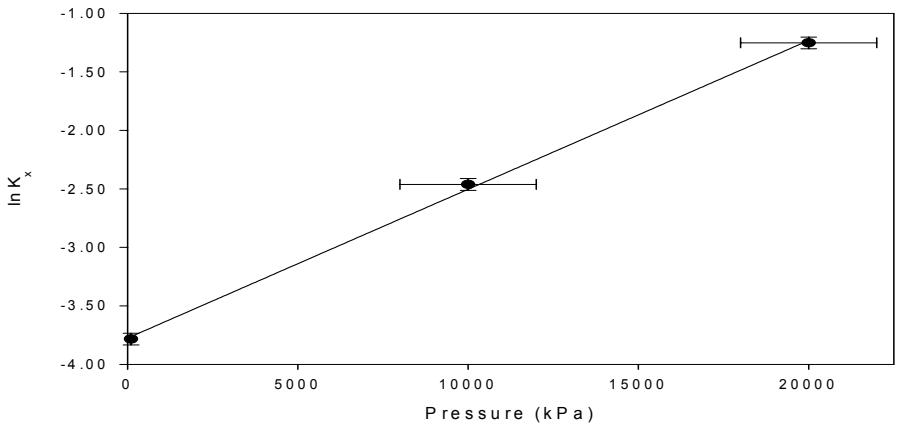

A volume changes reported correspond to about a 2% increase, using a value for the partial specific volume of 0.744 mL/g. The values obtained confirm the significant volume change expected due to the melting of the structured or denser water adsorbed to the protein surface.[21] The values that have been obtained for ΔV are in good agreement with some of the previous results as shown in Table 6.8 below. Some sources for the disparity in these reported values could be 1) the variation in sensitivity of the measurements,[47] 2) incorrect assumptions or approximations such as neglecting the effect on sheared samples on the extent of polyerization,[28] 3) the variation in species,[48] or 4) the slight dependence of ΔV on temperature as shown above and also on pressure.[49]

Figure 6.21 shows the dependence of r_p on pressure.

Figure 6.21 The trend of $r_p(T)$ at different pressures.

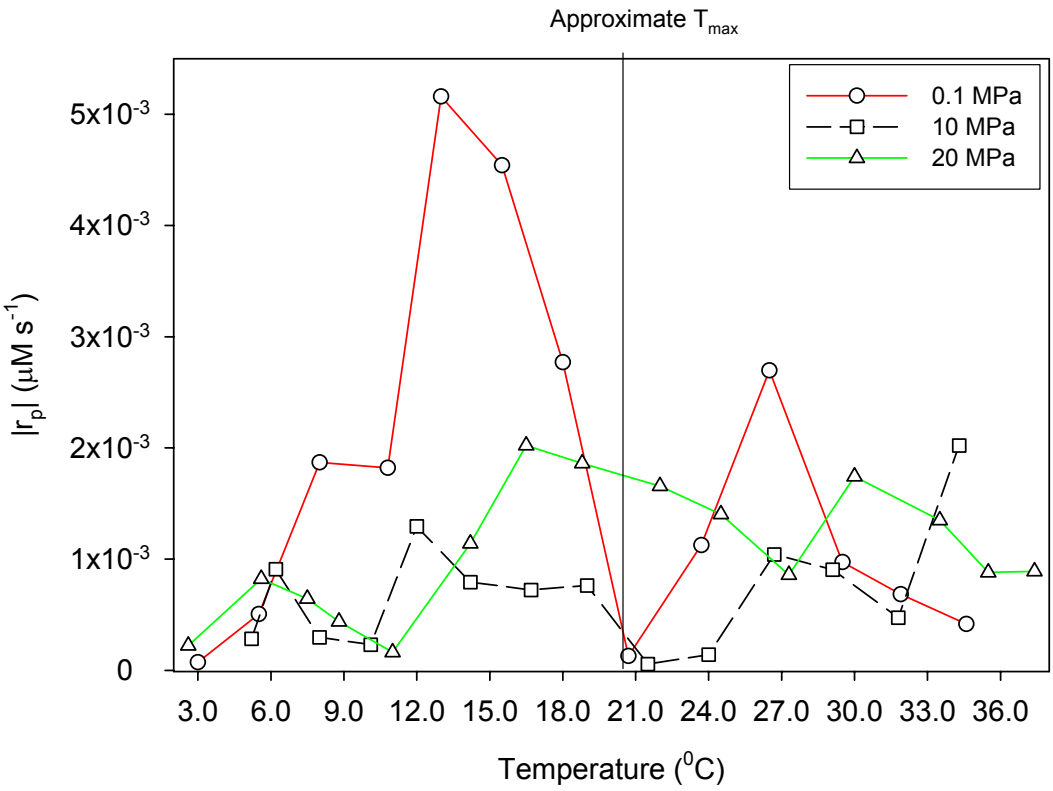

The plot in Figure 6.21 shows an interesting trend; the magnitude of r_p is largest for the lowest pressure, 0.1 MPa but seems to have it lowest values at 10 MPa. If there is an inverse proportionality of the overall magnitude of the initial rate, r_p, to pressure, then the suggestion can be made that increasing pressure decreases the initial rate with a minimum value at some pressure, and then it starts to go back up. Overall, no definitive conclusion can be drawn from this data comparing the initial rate at different pressures. Further study at intermediate pressures may provide better insight.

Chapter 7: Summary and Further Work

In this work, the extent of actin polymerization (ϕ) was measured as a function of time and temperature to yield key thermodynamic and kinetic data. The experimental methodology and improved equipment led to more data and better analysis for both the kinetics and thermodynamics of actin polymerization. Despite challenges in sample preparation and instrumental modification, the results showed remarkable consistency with prior work, while contributing to newer insights, and raising further questions.

Compelling results were the behavior of $\phi(T)$ and $\phi(t)$ under pressure and the behavior of the initial rate, r_p, with respect to temperature. A comprehensive plot showing the pressure effect $\phi(T)$ from various sources is given in Figure 7.1. A discussion of the major observations follows.

Figure 7.1. $\phi(T)$ from several sources showing the shift in T_p as pressure increases. The red symbols represent data at 0.1 MPa, the white symbols represent data taken at 10 MPa, and the blue symbols represent data at 20 MPa: Solvent = H_2O and $[G]_0$ = 3.0 mg/mL.

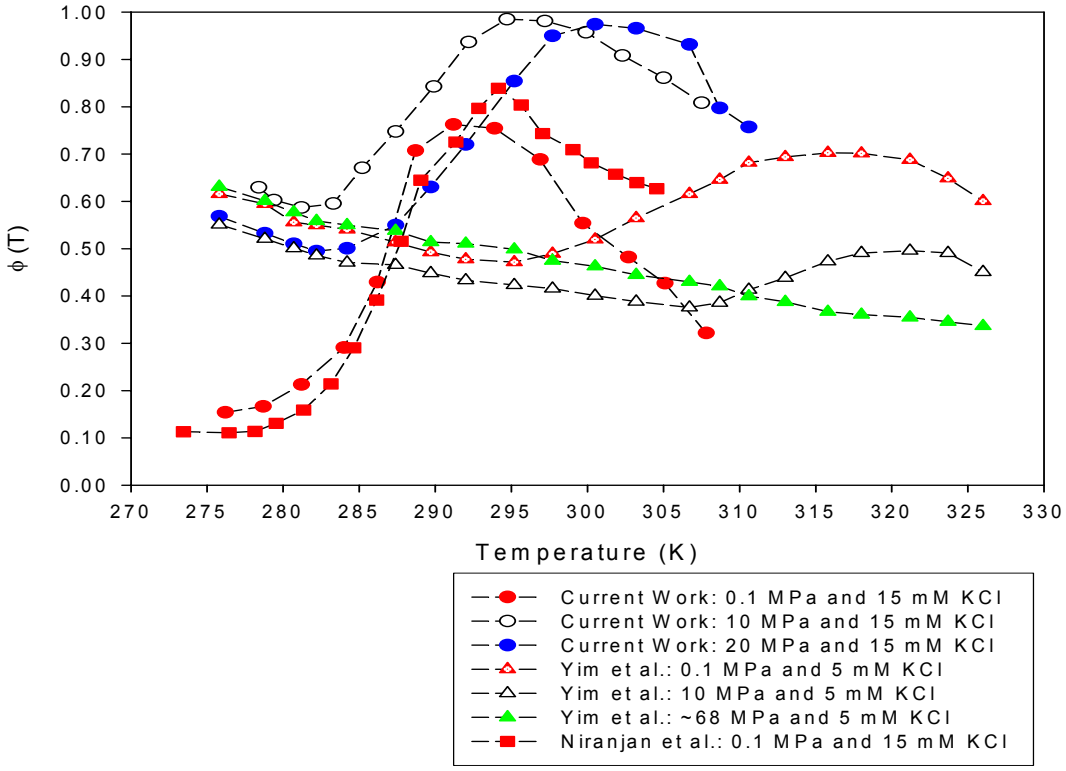

7.1 The Re-entrant Phase Transition

It was shown previously that actin polymerization reached a maximum extent and then decreased as temperature continued to increase.[18] This has not been observed for other such systems, but has been predicted for a form of silk polymerization and has been compared to the crystallization of Hemoglobin-S, which does exhibit a maximum.[50] The results of this study gave strong evidence of a re-entrant monomer region of the phase diagram. There are three major reasons to give strong consideration to a second transition temperature or a "ceiling" temperature in the depolymerization region:

a. All extent of polymerization plots,[14,16] including the current work, given an appropriate temperature range, exhibit this extremum and they all occur at different temperatures well below the denaturing temperature for actin of 60 ^{0}C.[39,40]

b. Since the transition temperature, T_p, has been defined as the inflection point in ϕ (T), the appearance of a second inflection point in some of the plots presented here for the first time confirms the existence of T_{p2}, the ceiling temperature.

c. The apparent rate constant, defined as the initial rate of polymerization shows a peak near T_p and in many cases also shows a peak where T_{p2} is or is expected to be.

d. Theories[41] propose that for entropically driven systems, there may be competing mechanisms for the dependence of hydrogen bonding and other unique non-covalent interactions can lead to the formation of closed two-

phase regions. Another recent theory suggests a competition between activation, which requires the polymer-bound monomers, and propagation.[17] This occurs because activation is also entropically driven and may have a floor temperature in the vicinity of T_p.

7.2 The Pressure Effect

The main extension of this work to the comprehensive study by Niranjan[15] was to apply a static pressure to the polymerizing actin system. The results showed that the extent of polymerization followed an identical trend as experiments done at atmospheric pressure. The major effect of the pressure was the shifting of the transition temperature, T_p, to a higher value (see Figure 7.2). It had been previously shown that an increase in pressure favors monomer.[27,48]

Figure 7.2 Effect of pressure on the transition temperature, T_p. Error bars are one standard deviation: Solvent = H_2O, $[G]_0$ = 3 mg/mL, [KCl] = 15 mM.

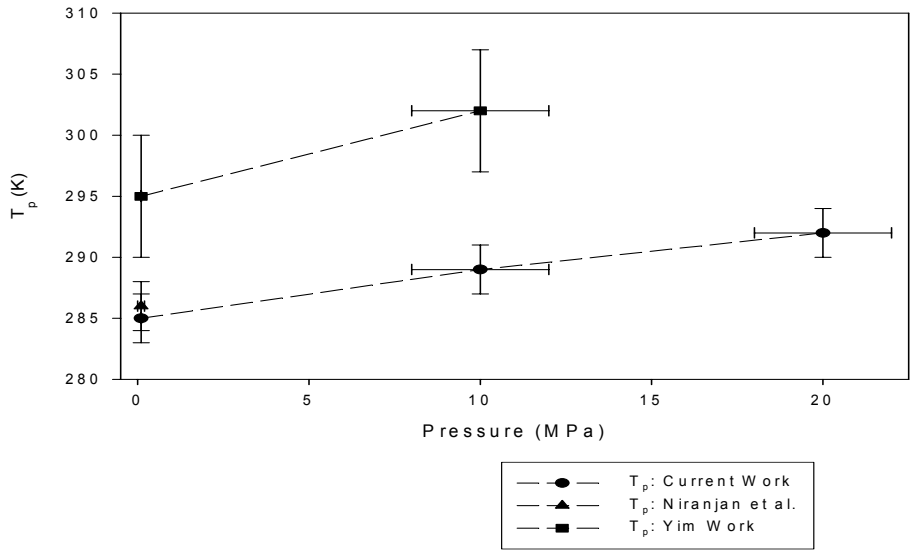

7.3 The Volume Change

The effect of pressure on the extent of polymerization for actin was used to estimate the change of volume during the polymerization of actin.

Table 7.1 Literature ΔV values from different methods for rabbit muscle actin. The salt (initiator) concentration is given below the actin concentration. The bold samples are results from the current work.

Method	**Actin Sample and Source**	**Method**	**Temperature**	**ΔV of Polymerization**
1	3.3 mg/ml actin 10 – 60 mM KCl[51]	Flow Birefringence	25 (+/-?) ^{0}C	+ 84 (+/-?) mL/mol
2	0.2 mg/ml actin 100 mM KCl[27]	Fluorescence Spectroscopy under Depolymerizing Pressure	25? ^{0}C	328 (+/-63) mL/mol
3	1.15 mg/ml actin 1.0 mM $MgCl_2$[51]	Dilatometry	25 ^{0}C	391 mL/mol
4	2.7 mg/ml actin 0.1 – 7 mM $MgCl_2$[52]	Vibrating Tube Densimetry	25 ^{0}C	-720 mL/mol
5a	***3.0 mg/ml actin 15 mM KCl***	***Static Pressure Fluorescence Spectroscopy***	***34 (+/-2) ^{0}C***	***324 (+/-63) cm^3/mol***
5b	***3.0 mg/ml actin 15 mM KCl***	***Static Pressure Fluorescence Spectroscopy***	***31 (+/-2) ^{0}C***	***415 (+/-57) cm^3/mol***
5c	***3.0 mg/ml actin 15 mM KCl***	***Static Pressure Fluorescence Spectroscopy***	***28 (+/-2) ^{0}C***	***484 (+/-63) cm^3/mol***

The results of the current work (Method 5a-c) compare well with the result of Method 2. The result of Method 1 is suspect because flow birefringence shears the sample which can have a significant effect on polymerization dynamics. Method 4 is

also unreliable because measurements in the vibrating tube can be strongly dependent on variable viscosity in the sample.

7.4 The Effect of Hydrogen Bonding

The substitution of H_2O solvent for D_2O was essentially an exchange for a stronger "hydrogen" bond. While $\phi(T)$ in D_2O exhibited the normal trend, there was clearly a shift in T_p - the value being about 3-4 degrees higher than its H_2O counterpart. This validates the importance of the role of the hydrogen bond, which is the primary interaction between the structured water and the surface residues on an actin monomer. As shown before,[16] the lower initial actin concentration increased T_p, further evidence that the initial monomer concentration has a significant effect on T_p.

The effect of D_2O on the rate was not readily apparent, but the results in chapter five clearly show that the initial polymerization rate in D_2O was a factor of ten lower than in H_2O. A possible explanation is that the substitution invokes a solvent isotope effect, where the substitution of a heavier isotope can have a dramatic effect on the kinetics. In this case, the stronger interaction between the bulk solvent and the protein also served to decrease the initial rate for D_2O based samples. The initial rate was even lower for the low actin concentration sample.

7.5 The Relationship between $r_p(T)$ and $\phi(T)$

Another finding of fundamental interest was the trend of the initial rate of polymerization, taken as the initial slope of $\phi(t)$, with temperature. It was noticed that r_p was correlated to $\phi(T)$: it reached a peak near T_p, decreased towards zero as $\phi(T)$ approached T_{max}, and then the rate of depolymerization increased and in some cases reached a peak near T_{p2}, before it began again to decrease towards zero. The maximum near T_p can be explained by the fact that actin viscosity increases dramatically above T_p, and the reaction becomes much more diffusion dependent.

7.6 The Effect of Thermal Cycling

Among the other questions answered was: What is the effect of a negative temperature perturbation on the polymerization dynamics? The results have shown that actin indeed exhibits a "frozen-in polymer state" observed in other equilibrium polymerization systems[53,54] and actin,[14] described as the "…tendency of the polymer, once formed, not to revert easily to monomer on retraversing the polymerization line.[55] In fact, actin exhibited hysteresis, a strong memory of the direction that it tended to before the negative perturbation – especially if this perturbation took place near the transition temperature. There were some cases where actin was essentially reversible in regions near T_{max} .

7.7 Summary and Further Work

Some further work stemming from this project could be to:

a. Measure the extent of polymerization of actin in D_2O buffer under pressure to understand the effect of both solvent and pressure on the dynamics of polymerization.

b. Study the extent of depolymerization to further understand the hysteresis observed under temperature reversals.

c. Apply a stretched exponential fit to the $\phi(t)$ data to obtain kinetic parameters such as a relaxation time. The stretched exponential is commonly applied to gelling systems where the relaxation process "…becomes critically slow at the gel point…" [56] for polymers above the glass transition temperature[57] and may apply to actin in the polymerizing region.[58] A detailed kinetic mechanism is being developed that factors in the length distributions in the polymerizing region[59] and will also be applied to the current data to obtain rate constants.

d. Vary the initiating salt concentration under pressure to study the effect of salt under pressure on T_p and ΔV.

e. Measure viscosity around the transition temperatures, T_p and T_{p2}, to better understand the effect of transport properties on the polymerization rate. This could be achieved by adding polystyrene beads to the polymerizing actin sample and measuring their diffusion coefficient to get the viscosity through the Stokes-Einstein equation.

Appendix. Tables of the extent of polymerization as a function of time - $\phi(t)$.

Run #1. $\phi(t)$ for 3.1 mg/mL in H_2O at 0.1 MPa.

3.0 ^{0}C		5.5 ^{0}C		8.0 ^{0}C		10.8A ^{0}C	
Time (s)	$\phi(t)$	Time (s)	$\phi(t)$	Time (s)	$\phi(t)$	Time (s)	$\phi(t)$
0	0.1529	0	0.1564	0	0.1932	0	0.2536
100	0.1530	100	0.1571	100	0.1957	100	0.2556
200	0.1531	200	0.1578	200	0.1985	200	0.2578
300	0.1532	300	0.1584	300	0.2014	300	0.2604
400	0.1533	400	0.1591	400	0.2042	400	0.2633
500	0.1535	500	0.1599	500	0.2065	500	0.2661
600	0.1536	600	0.1608	600	0.2084	600	0.2690
700	0.1537	700	0.1620	700	0.2098	700	0.2721
800	0.1537	800	0.1631	800	0.2110	800	0.2752
900	0.1538	900	0.1640	900	0.2121	900	0.2784
1000	0.1538	1000	0.1648	1000	0.2130	1000	0.2817
1100	0.1538	1100	0.1655	1100	0.2134	1100	0.2846
1200	0.1538	1200	0.1662	1200	0.2137	1200	0.2872
		1300	0.1665			1300	0.2892
		1400	0.1666			1400	0.2901
		1500	0.1667			1500	0.2910
		1600	0.1669			1600	0.2919

10.8B ^{0}C		13.0A ^{0}C		13.0B ^{0}C		15.5 ^{0}C	
Time (s)	$\phi(t)$	Time (s)	$\phi(t)$	Time (s)	$\phi(t)$	Time (s)	$\phi(t)$
0	0.5521	0	0.3397	0	0.5368	0	0.6254
100	0.5521	100	0.3469	100	0.5398	100	0.6314
200	0.5522	200	0.3534	200	0.5432	200	0.6372
300	0.5523	300	0.3610	300	0.5469	300	0.6433
400	0.5524	400	0.3685	400	0.5509	400	0.6499
500	0.5524	500	0.3753	500	0.5551	500	0.6571
600	0.5525	600	0.3821	600	0.5591	600	0.6636
700	0.5525	700	0.3882	700	0.5629	700	0.6690
800	0.5526	800	0.3938	800	0.5666	800	0.6742
900	0.5526	900	0.4001	900	0.5703	900	0.6790
1000	0.5526	1000	0.4067	1000	0.5739	1000	0.6838
1100	0.5526	1100	0.4136	1100	0.5771	1100	0.6887
1200	0.5527	1200	0.4200	1200	0.5799	1200	0.6936
1300	0.5527	1300	0.4258	1300	0.5825	1300	0.6983
		1400	0.4286	1400	0.5838	1400	0.7025
		1500	0.4313	1500	0.5843	1500	0.7062
		1600	0.4340	1600	0.5849	1600	0.7083
		1700	0.4363			1700	0.7100
						1800	0.7116
						1900	0.7131

18.0 ^{0}C		20.7A ^{0}C		20.7B ^{0}C		23.7A ^{0}C	
Time (s)	ϕ(t)	Time (s)	ϕ(t)	Time (s)	ϕ(t)	Time (s)	ϕ(t)
0	0.7176	0	0.7514	0	0.7130	0	0.7075
100	0.7210	100	0.7516	100	0.7108	100	0.7061
200	0.7247	200	0.7517	200	0.7085	200	0.7045
300	0.7287	300	0.7519	300	0.7058	300	0.7030
400	0.7327	400	0.7521	400	0.7031	400	0.7013
500	0.7367	500	0.7523	500	0.7007	500	0.6997
600	0.7407	600	0.7526	600	0.6985	600	0.6984
700	0.7446	700	0.7529	700	0.6964	700	0.6972
800	0.7484	800	0.7532	800	0.6945	800	0.6959
900	0.7517	900	0.7534	900	0.6927	900	0.6947
1000	0.7546	1000	0.7536	1000	0.6910	1000	0.6935
1100	0.7573	1100	0.7537	1100	0.6894	1100	0.6924
1200	0.7597	1200	0.7539	1200	0.6879	1200	0.6914
1300	0.7616	1300	0.7540	1300	0.6866	1300	0.6904
1400	0.7631	1400	0.7540	1400	0.6855	1400	0.6895
1500	0.7642	1500	0.7541	1500	0.6845	1500	0.6887
1600	0.7651	1600	0.7541	1600	0.6837	1600	0.6881
1700	0.7653	1700	0.7541	1700	0.6830	1700	0.6877
		1800	0.7541	1800	0.6827	1800	0.6873
				1900	0.6824		

23.7B ^{0}C		26.5 ^{0}C		29.5A ^{0}C		29.5B ^{0}C	
Time (s)	ϕ(t)	Time (s)	ϕ(t)	Time (s)	ϕ(t)	Time (s)	ϕ(t)
0	0.6393	0	0.5888	0	0.5028	0	0.4137
100	0.6384	100	0.5855	100	0.5016	100	0.4135
200	0.6376	200	0.5816	200	0.5003	200	0.4133
300	0.6366	300	0.5777	300	0.4989	300	0.4129
400	0.6356	400	0.5739	400	0.4975	400	0.4126
500	0.6345	500	0.5703	500	0.4961	500	0.4122
600	0.6334	600	0.5672	600	0.4947	600	0.4117
700	0.6321	700	0.5647	700	0.4934	700	0.4111
800	0.6309	800	0.5627	800	0.4921	800	0.4105
900	0.6295	900	0.5612	900	0.4910	900	0.4099
1000	0.6282	1000	0.5600	1000	0.4898	1000	0.4093
1100	0.6269	1100	0.5590	1100	0.4887	1100	0.4088
1200	0.6258	1200	0.5582	1200	0.4877	1200	0.4084
1300	0.6247	1300	0.5576	1300	0.4867	1300	0.4080
1400	0.6237	1400	0.5571	1400	0.4857	1400	0.4076
1500	0.6227	1500	0.5567	1500	0.4848	1500	0.4073
1600	0.6219	1600	0.5562	1600	0.4838	1600	0.4072
1700	0.6211	1700	0.5557	1700	0.4830	1700	0.4070
1800	0.6204	1800	0.5552	1800	0.4823	1800	0.4069
1900	0.6201	1900	0.5546	1900	0.4819	1900	0.4069
2000	0.6198	2000	0.5539	2000	0.4815	2000	0.4068
2100	0.6195	2100	0.5533	2100	0.4812	2100	0.4068
2200	0.6192	2200	0.5529	2200	0.4808	2200	0.4067

31.9A ^{0}C		**31.9B ^{0}C**		**34.6 ^{0}C**	
Time (s)	ϕ(t)	Time (s)	ϕ(t)	Time (s)	ϕ(t)
0	0.4415	0	0.3702	0	0.3323
100	0.4406	100	0.3692	100	0.3318
200	0.4398	200	0.3682	200	0.3313
300	0.4388	300	0.3671	300	0.3307
400	0.4378	400	0.3660	400	0.3301
500	0.4367	500	0.3649	500	0.3294
600	0.4357	600	0.3639	600	0.3287
700	0.4346	700	0.3632	700	0.3280
800	0.4336	800	0.3625	800	0.3272
900	0.4326	900	0.3619	900	0.3265
1000	0.4316	1000	0.3614	1000	0.3258
1100	0.4306	1100	0.3610	1100	0.3251
1200	0.4297	1200	0.3608	1200	0.3245
1300	0.4288	1300	0.3606	1300	0.3239
1400	0.4280	1400	0.3605	1400	0.3233
1500	0.4273	1500	0.3605	1500	0.3228
1600	0.4269	1600	0.3604	1600	0.3223
1700	0.4265	1700	0.3604	1700	0.3219
1800	0.4262	1800	0.3604	1800	0.3215
1900	0.4258	1900	0.3604	1900	0.3212
		2000	0.3604	2000	0.3211
		2100	0.3604	2100	0.3210

Run #2. $\phi(t)$ for 3.1 mg/mL in D_2O at 0.1 MPa.

8.0 ^{0}C		11.3 ^{0}C		12.8 ^{0}C		14.4A ^{0}C	
Time (s)	$\phi(t)$	Time (s)	$\phi(t)$	Time (s)	$\phi(t)$	Time (s)	$\phi(t)$
0	0.4383	0	0.4327	0	0.4498	0	0.4949
100	0.4383	100	0.4328	100	0.4503	100	0.4957
200	0.4384	200	0.4330	200	0.4509	200	0.4965
300	0.4384	300	0.4332	300	0.4516	300	0.4976
400	0.4385	400	0.4334	400	0.4524	400	0.4988
500	0.4385	500	0.4336	500	0.4533	500	0.5001
600	0.4386	600	0.4339	600	0.4543	600	0.5017
700	0.4387	700	0.4343	700	0.4555	700	0.5033
800	0.4387	800	0.4346	800	0.4568	800	0.5051
900	0.4388	900	0.4350	900	0.4582	900	0.5070
1000	0.4388	1000	0.4355	1000	0.4596	1000	0.5090
1100	0.4389	1100	0.4359	1100	0.4612	1100	0.5111
1200	0.4389	1200	0.4364	1200	0.4627	1200	0.5132
1300	0.4390	1300	0.4370	1300	0.4643	1300	0.5153
1400	0.4391	1400	0.4375	1400	0.4659	1400	0.5175
1500	0.4392	1500	0.4381	1500	0.4674	1500	0.5195
1600	0.4393	1600	0.4386	1600	0.4688	1600	0.5215
1700	0.4394	1700	0.4391	1700	0.4702	1700	0.5233
1800	0.4395	1800	0.4396	1800	0.4715	1800	0.5251
1900	0.4397	1900	0.4400	1900	0.4727	1900	0.5267
2000	0.4398	2000	0.4404	2000	0.4738	2000	0.5282
2100	0.4400	2100	0.4408	2100	0.4747	2100	0.5294
2200	0.4401	2200	0.4411	2200	0.4755	2200	0.5305
2300	0.4402	2300	0.4413	2300	0.4762	2300	0.5314
2400	0.4404	2400	0.4415	2400	0.4768	2400	0.5322
2500	0.4405	2500	0.4416	2500	0.4772	2500	0.5327
2600	0.4405	2600	0.4417	2600	0.4775	2600	0.5331
2700	0.4406	2700	0.4418	2700	0.4777	2700	0.5334
2800	0.4406	2800	0.4419	2800	0.4779	2800	0.5337

14.4B ^{0}C		17.0A ^{0}C		17.0B ^{0}C		18.1 ^{0}C	
Time (s)	$\phi(t)$	Time (s)	$\phi(t)$	Time (s)	$\phi(t)$	Time (s)	$\phi(t)$
0	0.6505	0	0.5546	0	0.6572	0	0.6742
100	0.6508	100	0.5559	100	0.6574	100	0.6749
200	0.6510	200	0.5574	200	0.6578	200	0.6757
300	0.6513	300	0.5591	300	0.6582	300	0.6765
400	0.6516	400	0.5610	400	0.6587	400	0.6775
500	0.6520	500	0.5631	500	0.6592	500	0.6786
600	0.6524	600	0.5654	600	0.6598	600	0.6797
700	0.6529	700	0.5679	700	0.6604	700	0.6808
800	0.6535	800	0.5706	800	0.6611	800	0.6819
900	0.6541	900	0.5734	900	0.6618	900	0.6831
1000	0.6547	1000	0.5763	1000	0.6626	1000	0.6842
1100	0.6553	1100	0.5794	1100	0.6634	1100	0.6854
1200	0.6560	1200	0.5825	1200	0.6642	1200	0.6864
1300	0.6566	1300	0.5857	1300	0.6650	1300	0.6874
1400	0.6573	1400	0.5888	1400	0.6658	1400	0.6883
1500	0.6579	1500	0.5919	1500	0.6667	1500	0.6891

1600	0.6585	1600	0.5949	1600	0.6675	1600	0.6897
1700	0.6590	1700	0.5978	1700	0.6683	1700	0.6903
1800	0.6595	1800	0.6005	1800	0.6690	1800	0.6907
1900	0.6600	1900	0.6031	1900	0.6698	1900	0.6911
2000	0.6603	2000	0.6054	2000	0.6704	2000	0.6913
2100	0.6607	2100	0.6076	2100	0.6710	2100	0.6915
2200	0.6609	2200	0.6094	2200	0.6715	2200	0.6917
2300	0.6612	2300	0.6111	2300	0.6720	2300	0.6918
2400	0.6614	2400	0.6125	2400	0.6724		
2500	0.6615	2500	0.6133	2500	0.6726		
2600	0.6616	2600	0.6140	2600	0.6728		
2700	0.6616	2700	0.6147	2700	0.6730		
2800	0.6617	2800	0.6153	2800	0.6731		

20.0 ^{0}C		**22.0A ^{0}C**		**22.0B ^{0}C**		**24.1A ^{0}C**		**24.1B ^{0}C**	
Time (s)	ϕ(t)	Time (s)	ϕ(t)	Time (s)	ϕ(t)	Time(s)	ϕ(t)	Time (s)	ϕ(t)
0	0.6991	0	0.7078	0	0.7159	0	0.6937	0	0.6094
100	0.6996	100	0.7081	100	0.7158	100	0.6923	100	0.6093
200	0.7002	200	0.7083	200	0.7157	200	0.6913	200	0.6092
300	0.7008	300	0.7086	300	0.7157	300	0.6905	300	0.6092
400	0.7016	400	0.7090	400	0.7156	400	0.6899	400	0.6091
500	0.7024	500	0.7094	500	0.7155	500	0.6898	500	0.6090
600	0.7033	600	0.7098	600	0.7153	600	0.6899	600	0.6089
700	0.7043	700	0.7103	700	0.7151	700	0.6902	700	0.6087
800	0.7052	800	0.7107	800	0.7148	800	0.6905	800	0.6086
900	0.7062	900	0.7112	900	0.7144	900	0.6909	900	0.6085
1000	0.7072	1000	0.7117	1000	0.7139	1000	0.6914	1000	0.6084
1100	0.7081	1100	0.7122	1100	0.7134	1100	0.6918	1100	0.6083
1200	0.7090	1200	0.7127	1200	0.7129	1200	0.6921	1200	0.6082
1300	0.7098	1300	0.7132	1300	0.7123	1300	0.6923	1300	0.6081
1400	0.7105	1400	0.7136	1400	0.7117	1400	0.6924	1400	0.6081
1500	0.7112	1500	0.7140	1500	0.7111	1500	0.6924	1500	0.6080
1600	0.7117	1600	0.7144	1600	0.7105	1600	0.6925	1600	0.6080
1700	0.7122	1700	0.7147	1700	0.7100	1700	0.6925	1700	0.6079
1800	0.7126	1800	0.7150	1800	0.7095	1800	0.6925	1800	0.6079
1900	0.7128	1900	0.7152	1900	0.7092	1900	0.6925	1900	0.6079
2000	0.7130	2000	0.7154	2000	0.7089	2000	0.6924	2000	0.6079
2100	0.7132	2100	0.7155	2100	0.7086	2100	0.6923	2100	0.6079
2200	0.7134	2200	0.7156	2200	0.7085	2200	0.6923	2200	0.6079
		2300	0.7157	2300	0.7083	2300	0.6922	2300	0.6079
				2400	0.7082	2400	0.6921		
				2500	0.7082	2500	0.6921		
				2600	0.7081	2600	0.6921		
				2700	0.7081				
				2800	0.7081				

26.4 ^{0}C		29.0A ^{0}C		29.0B ^{0}C		31.6A ^{0}C		31.6B ^{0}C	
Time (s)	ϕ(t)	Time (s)	ϕ(t)	Time (s)	ϕ(t)	Time(s)	ϕ(t)	Time (s)	ϕ(t)
0	0.6144	0	0.5683	0	0.5399	0	0.5296	0	0.5064
100	0.6138	100	0.5679	100	0.5402	100	0.5294	100	0.5056
200	0.6133	200	0.5674	200	0.5405	200	0.5291	200	0.5049
300	0.6127	300	0.5669	300	0.5408	300	0.5289	300	0.5042
400	0.6121	400	0.5663	400	0.5410	400	0.5286	400	0.5036
500	0.6114	500	0.5657	500	0.5412	500	0.5284	500	0.5030
600	0.6109	600	0.5651	600	0.5413	600	0.5281	600	0.5025
700	0.6103	700	0.5644	700	0.5414	700	0.5278	700	0.5020
800	0.6098	800	0.5637	800	0.5415	800	0.5276	800	0.5016
900	0.6093	900	0.5630	900	0.5415	900	0.5273	900	0.5012
1000	0.6089	1000	0.5623	1000	0.5415	1000	0.5270	1000	0.5008
1100	0.6084	1100	0.5617	1100	0.5415	1100	0.5268	1100	0.5005
1200	0.6081	1200	0.5611	1200	0.5414	1200	0.5265	1200	0.5001
1300	0.6077	1300	0.5605	1300	0.5413	1300	0.5262	1300	0.4998
1400	0.6074	1400	0.5600	1400	0.5412	1400	0.5259	1400	0.4995
1500	0.6071	1500	0.5595	1500	0.5411	1500	0.5257	1500	0.4992
1600	0.6068	1600	0.5590	1600	0.5409	1600	0.5254	1600	0.4989
1700	0.6065	1700	0.5586	1700	0.5408	1700	0.5252	1700	0.4986
1800	0.6062	1800	0.5583	1800	0.5406	1800	0.5249	1800	0.4984
1900	0.6059	1900	0.5580	1900	0.5404	1900	0.5247	1900	0.4982
2000	0.6057	2000	0.5577	2000	0.5402	2000	0.5246	2000	0.4981
2100	0.6054	2100	0.5575	2100	0.5401	2100	0.5245	2100	0.4980
2200	0.6051	2200	0.5574	2200	0.5399	2200	0.5244	2200	0.4980
2300	0.6049	2300	0.5573	2300	0.5398	2300	0.5243	2300	0.4980
2400	0.6047	2400	0.5572	2400	0.5397			2400	0.4980
2500	0.6046	2500	0.5572	2500	0.5397			2500	0.4980
2600	0.6044	2600	0.5571	2600	0.5397			2600	0.4980
2700	0.6043	2700	0.5571	2700	0.5397			2700	0.4980
2800	0.6042	2800	0.5570	2800	0.5396			2800	0.4981

Run #3. ϕ(t) for 1.0 mg/mL in D_2O at 0.1 MPa.

8.0 ^{0}C		11.3 ^{0}C		12.8 ^{0}C		14.4A ^{0}C	
Time (s)	ϕ(t)	Time (s)	ϕ(t)	Time (s)	ϕ(t)	Time (s)	ϕ(t)
0	0.4240	0	0.4096	0	0.3971	0	0.3928
100	0.4240	100	0.4094	100	0.3971	100	0.3932
200	0.4239	200	0.4092	200	0.3971	200	0.3936
300	0.4239	300	0.4089	300	0.3971	300	0.3940
400	0.4238	400	0.4087	400	0.3971	400	0.3945
500	0.4237	500	0.4084	500	0.3971	500	0.3949
600	0.4236	600	0.4081	600	0.3971	600	0.3954
700	0.4235	700	0.4078	700	0.3971	700	0.3961
800	0.4234	800	0.4075	800	0.3971	800	0.3967
900	0.4232	900	0.4073	900	0.3972	900	0.3975
1000	0.4231	1000	0.4070	1000	0.3972	1000	0.3982
1100	0.4230	1100	0.4068	1100	0.3973	1100	0.3990
1200	0.4228	1200	0.4066	1200	0.3973	1200	0.3998
1300	0.4227	1300	0.4064	1300	0.3974	1300	0.4006
1400	0.4225	1400	0.4062	1400	0.3975	1400	0.4013
1500	0.4224	1500	0.4061	1500	0.3976	1500	0.4021

1600	0.4223	1600	0.4059	1600	0.3977	1600	0.4027
1700	0.4222	1700	0.4058	1700	0.3978	1700	0.4034
1800	0.4221	1800	0.4057	1800	0.3979	1800	0.4039
1900	0.4220	1900	0.4056	1900	0.3980	1900	0.4044
2000	0.4219	2000	0.4055	2000	0.3981	2000	0.4048
2100	0.4218	2100	0.4055	2100	0.3982	2100	0.4051
2200	0.4218	2200	0.4054	2200	0.3983	2200	0.4052
2300	0.4217	2300	0.4054	2300	0.3984	2300	0.4053
2400	0.4217	2400	0.4053	2400	0.3985	2400	0.4054
2500	0.4217	2500	0.4053	2500	0.3986	2500	0.4055
2600	0.4216	2600	0.4053	2600	0.3987	2600	0.4056
2700	0.4216	2700	0.4053	2700	0.3987	2700	0.4055
2800	0.4216	2800	0.4053	2800	0.3987	2800	0.4055
2900	0.4216	2900	0.4053	2900	0.3988	2900	0.4054

14.4B ^{0}C		**17.0A ^{0}C**		**17.0B ^{0}C**		**18.1 ^{0}C**	
Time (s)	ϕ(t)	Time (s)	ϕ(t)	Time (s)	ϕ(t)	Time (s)	ϕ(t)
0	0.4367	0	0.4036	0	0.4380	0	0.4518
100	0.4370	100	0.4039	100	0.4382	100	0.4524
200	0.4373	200	0.4043	200	0.4384	200	0.4531
300	0.4377	300	0.4048	300	0.4387	300	0.4538
400	0.4381	400	0.4053	400	0.4390	400	0.4546
500	0.4385	500	0.4059	500	0.4394	500	0.4555
600	0.4390	600	0.4067	600	0.4398	600	0.4564
700	0.4394	700	0.4075	700	0.4402	700	0.4572
800	0.4398	800	0.4083	800	0.4407	800	0.4581
900	0.4403	900	0.4093	900	0.4412	900	0.4590
1000	0.4407	1000	0.4103	1000	0.4418	1000	0.4599
1100	0.4411	1100	0.4114	1100	0.4424	1100	0.4608
1200	0.4415	1200	0.4125	1200	0.4431	1200	0.4617
1300	0.4420	1300	0.4137	1300	0.4437	1300	0.4625
1400	0.4424	1400	0.4149	1400	0.4444	1400	0.4632
1500	0.4428	1500	0.4161	1500	0.4451	1500	0.4638
1600	0.4432	1600	0.4172	1600	0.4458	1600	0.4642
1700	0.4435	1700	0.4184	1700	0.4466	1700	0.4646
1800	0.4439	1800	0.4196	1800	0.4473	1800	0.4649
1900	0.4443	1900	0.4207	1900	0.4480	1900	0.4652
2000	0.4447	2000	0.4218	2000	0.4486	2000	0.4654
2100	0.4451	2100	0.4230	2100	0.4493	2100	0.4656
2200	0.4454	2200	0.4240	2200	0.4499	2200	0.4657
2300	0.4457	2300	0.4249	2300	0.4504		
2400	0.4460	2400	0.4258	2400	0.4509		
2500	0.4462	2500	0.4266	2500	0.4514		
2600	0.4463	2600	0.4271	2600	0.4516		
2700	0.4465	2700	0.4276	2700	0.4519		
2800	0.4466	2800	0.4280	2800	0.4520		
		2900	0.4284	2900	0.4522		

20.0 ^{0}C		22.0A ^{0}C		22.0B ^{0}C		24.1A ^{0}C		24.1B ^{0}C	
Time (s)	ϕ(t)	Time (s)	ϕ(t)	Time (s)	ϕ(t)	Time(s)	ϕ(t)	Time (s)	ϕ(t)
0	0.4731	0	0.4989	0	0.6099	0	0.5370	0	0.6094
100	0.4743	100	0.4996	100	0.6104	100	0.5380	100	0.6093
200	0.4756	200	0.5005	200	0.6110	200	0.5391	200	0.6092
300	0.4771	300	0.5016	300	0.6115	300	0.5403	300	0.6092
400	0.4786	400	0.5031	400	0.6121	400	0.5417	400	0.6091
500	0.4802	500	0.5047	500	0.6127	500	0.5431	500	0.6090
600	0.4818	600	0.5065	600	0.6133	600	0.5446	600	0.6089
700	0.4834	700	0.5084	700	0.6139	700	0.5462	700	0.6087
800	0.4850	800	0.5104	800	0.6145	800	0.5478	800	0.6086
900	0.4864	900	0.5124	900	0.6150	900	0.5494	900	0.6085
1000	0.4878	1000	0.5145	1000	0.6155	1000	0.5511	1000	0.6084
1100	0.4891	1100	0.5166	1100	0.6160	1100	0.5528	1100	0.6083
1200	0.4903	1200	0.5189	1200	0.6164	1200	0.5545	1200	0.6082
1300	0.4913	1300	0.5211	1300	0.6168	1300	0.5562	1300	0.6081
1400	0.4923	1400	0.5235	1400	0.6171	1400	0.5578	1400	0.6081
1500	0.4932	1500	0.5257	1500	0.6174	1500	0.5594	1500	0.6080
1600	0.4940	1600	0.5278	1600	0.6177	1600	0.5609	1600	0.6080
1700	0.4947	1700	0.5297	1700	0.6180	1700	0.5624	1700	0.6079
1800	0.4953	1800	0.5314	1800	0.6182	1800	0.5639	1800	0.6079
1900	0.4958	1900	0.5329	1900	0.6184	1900	0.5652	1900	0.6079
2000	0.4963	2000	0.5342	2000	0.6186	2000	0.5664	2000	0.6079
2100	0.4967	2100	0.5354	2100	0.6188	2100	0.5675	2100	0.6079
2200	0.4970	2200	0.5365	2200	0.6189	2200	0.5683	2200	0.6079
2300	0.4972	2300	0.5375	2300	0.6191	2300	0.5690	2300	0.6079
2400	0.4973	2400	0.5384	2400	0.6192	2400	0.5695		
		2500	0.5392	2500	0.6193	2500	0.5700		
		2600	0.5398	2600	0.6193	2600	0.5702		
		2700	0.5403	2700	0.6194				
		2800	0.5405	2800	0.6194				

26.4 ^{0}C		29.0A ^{0}C		29.0B ^{0}C		31.6A ^{0}C		31.6B ^{0}C	
Time (s)	ϕ(t)	Time (s)	ϕ(t)	Time (s)	ϕ(t)	Time(s)	ϕ(t)	Time (s)	ϕ(t)
0	0.5918	0	0.5788	0	0.5725	0	0.5515	0	0.5317
100	0.5921	100	0.5788	100	0.5725	100	0.5515	100	0.5314
200	0.5923	200	0.5788	200	0.5725	200	0.5515	200	0.5311
300	0.5926	300	0.5788	300	0.5725	300	0.5515	300	0.5307
400	0.5930	400	0.5788	400	0.5725	400	0.5515	400	0.5302
500	0.5933	500	0.5788	500	0.5724	500	0.5515	500	0.5297
600	0.5937	600	0.5787	600	0.5724	600	0.5515	600	0.5292
700	0.5942	700	0.5787	700	0.5724	700	0.5515	700	0.5287
800	0.5947	800	0.5787	800	0.5724	800	0.5515	800	0.5281
900	0.5952	900	0.5787	900	0.5724	900	0.5515	900	0.5276
1000	0.5957	1000	0.5787	1000	0.5723	1000	0.5515	1000	0.5270
1100	0.5962	1100	0.5786	1100	0.5723	1100	0.5515	1100	0.5264
1200	0.5967	1200	0.5786	1200	0.5723	1200	0.5515	1200	0.5258
1300	0.5972	1300	0.5786	1300	0.5722	1300	0.5515	1300	0.5253
1400	0.5977	1400	0.5785	1400	0.5722	1400	0.5515	1400	0.5247
1500	0.5982	1500	0.5785	1500	0.5721	1500	0.5515	1500	0.5242
1600	0.5987	1600	0.5785	1600	0.5721	1600	0.5515	1600	0.5237
1700	0.5991	1700	0.5784	1700	0.5721	1700	0.5515	1700	0.5232
1800	0.5995	1800	0.5784	1800	0.5720	1800	0.5515	1800	0.5228
1900	0.5998	1900	0.5784	1900	0.5720	1900	0.5515	1900	0.5224
2000	0.6001	2000	0.5783	2000	0.5719	2000	0.5515	2000	0.5220

2100	0.6003	2100	0.5783	2100	0.5719	2100	0.5515	2100	0.5216
2200	0.6005	2200	0.5783	2200	0.5718	2200	0.5515	2200	0.5213
2300	0.6006	2300	0.5783	2300	0.5718	2300	0.5515	2300	0.5211
2400	0.6007	2400	0.5782	2400	0.5718	2400	0.5515	2400	0.5208
		2500	0.5782	2500	0.5718	2500	0.5515	2500	0.5206
		2600	0.5782	2600	0.5718	2600	0.5515	2600	0.5205
		2700	0.5782	2700	0.5717	2700	0.5515	2700	0.5204
		2800	0.5782	2800	0.5717	2800	0.5515	2800	0.5203
		2900	0.5782	2900	0.5717	2900	0.5515	2900	0.5202

Run #1. $\phi(t)$ for 2.93 mg/mL in H_2O at 10 MPa.

5.2 ^{0}C		**6.2 ^{0}C**		**8.0 ^{0}C**		**10.1 ^{0}C**	
Time (s)	$\phi(t)$	Time (s)	$\phi(t)$	Time (s)	$\phi(t)$	Time (s)	$\phi(t)$
0	0.6354	0	0.6206	0	0.5936	0	0.5892
100	0.6351	100	0.6194	100	0.5932	100	0.5892
200	0.6347	200	0.6182	200	0.5928	200	0.5892
300	0.6343	300	0.6169	300	0.5924	300	0.5893
400	0.6338	400	0.6155	400	0.5920	400	0.5893
500	0.6334	500	0.6141	500	0.5914	500	0.5894
600	0.6330	600	0.6128	600	0.5907	600	0.5895
700	0.6327	700	0.6117	700	0.5901	700	0.5896
800	0.6323	800	0.6105	800	0.5895	800	0.5897
900	0.6321	900	0.6094	900	0.5890	900	0.5899
1000	0.6317	1000	0.6085	1000	0.5884	1000	0.5901
1100	0.6314	1100	0.6075	1100	0.5880	1100	0.5903
1200	0.6310	1200	0.6067	1200	0.5875	1200	0.5906
1300	0.6307	1300	0.6059	1300	0.5872	1300	0.5909
1400	0.6305	1400	0.6052	1400	0.5869	1400	0.5912
1500	0.6302	1500	0.6045	1500	0.5866	1500	0.5915
1600	0.6300	1600	0.6039	1600	0.5864	1600	0.5919
1700	0.6298	1700	0.6033	1700	0.5863	1700	0.5922
1800	0.6296	1800	0.6030	1800	0.5863	1800	0.5926
1900	0.6295	1900	0.6028	1900	0.5862	1900	0.5930
2000	0.6294	2000	0.6027	2000	0.5862	2000	0.5934
2100	0.6294	2100	0.6026	2100	0.5862	2100	0.5937
2200	0.6294	2200	0.6026	2200	0.5863	2200	0.5941
2300	0.6295	2300	0.6025	2300	0.5863	2300	0.5944
2400	0.6295	2400	0.6026	2400	0.5864	2400	0.5947
2500	0.6295	2500	0.6026	2500	0.5864	2500	0.5950
2600	0.6296	2600	0.6026	2600	0.5865	2600	0.5952
2700	0.6296	2700	0.6026	2700	0.5866	2700	0.5953
2800	0.6296	2800	0.6025	2800	0.5867	2800	0.5955
2900	0.6296	2900	0.6025	2900	0.5868	2900	0.5956

11.8 ^{0}C **14.2 ^{0}C** **16.7 ^{0}C** **19.0 ^{0}C**

Time (s)	$\phi(t)$	Time (s)	$\phi(t)$	Time (s)	$\phi(t)$	Time (s)	$\phi(t)$
0	0.6067	0	0.6931	0	0.7979	0	0.8930
100	0.6081	100	0.6939	100	0.7988	100	0.8938
200	0.6097	200	0.6949	200	0.7997	200	0.8948
300	0.6116	300	0.6961	300	0.8006	300	0.8959
400	0.6136	400	0.6973	400	0.8016	400	0.8971
500	0.6159	500	0.6988	500	0.8033	500	0.8984
600	0.6184	600	0.7006	600	0.8050	600	0.8999
700	0.6210	700	0.7027	700	0.8068	700	0.9015
800	0.6236	800	0.7048	800	0.8087	800	0.9033
900	0.6264	900	0.7071	900	0.8108	900	0.9052
1000	0.6293	1000	0.7094	1000	0.8129	1000	0.9073
1100	0.6322	1100	0.7116	1100	0.8151	1100	0.9094
1200	0.6352	1200	0.7140	1200	0.8173	1200	0.9115
1300	0.6381	1300	0.7165	1300	0.8195	1300	0.9137
1400	0.6411	1400	0.7193	1400	0.8218	1400	0.9160
1500	0.6440	1500	0.7221	1500	0.8241	1500	0.9182
1600	0.6468	1600	0.7250	1600	0.8263	1600	0.9204
1700	0.6497	1700	0.7281	1700	0.8285	1700	0.9226
1800	0.6525	1800	0.7313	1800	0.8307	1800	0.9246
1900	0.6552	1900	0.7346	1900	0.8328	1900	0.9265
2000	0.6579	2000	0.7379	2000	0.8349	2000	0.9283
2100	0.6605	2100	0.7404	2100	0.8361	2100	0.9300
2200	0.6629	2200	0.7420	2200	0.8372	2200	0.9316
2300	0.6651	2300	0.7435	2300	0.8384	2300	0.9330
2400	0.6671	2400	0.7449	2400	0.8395	2400	0.9344
2500	0.6689	2500	0.7463	2500	0.8406	2500	0.9356
2600	0.6700	2600	0.7470	2600	0.8417	2600	0.9362
2700	0.6709	2700	0.7477	2700	0.8427	2700	0.9367
2800	0.6718	2800	0.7484	2800	0.8437	2800	0.9373
2900	0.6726	2900	0.7490	2900	0.8445	2900	0.9378

21.5 ^{0}C		**24.0 ^{0}C**		**26.7 ^{0}C**		**29.1 ^{0}C**	
Time (s)	$\phi(t)$	Time (s)	$\phi(t)$	Time (s)	$\phi(t)$	Time (s)	$\phi(t)$
0	0.9662	0	0.9847	0	0.9722	0	0.9379
100	0.9662	100	0.9845	100	0.9707	100	0.9368
200	0.9663	200	0.9843	200	0.9692	200	0.9357
300	0.9665	300	0.9842	300	0.9677	300	0.9345
400	0.9665	400	0.9840	400	0.9662	400	0.9333
500	0.9666	500	0.9837	500	0.9648	500	0.9313
600	0.9666	600	0.9833	600	0.9635	600	0.9285
700	0.9667	700	0.9830	700	0.9624	700	0.9257
800	0.9670	800	0.9827	800	0.9614	800	0.9231
900	0.9674	900	0.9824	900	0.9605	900	0.9206
1000	0.9680	1000	0.9822	1000	0.9598	1000	0.9186
1100	0.9689	1100	0.9819	1100	0.9592	1100	0.9168
1200	0.9701	1200	0.9817	1200	0.9588	1200	0.9153
1300	0.9714	1300	0.9815	1300	0.9584	1300	0.9140
1400	0.9727	1400	0.9814	1400	0.9581	1400	0.9129
1500	0.9741	1500	0.9813	1500	0.9579	1500	0.9121
1600	0.9755	1600	0.9812	1600	0.9577	1600	0.9115
1700	0.9771	1700	0.9811	1700	0.9576	1700	0.9109
1800	0.9788	1800	0.9811	1800	0.9576	1800	0.9105
1900	0.9803	1900	0.9810	1900	0.9575	1900	0.9100
2000	0.9818	2000	0.9810	2000	0.9574	2000	0.9095
2100	0.9829	2100	0.9810	2100	0.9574	2100	0.9091

2200	0.9835	2200	0.9810	2200	0.9573	2200	0.9089
2300	0.9839	2300	0.9810	2300	0.9573	2300	0.9087
2400	0.9843	2400	0.9810	2400	0.9573	2400	0.9085
2500	0.9846	2500	0.9811	2500	0.9573	2500	0.9084
2600	0.9848	2600	0.9811	2600	0.9573	2600	0.9083
2700	0.9850	2700	0.9811	2700	0.9573	2700	0.9082
2800	0.9853	2800	0.9812	2800	0.9573	2800	0.9081
2900	0.9855	2900	0.9812	2900	0.9573	2900	0.9081

31.8 ^{0}C		**34.3 ^{0}C**	
Time (s)	ϕ(t)	Time (s)	ϕ(t)
0	0.8849	0	0.8439
100	0.8845	100	0.8412
200	0.8841	200	0.8384
300	0.8834	300	0.8355
400	0.8825	400	0.8325
500	0.8815	500	0.8295
600	0.8802	600	0.8265
700	0.8789	700	0.8239
800	0.8774	800	0.8217
900	0.8758	900	0.8197
1000	0.8741	1000	0.8181
1100	0.8724	1100	0.8167
1200	0.8708	1200	0.8156
1300	0.8693	1300	0.8147
1400	0.8680	1400	0.8140
1500	0.8669	1500	0.8134
1600	0.8658	1600	0.8128
1700	0.8649	1700	0.8122
1800	0.8641	1800	0.8117
1900	0.8634	1900	0.8112
2000	0.8628	2000	0.8107
2100	0.8623	2100	0.8102
2200	0.8619	2200	0.8097
2300	0.8615	2300	0.8093
2400	0.8612	2400	0.8090
2500	0.8610	2500	0.8087
2600	0.8609	2600	0.8085
2700	0.8609	2700	0.8085
2800	0.8608	2800	0.8084
2900	0.8608	2900	0.8083

Run #1. ϕ(t) for 3.0 mg/mL in H_2O at 20 MPa.

2.6 ^{0}C		5.6 ^{0}C		7.5 ^{0}C		8.8 ^{0}C	
Time (s)	ϕ(t)	Time (s)	ϕ(t)	Time (s)	ϕ(t)	Time (s)	ϕ(t)
0	0.5799	0	0.5562	0	0.5203	0	0.5036
100	0.5797	100	0.5552	100	0.5194	100	0.5031
200	0.5794	200	0.5541	200	0.5185	200	0.5025
300	0.5791	300	0.5529	300	0.5176	300	0.5019
400	0.5788	400	0.5517	400	0.5166	400	0.5012
500	0.5784	500	0.5505	500	0.5157	500	0.5006
600	0.5780	600	0.5492	600	0.5148	600	0.4999
700	0.5776	700	0.5479	700	0.5140	700	0.4993
800	0.5771	800	0.5466	800	0.5133	800	0.4986
900	0.5766	900	0.5454	900	0.5126	900	0.4981
1000	0.5760	1000	0.5442	1000	0.5121	1000	0.4975
1100	0.5755	1100	0.5430	1100	0.5116	1100	0.4971
1200	0.5749	1200	0.5419	1200	0.5113	1200	0.4966
1300	0.5743	1300	0.5409	1300	0.5110	1300	0.4962
1400	0.5737	1400	0.5399	1400	0.5107	1400	0.4959
1500	0.5730	1500	0.5389	1500	0.5106	1500	0.4956
1600	0.5724	1600	0.5380	1600	0.5104	1600	0.4954
1700	0.5719	1700	0.5372	1700	0.5103	1700	0.4952
1800	0.5713	1800	0.5363	1800	0.5103	1800	0.4951
1900	0.5708	1900	0.5356	1900	0.5102	1900	0.4950
2000	0.5703	2000	0.5349	2000	0.5102	2000	0.4948
2100	0.5698	2100	0.5343	2100	0.5102	2100	0.4948
2200	0.5694	2200	0.5337	2200	0.5102	2200	0.4947
2300	0.5690	2300	0.5332	2300	0.5102	2300	0.4946
2400	0.5687	2400	0.5328	2400	0.5102	2400	0.4946
2500	0.5684	2500	0.5325	2500	0.5103	2500	0.4946
2600	0.5681	2600	0.5323	2600	0.5103	2600	0.4945
2700	0.5680	2700	0.5322	2700	0.5103	2700	0.4945
2800	0.5679	2800	0.5321	2800	0.5103	2800	0.4945

11.0 ^{0}C		14.2 ^{0}C		16.5 ^{0}C		18.8 ^{0}C	
Time (s)	ϕ(t)	Time (s)	ϕ(t)	Time (s)	ϕ(t)	Time (s)	ϕ(t)
0	0.4956	0	0.5187	0	0.5697	0	0.6667
100	0.4956	100	0.5188	100	0.5708	100	0.6680
200	0.4956	200	0.5189	200	0.5720	200	0.6694
300	0.4956	300	0.5190	300	0.5732	300	0.6709
400	0.4956	400	0.5191	400	0.5745	400	0.6726
500	0.4957	500	0.5193	500	0.5759	500	0.6743
600	0.4957	600	0.5197	600	0.5774	600	0.6762
700	0.4958	700	0.5201	700	0.5790	700	0.6782
800	0.4959	800	0.5206	800	0.5808	800	0.6803
900	0.4960	900	0.5213	900	0.5828	900	0.6826
1000	0.4961	1000	0.5222	1000	0.5850	1000	0.6850
1100	0.4963	1100	0.5233	1100	0.5874	1100	0.6875
1200	0.4965	1200	0.5246	1200	0.5900	1200	0.6901
1300	0.4967	1300	0.5262	1300	0.5929	1300	0.6928
1400	0.4969	1400	0.5279	1400	0.5959	1400	0.6955
1500	0.4972	1500	0.5299	1500	0.5990	1500	0.6983
1600	0.4975	1600	0.5319	1600	0.6023	1600	0.7011
1700	0.4979	1700	0.5341	1700	0.6056	1700	0.7038
1800	0.4982	1800	0.5363	1800	0.6090	1800	0.7065
1900	0.4986	1900	0.5385	1900	0.6123	1900	0.7091
2000	0.4989	2000	0.5407	2000	0.6156	2000	0.7115
2100	0.4993	2100	0.5427	2100	0.6187	2100	0.7138

2200	0.4997	2200	0.5446	2200	0.6216	2200	0.7160
2300	0.5000	2300	0.5462	2300	0.6243	2300	0.7178
2400	0.5004	2400	0.5477	2400	0.6269	2400	0.7194
2500	0.5006	2500	0.5485	2500	0.6287	2500	0.7206
2600	0.5008	2600	0.5493	2600	0.6300	2600	0.7213
2700	0.5008	2700	0.5499	2700	0.6307	2700	0.7218

22.0 ^{0}C		**24.5 ^{0}C**		**27.3 ^{0}C**		**30.0 ^{0}C**	
Time (s)	ϕ(t)	Time (s)	ϕ(t)	Time (s)	ϕ(t)	Time (s)	ϕ(t)
0	0.8032	0	0.8969	0	0.9966	0	0.9997
100	0.8033	100	0.8994	100	0.9956	100	0.9995
200	0.8035	200	0.9022	200	0.9944	200	0.9991
300	0.8037	300	0.9052	300	0.9931	300	0.9986
400	0.8041	400	0.9083	400	0.9917	400	0.9978
500	0.8046	500	0.9114	500	0.9903	500	0.9969
600	0.8053	600	0.9145	600	0.9887	600	0.9956
700	0.8062	700	0.9175	700	0.9871	700	0.9941
800	0.8073	800	0.9205	800	0.9855	800	0.9924
900	0.8087	900	0.9232	900	0.9839	900	0.9904
1000	0.8102	1000	0.9258	1000	0.9824	1000	0.9883
1100	0.8120	1100	0.9283	1100	0.9809	1100	0.9860
1200	0.8141	1200	0.9305	1200	0.9796	1200	0.9835
1300	0.8163	1300	0.9326	1300	0.9784	1300	0.9810
1400	0.8188	1400	0.9346	1400	0.9774	1400	0.9785
1500	0.8215	1500	0.9365	1500	0.9765	1500	0.9759
1600	0.8244	1600	0.9382	1600	0.9758	1600	0.9734
1700	0.8275	1700	0.9398	1700	0.9753	1700	0.9710
1800	0.8306	1800	0.9413	1800	0.9749	1800	0.9689
1900	0.8339	1900	0.9427	1900	0.9746	1900	0.9672
2000	0.8372	2000	0.9440	2000	0.9744	2000	0.9659
2100	0.8404	2100	0.9452	2100	0.9743	2100	0.9650
2200	0.8436	2200	0.9463	2200	0.9742	2200	0.9647
2300	0.8466	2300	0.9473	2300	0.9741		
2400	0.8494	2400	0.9481	2400	0.9741		
2500	0.8519	2500	0.9488	2500	0.9741		
2600	0.8540	2600	0.9494	2600	0.9741		
2700	0.8549	2700	0.9499	2700	0.9741		
2800	0.8554	2800	0.9501	2800	0.9741		

33.5 ^{0}C		**35.5 ^{0}C**		**37.4 ^{0}C**	
Time (s)	ϕ(t)	Time (s)	ϕ(t)	Time (s)	ϕ(t)
0	0.9708	0	0.8242	0	0.7818
100	0.9693	100	0.8230	100	0.7811
200	0.9675	200	0.8217	200	0.7802
300	0.9656	300	0.8203	300	0.7792
400	0.9636	400	0.8188	400	0.7782
500	0.9615	500	0.8172	500	0.7770
600	0.9593	600	0.8155	600	0.7758
700	0.9572	700	0.8138	700	0.7746
800	0.9551	800	0.8122	800	0.7733
900	0.9530	900	0.8105	900	0.7720
1000	0.9510	1000	0.8090	1000	0.7707
1100	0.9492	1100	0.8075	1100	0.7694
1200	0.9474	1200	0.8061	1200	0.7682

1300	0.9458	1300	0.8048	1300	0.7669
1400	0.9442	1400	0.8037	1400	0.7658
1500	0.9428	1500	0.8027	1500	0.7647
1600	0.9414	1600	0.8018	1600	0.7636
1700	0.9401	1700	0.8010	1700	0.7626
1800	0.9389	1800	0.8003	1800	0.7617
1900	0.9377	1900	0.7996	1900	0.7609
2000	0.9366	2000	0.7991	2000	0.7601
2100	0.9356	2100	0.7987	2100	0.7594
2200	0.9346	2200	0.7983	2200	0.7588
2300	0.9337	2300	0.7979	2300	0.7583
2400	0.9329	2400	0.7977	2400	0.7578
2500	0.9322	2500	0.7974	2500	0.7574
2600	0.9317	2600	0.7972	2600	0.7571
2700	0.9313	2700	0.7972	2700	0.7570
2800	0.9312	2800	0.7971	2800	0.7569

Bibliography

(1) Grosberg, A. Y.; Khokhlov, A. R. *Giant Molecules*; Academic Press: San Diego, 1997.

(2) Oosawa, F.; Asakura, S. *Thermodynamics of the Polymerization of Protein*; Academic Press: New York, 1975.

(3) Wheeler, J. C.; Kennedy, S. J.; Pfeuty, P. *Phys. Rev. Lett.* **1980**, *45*, 1748.

(4) Vandekerckhove, J.; Weber, K. *Eur. J. Biochem.* **1978**, *90*, 451.

(5) Alberts, B.; Johnson, A. *Molecular Biology of the Cell*; Taylor and Francis: New York, 2002.

(6) Pollard, T. D.; Balnchoin, L.; Mullins, R. D. *Ann. Rev. Biophys. Biomol. Struc.* **2000**, *29*, 545.

(7) Kabsch, W.; Mannherz, H. G.; Suck, D.; Pai, E. F.; Holmes, K. C. *Nature* **1990**, *347*, 37.

(8) Howard, J. *Mechanics of Motor Proteins and the Cytoskeleton*; Sinauer Associates Publishers: Sunderland, Mass., 2001.

(9) Kasai, M.; Asakura, S.; Oosawa, F. *Biochim. Biophys. Acta* **1962**, *57*, 13.

(10) Carlier, M.-F.; Pantaloni, D.; Korn, E. D. *J. Biol. Chem.* **1984**, *259*, 9987.

(11) Drenckhahn, D.; Pollard, T. *J. Biol. Chem.* **1986**, *261*, 12754.

(12) Kawamura, M.; Maruyama, K. *J. Biochem.* **1970**, *67*, 437.

(13) Kasai, M.; Asakura, S.; Oosawa, F. *Biochimica et Biophysica Acta* **1962**, *57*, 22.

(14) Ivkov, R.; Forbes, J. G.; Greer, S. C. *J. Chem. Phys.* **1998**, *108*, 5599.

(15) Niranjan, P. S. Thermodynamics of Actin Polymerization: Extent of Polymerization Studies. Ph. D., University of Maryland at College Park, 2000.

(16) Niranjan, P. S.; Yim, P. B.; Forbes, J. G.; Greer, S. C.; Dudowicz, J.; Freed, K. F.; Douglas, J. F. *J. Chem. Phys.* **2003**, *119*, 4070.

(17) Dudowicz, J.; Freed, K. F.; Douglas, J. F. *J. Chem. Phys.* **1999**, *111*, 7116.

(18) Niranjan, P. S.; Forbes, J. G.; Greer, S. C.; Dudowicz, J.; Freed, K. F.; Douglas, J. F. *J. Chem. Phys.* **2001**, *114*, 10573.

(19) Okamoto, K. I.; Nagai, T.; Miyawaki, A.; Hayashi, Y. *Nature Neuroscience* **2004**, *7*, 1104.

(20) Marx, J. *Science* **2003**, *302*, 214.

(21) Pollack, G. H. *Cells, Gels, and the Engines of Life: A New, Unifying Approach to Cell Function*; Ebner and Sons: Seattle, 2001.

(22) O'Shaughnessy, B.; Vavylonis, D. *preprint* **2001**.

(23) Kresheck, G. C.; Schneider, H.; Scheraga, H. A. *J. Phys. Chem.* **1965**, *69*, 3132.

(24) Ikeuchi, Y.; Suzuki, A.; Oota, T.; Hagiwara, K.; Tatsumi, R.; Ito, T.; Balny, C. *Eur J Biochem* **2002**, *269*, 364.

(25) Swezey, R. R.; Somero, G. N. *Biochemistry* **1982**, *21*, 4496.

(26) Isaacs, N. S. *Liquid Phase High Pressure Chemistry*; Wiley-Interscience: New York, 1981.

(27) Garcia, C. R.; J. Adalbarto Amaral, J.; Abrahamsohn, P.; Verjovski-Almeida, S. *Eur. J. Biochem.* **1992**, *209*, 1005.

(28) Ikkai, T.; Ooi, T. *Biochemistry* **1966**, *5*, 1551.

(29) Zimmerle, C. T.; Frieden, C. *Biochemistry* **1988**, *27*, 7759.

(30) Kitamura, Y.; Itoh, T. *J. Solution Chem.* **1987**, *16*, 715.

(31) Amos, L. A.; Amos, W. B. *Molecules of the Cytoskeleton*; The Guilford Press: New York, 1991.

(32) Kinosian, H. J.; Selden, L. A.; Estes, J. E.; Gershman, L. C. *Biochim. Biophys. Acta* **1991**, *1077*, 151.

(33) Kasai, M.; Nakano, E.; Oosawa, F. *Biochim. Biophys. Acta* **1965**, *94*, 494.

(34) Kouyama, T.; Mihashi, K. *Eur. J. Biochem.* **1981**, *114*, 33.

(35) Houk, T. W.; Ue, K. *Anal. Biochem.* **1974**, *62*, 66.

(36) Weber, G. *J. Phys. Chem.* **1993**, *97*, 7108.

(37) Zimmerle, C. T.; Frieden, C. *Biochemistry* **1986**, *25*, 6432.

(38) Lauffer, M. A. *Entropy-Driven Processes in Biology*; Springer-Verlag: New York, 1975.

(39) Belagyi, J.; Damerau, W.; G., P. *Acta Biochim Biophys Acad Sci Hung* **1978**, *13*, 85.

(40) Schuler, H.; Lindberg, U.; Schutt, C. E.; Karlsson, R. *Eur J Biochem* **2000**, *267*, 476.

(41) Moelbert, S.; De los Rios, P. *Macromolecules* **2003**, *36*, 5845.

(42) Sept, D.; Xu, J.; Pollard, T. D.; McCammon, J. A. *Biophys. J.* **1999**, *77*, 2911.

(43) Ruiz-Garcia, J.; Anderson, E. M.; Greer, S. C. *J. Phys. Chem.* **1989**, *93*, 6980.

(44) Touro, F. J.; Wiewiorowski, T. K. *J. Phys. Chem.* **1966**, *70*, 239.

(45) Zhuang, J.; Das, S. S.; Nowakowski, M.; Greer, S. C. *Physica A* **1997**, *244*, 522.

(46) Miyake, A.; Stockmayer, W. H. *Die Makromolekulare Chemie* **1965**, *88*, 90.

(47) Yim, P. B.; Jacobs, D. T.; Peters, N. D.; Forbes, J. G.; Alessi, M. L.; Greer, S. C. **unpublished**.

(48) Swezey, R. R.; Somero, G. N. *Biochemistry* **1985**, *24*, 852.

(49) Morita, T. *Journal of Biological Chemistry* **2003**, *278*, 28060.

(50) Hofrichter, J.; Christoph, G. W.; Eaton, W. A. *Biophysical Journal* **1993**, *64*, A43.

(51) Ikkai, T.; Ooi, T. *Science* **1966**, *152*, 1756.

(52) Quirion, F.; Gicqaud, C. *Biochem. J.* **1993**, *295*, 671.

(53) Andrews, A. P.; Andrews, K. P.; Greer, S. C.; Boue, F.; Pfeuty, P. *Macromolecules* **1994**, *27*, 3902.

(54) Gu, X. Density as a function of temperature near the ceiling temperature of alpha-methylstyrene. M. S., University of Maryland, College Park, 1997.

(55) Greer, S. C. *J. Phys. Chem.* **1998**, *102*, 5413.

(56) de Arcangelis, L.; Del Gado, E.; Fierro, A.; Coniglio, A. *Braz. J. Phys.* **2003**, *33*, 594.

(57) Bahar, I.; Erman, B.; Fytas, G.; Steffen, W. *Macromolecules* **1994**, *27*, 5200.

(58) Douglas, J. F., personal communication.

(59) Freed, K. *unpublished* **2003**.